Robust control of platooning systems over imperfect wireless channels

Tiago Rocha Gonçalves

université
PARIS-SACLAY

Robust control of platooning systems over imperfect wireless channels

Contrôle robuste de pelotons de véhicules sur un canal radio avec imperfections

Thèse de doctorat de l'université Paris-Saclay

École doctorale n° 580, sciences et technologies de l'information et de la communication (STIC)
Spécialité de doctorat: Réseaux, information et communications
Unité de recherche: Laboratoire des signaux et systèmes (Université Paris-Saclay, CNRS, CentraleSupélec)
Référent: : Faculté des sciences d'Orsay

Thèse présentée et soutenue à Paris-Saclay, le 23 novembre 2021, par

Tiago ROCHA GONÇALVES

Composition du jury:

Fawzi NASHASHIBI Directeur de recherche, INRIA Paris-Rocquencourt	Président
Francesco DE PELLEGRINI Professeur, Université d'Avignon	Rapporteur & Examinateur
Loutfi NUAYMI Professeur, Institut Mines Télécom / IMT Atlantique	Rapporteur & Examinateur
Irinel-Constantin MORĂRESCU Professeur, Université de Lorraine	Examinateur
Chung Shue (Calvin) CHEN Chercheur, Nokia Bell Labs	Examinateur

Direction de la thèse:

Salah Eddine ELAYOUBI Professeur, CentraleSupélec, Université de Paris-Saclay	Directeur de thèse
Vineeth S. VARMA Chargé de recherche, CNRS, Université de Lorraine	Co-encadrant

Thèse de doctorat

NNT: 2021UPASG089

Synthèse en français

Les systèmes de transport sont essentiels pour la société, car le rythme soutenu de la croissance économique est étroitement lié à l'accroissement des activités de transport. Dans ce contexte, le domaine des systèmes de transport intelligents (ITS) est apparu comme un sujet de recherche d'actualité pour améliorer et relever les nouveaux défis des systèmes de circulation. Les systèmes de pelotons représentent une approche relativement simple en termes de déploiement vers des solutions économes en carburant, la réduction de la congestion du trafic et l'amélioration de la sécurité routière. En particulier, le peloton de véhicules est une formation spécifique par un groupe de véhicules coordonnés, dans laquelle une courte distance inter-véhicules est maintenue grâce à l'automatisation et aux technologies de communication entre véhicules. Le déploiement de tels systèmes est étroitement lié à une évaluation minutieuse de la synergie entre les deux technologies de base.

Cette thèse a été consacrée au contrôle robuste des systèmes de platooning sur des canaux sans fil imparfait. Nous avons soigneusement considéré la coexistence des aspects de communication et de contrôle, car ils sont tous deux cruciaux pour le déploiement des véhicules de platooning.

Nous avons couvert plusieurs aspects importants dans ce travail, le premier étant la proposition d'un schéma de contrôle adaptatif basé sur la qualité du lien de communication, comme abordé au Chapitre 3. Dans ce contexte, nous présentons l'algorithme dynamique proposé, pour lequel nous effectuons une optimisation heuristique hors ligne afin d'établir les meilleurs paramètres de contrôle pour toute valeur donnée de PER (Packet Error Rate). Cette proposition est vérifiée via notre environnement de simulation de peloton construit sur Simulink et Matlab qui sont chargés de permettre l'interaction entre les systèmes de contrôle et de communication. Nous avons réussi à atteindre notre objectif puisque notre approche dynamique surpasse les stratégies de contrôle statiques. En outre, nous avons identifié une dépendance substantielle de la qualité du canal de liaison du leader avec le dernier véhicule du peloton, ce qui a considérablement limité notre approche dynamique.

En cherchant à améliorer la qualité du canal, nous avons proposé au Chapitre 4 une modélisation analytique du peloton sous deux schémas de relais différents. En particulier, nous avons considérablement amélioré le modèle d'accès au canal en introduisant un modèle de chaîne de Markov qui quantifie la fiabilité des différents liens de communication tels que le lien véhicule-véhicule et le lien véhicule-RSU (Roadside Unit). Nous proposons ensuite une approche intercouche qui ajuste la couche application, c'est-à-dire la distance inter-véhicules du peloton, aux performances observées de la couche contrôle d'accès au support. En outre, nous fournissons une optimisation du protocole de communication pour le peloton en tenant compte de la performance du peloton. Plus précisément, nous déterminons le meilleur compromis entre la taille de la fenêtre de contention, qui affecte directement le délai des paquets, et la performance du peloton de contrôle, qui se traduit par des distances inter-véhicules plus courtes. En plus de l'analyse des performances ci-dessus, nous avons fourni une comparaison avec les approches classiques qui ne prennent pas en compte l'interaction bidirectionnelle entre les paramètres de contrôle et de communication dans le Chapitre 4. Comme nous l'avons montré, il devient évident qu'il est nécessaire de procéder à l'analyse de cette interaction puisque des résultats avec des collisions ont été observés lorsqu'une analyse partielle seulement a été effectuée. Cette observation renforce l'objectif principal de cette thèse.

Néanmoins, notez que jusqu'à présent, toute l'attention est concentrée sur l'optimisation de la distance inter-véhicules du peloton en prenant en compte les caractéristiques essentielles de la conception de la communication/contrôle conjointe. Malgré la pertinence de cette approche, nous manquons d'analyse pour quantifier de tels développements en termes de consommation de carburant, qui est l'aspect le plus important dans la perspective économique et la faisabilité du platooning à des fins commerciales. Afin de combler cette lacune, nous proposons dans le Chapitre 5 une analyse complète pour améliorer l'efficacité énergétique du système de platooning.

Nous avons commencé le Chapitre 5 en abordant les forces externes et le modèle de consommation de carburant d'un point de vue plus axé sur le contrôle. Ceci sexplique par le fait que nous souhaitions observer l'effet de la distance inter-véhicules, qui est un paramètre de contrôle, sur le rendement énergétique du peloton. Nous avons ensuite présenté une comparaison des performances de carburant des deux contrôleurs évalués, ACC (Adaptive Cruise Control) et CACC (Cooperative Adaptive Cruise Control), ce qui nous a permis d'observer le fait suivant. Il existe un compromis non trivial entre une consommation de carburant plus élevée due à l'effort de contrôle et une consommation de carburant plus faible due à la formation de pelotons. Par conséquent, notre objectif dans ce chapitre est de tenter de résoudre ce dilemme. Dans ce contexte, nous avons proposé une commande

améliorée, qui est une combinaison linéaire des commandes ACC et CACC, mais paramétrée par un facteur de lissage β pour permettre des transitions douces et réduire les pertes de carburant. Cependant, nous sommes maintenant confrontés à une question : quand chaque contrôleur doit-il être utilisé lors d'une opération de platooning ? En fait, cette question est associée au compromis non trivial mentionné ci-dessus, et c'est une tâche très complexe puisque le peloton est soumis à des perturbations inconnues. Nous modélisons cette dynamique inconnue comme un processus stochastique, pour lequel nous proposons un modèle de chaîne de Markov qui quantifie le profil de vitesse du véhicule brouilleur. Afin de tenter de répondre à la question ci-dessus, nous proposons deux approches différentes.

La première approche est une commande à seuil qui, sur la base de certaines fonctions de l'accélération du véhicule, détermine le meilleur contrôleur à adopter par le peloton. La seconde adopte une approche d'apprentissage par renforcement profond qui, sur la base d'expériences par essais et erreurs, apprend le comportement des perturbations et adapte l'action qui maximise une certaine fonction de récompense. Pour surmonter les problèmes de sécurité et de convergence des algorithmes DRL (Deep Reinforcement Learning), notre approche définit la période de fonctionnement des contrôleurs ACC et CACC bien connus, au lieu de contrôler directement les véhicules. Notez que dans les deux approches, nous adoptons un contrôleur homogène, ce qui signifie que tous les membres du peloton agissent selon la même politique de contrôle. Nous avons montré que les deux approches proposées sont des solutions prometteuses pour déterminer l'ensemble des temps de transition, et, par conséquent, pour répondre à la question. En particulier, le DRL surpasse tous les cas évalués dans notre scénario de peloton, mais, d'un autre côté, il impose certains défis de déploiement pour traiter toutes les informations et prendre des décisions en temps réel.

Il convient de noter que de nombreux efforts ont été déployés pour appliquer les techniques d'apprentissage automatique aux véhicules autonomes connectés. Il ne fait aucun doute que les progrès en matière d'algorithmes convergents plus rapides et de ressources informatiques plus puissantes sont des points clés techniques pour un déploiement massif de ces technologies. En outre, il est tout aussi important de comprendre la confiance que les conducteurs accordent à ces systèmes, car il n'est peut-être pas possible de démontrer la sécurité des véhicules autonomes en termes de décès et de blessures. Quoi qu'il en soit, les progrès de la sensibilisation à l'environnement et à l'évolution des technologies rendent la mise en uvre de tels systèmes très probable dans un avenir proche.

Acknowledgements

First of all, I would like to thank all the support of my parents in Brazil, Sérgio and Edna. They have always supported me and encouraged me to go further in my studies, and gave me all the support I needed. Since the beginning of my studies, I have virtual family meetings on Sundays, so this is the day when I feel most in Brazil. On this occasion, they always ask me how my research is going, so since them they have been following my little steps. I would like also to thank my brothers, Tomaz and Júlia. They are amazing people and I am happy to have them as family.

I would like to express my deepest gratitude to my thesis supervisors, Salah E. Elayoubi and Vineeth S. Varma. I appreciate all the support and conversation I had with both of them. It was a huge privilege to work with them. I am grateful for all their help, for all the corrections, and especially for the technical and professional guidance. Instead of Sundays, fortunately, we had meetings on Tuesdays. Therefore, defending my doctoral thesis on a Tuesday seems like a perfect occasion to close this cycle in my life.

All my thanks also go to Francesco de Pellegrini and Loutfi Nuaymi for their interest in my work by agreeing to be the reviewers of my manuscript. I also thank Fawzi Nashashibi, Irinel-Constantin Morarescu, and Calvin Chen for kindly agreeing to be part of the jury.

I would like to thank from the bottom of my heart all my friends in France, who have become my second family. I really appreciate the relaxing time during the weekends, and all the trips we have done together. Those moments and meeting all of you make me feel fortunate to be living abroad. Special thanks to Icaro, Pedro, Vinícius, Monacer, Priscila, Thaís T., Thaís A., Alex, Michele and Monique. I also appreciate the good times that I shared with my colleagues in L2S laboratory with Siyang, Raul, José and Hung. A big thank goes to Rafael, with whom I had the pleasure to work with. Our discussions really motivated me during these last months of my thesis.

I could not forget to mention Déborah who has lived a good part of this journey with me. Her love and unconditional support were essential for me to finish my studies. I am happy to have her by my side. Also, I thank her family, Charlety,

who made me feel included not only in the family but also in my new home, France.

Finally, my decision to cross the Atlantic to start a PhD in a country I have never lived before and barely spoke the language was not easy. But fortunately, everyone around me encouraged me to go for it. Especially, my sister Júlia who has a genetic disorder, and my mother refers to her as an angel on earth. She has motivated me every day. I only wish she could fully understand how much important she is to me, despite our distance. This is for you, sister.

Contents

Synthèse en français i
Acknowledgements iv

1 Introduction **1**
1.1 Background and Motivation 1
1.2 Main contributions 7
1.3 Thesis overview and Organization 8
1.4 List of publications 10

2 Enabling technologies for platooning **11**
2.1 Vehicular Communication Technologies 11
2.1.1 ITS-G5 protocol 12
2.2 Control aspects for platooning 15
2.2.1 Vehicle dynamics 16
2.2.2 Cruise Control (CC) 19
2.2.3 Adaptive Cruise Control (ACC) 19
2.2.4 Cooperative Adaptive Cruise Control (CACC) 20
2.2.5 Predictive Cooperative Adaptive Cruise Control 21
2.2.6 Semi-Autonomous Control 22
2.3 Information flow topology 24
2.4 Platooning research projects 25
2.5 Summary 27

3 Adaptive control scheme based on communication link quality **28**
3.1 Introduction 28
3.2 General system outline 33
3.3 Control Platooning System 36
3.3.1 Vehicle dynamics 36
3.3.2 Proposed dynamic scheme based on PCACC 36
3.4 Simulation system implementation 39
3.4.1 Communication Platooning system 39
3.4.2 Simulation Assumptions and Platoon Scenario 46

3.5 Performance Evaluation . . . 50
3.5.1 Offline optimization . . . 51
3.5.2 Online adaptation of the control parameters . . . 51
3.6 Concluding Remarks . . . 54

4 Analytical modeling of platoon under V2X relaying scheme 57
4.1 Introduction . . . 58
4.2 Platooning control system . . . 61
4.2.1 Vehicle dynamics and objective of platoon control . . . 62
4.2.2 Platoon controller with delay factor . . . 62
4.3 Communication mechanisms for platooning . . . 63
4.3.1 Baseline scheme with V2V communications only . . . 63
4.3.2 Relaying of the leader's packets . . . 64
4.4 Communication performance analysis . . . 67
4.4.1 Mean access delay . . . 68
4.4.2 Packet loss probability for V2V links . . . 69
4.4.3 Performance analysis for V2V relaying . . . 75
4.4.4 Performance with RSU relaying . . . 76
4.5 Simulation results . . . 77
4.5.1 Simulation environment description . . . 77
4.5.2 Communication system performance . . . 80
4.5.3 Platoon performance: inter-vehicle distance . . . 81
4.6 Extended performance analysis . . . 83
4.6.1 Comparison with classical approaches . . . 83
4.6.2 Impact of the RSU density . . . 84
4.6.3 Impact of the platoon size . . . 85
4.7 Concluding Remarks . . . 87

5 Fuel efficiency improvements to platooning systems 89
5.1 Introduction . . . 90
5.2 System Model and Problem Statement . . . 93
5.2.1 Platoon modelling with external forces . . . 93
5.2.2 Fuel consumption model . . . 95
5.2.3 Classical control schemes for platooning . . . 97
5.2.4 Enhanced proposed controller . . . 102
5.2.5 Objective . . . 104
5.3 Optimal policy for constant jammers . . . 105
5.4 Stochastic disturbances . . . 107
5.4.1 Jammer profile modeled with Markov chains . . . 108
5.4.2 Troublesome conditions . . . 109
5.5 Proposed switch controllers . . . 110

5.5.1 Threshold control . . . 110
5.5.2 Deep reinforcement learning for switching platoon controller 111
5.5.3 Experimental settings . . . 114
5.6 Performance evaluation . . . 114
5.6.1 Numerical stochastic profiles of the jammer . . . 114
5.6.2 Simulation environment . . . 116
5.6.3 Performance over baseline . . . 118
5.7 Conclusions . . . 122

6 General conclusion and perspectives 124
6.1 General conclusion . . . 124
6.2 Future perspectives . . . 126
6.2.1 Direct extensions . . . 126
6.2.2 Application to other domains . . . 127

List of Figures

1.1 Number of citations of "vehicle platoons" in the IEEE Xplore Digital Library, and in the ScienceDirect Library. 3
1.2 Connected vehicle benefits. 4
1.3 Costumer operating costs for a European long haulage [1]. 6
1.4 Manuscript organization. 9

2.1 Closed loop block diagram of the control system framework. 16
2.2 Block diagram of the platoon system with a PCACC control between vehicle $i-1$ and vehicle i. 22
2.3 Impact of actuator lag τ in the platoon performance for different control schemes under an average velocity of the leader of $18m/s$. . 23
2.4 Typical information flow topology of platooning systems. The vehicle in green is the leader, while the blue ones are the platoon members. 24

3.1 General system outline for two platoon members only. 34
3.2 Block diagram overview with control and communication system interaction. 35
3.3 Offline and online parameter election diagram. 38
3.4 Block diagram simulation overview. 39
3.5 Illustration of Highway NLOS and LOS profiles from WLAN Toolbox. 41
3.6 Traffic interference in respect to the leader vehicle in green. The transmission range is denoted by R, and the length of the platoon size by L_{PS}. Platoon members and external vehicles are illustrated in blue and red, respectively. 43
3.7 Loss probability comparison for consecutive vehicles for ALOHA protocol in dashed blue. 44
3.8 PER of Highway environment with NLOS condition. Interferences are expressed in orange, while no interference conditions in blue. . . 45
3.9 Traffic scenario including a platoon with V2V communication approach. 47

3.10 Illustration of the jammer velocity profile adopted with 2 cycles. . . 48
3.11 Burst size with different probabilities to occur. The dashed blue, solid red, and dashed yellow corresponds to probabilities of burst to occur of 10^{-1},10^{-5}, and 10^{-10}, respectively. We have adopted the solid red line $\nu = -5$, while dash lines are shown for comparison purposes. 49
3.12 Illustration of the average inter-vehicular distance with $\text{PER}_{i,i+1} = 0.0245$ for different C values. Several cases of PER_{LLV} are considered. 52
3.13 Illustration of the optimum C and D_{des} parameters for different PER_{LLV} values. 53
3.14 Traffic density pattern adopted for the best and the worst communication link with the leader, illustrated in blue and orange, respectively. 54
3.15 Illustration of the average inter-vehicular distance for the first two and last two vehicles considering the Case 4 simulation. 55

4.1 Arrangement of a platoon with V2V and V2I relaying communication technologies. The solid blue lines are the vehicle to neighbour links, the dashed green and red lines are the broadcast links for V2V and RSU relaying, respectively, and the dotted black lines are the outside interference links from outside the platoon. 59
4.2 Proposed Markov chain for baseline scheme. 70
4.3 Loss probability comparison, for consecutive vehicles, of CSMA/CA with no retransmission ($m = 1$), and one retransmission ($m = 2$) in dashed orange and solid yellow lines, respectively. Aloha is kept for comparison purposes in dashed blue. 74
4.4 Block diagram of system simulator with control and communication interaction. 78
4.5 Illustration of different profiles adopted over time. 79
4.6 PER for 20th vehicle for the different communication scenarios with $m = m_l = m_r = 2$ retransmission attempts. 80
4.7 Average packet error rate for 10th and 20th vehicle under V2V relay $r = [5\ 10\ 15]$ approach in solid blue and red lines, and average inter-vehicular distance of the platoon for different contention window sizes in dashed yellow line, respectively. 83
4.8 PER for between leader and last vehicle for different RSU densities. 85
4.9 PER for 10th vehicle for the different communication scenarios with $m = m_l = m_r = 2$ retransmission attempts. 86
4.10 Average inter-vehicular distance for platoon size of $N = 11$ under baseline approach in solid blue, and traffic density profile over time in dashed red lines. 87

5.1 Air-drag reduction for trucks in a platoon at $80km/h$ empirically obtained. The figure is adapted from [2]. 96
5.2 Behavior of ACC controller. 99
5.3 Behavior of CACC controller. 100
5.4 Fuel consumption comparison for ACC and CACC controllers under constant and aggressive condition. 101
5.5 Performance comparison between non-enhanced, enhanced and no switch control in dashed-dotted blue, solid orange, and dashed yellow, respectively, under constant jammer and with transition time $t_1 = 50$ s. The two figures on the top correspond to the switching from ACC to CACC, whereas the bottom two are from CACC to ACC. 103
5.6 The transition rate for the Markov chain of the Jammer profile. . . 108
5.7 Illustration of troublesome conditions. 110
5.8 Reinforcement learning overall diagram. 112
5.9 Overview of the DRL framework for our platoon system. 116
5.10 Illustration of a particular jammer profile investigated in (a), and the corresponding fuel platoon performance for all evaluated cases in (b). 120
5.11 The fuel performance relative to the baseline approach in (a), and the smooth control design parameter $\beta(t)$ for the DRL and both threshold switch control approaches in (b). 121

List of Tables

2.1 Differences in PHY parameters between IEEE 802.11a and IEEE 802.11p (source [3]). 14
2.2 EDCA parameters in IEEE 802.11p (source [4]). 15

3.1 Parameters for the MATLAB WLAN Toolbox PHY layer of 802.11p. 40
3.2 Communication and Controller Parameters 50
3.3 Case comparison for the online implementation. 53

4.1 Communication and control and traffic simulation parameters . . . 79
4.2 Performance metrics over different communication schemes for platoon size N=21, $m = m_l = m_r = 1$. 81
4.3 Performance metrics over different communication schemes for platoon size N=21, $m = m_l = m_r = 2$. 81
4.4 Performance metrics over different RSU relaying densities for platoon size N=21 with 0 db shadowing. 85
4.5 Performance metrics over different communication schemes for platoon size N=11, $m = m_l = m_r = 1$. 86
4.6 Performance metrics over different communication schemes for platoon size N=11, $m = m_l = m_r = 2$. 87

5.1 Neural network, control and traffic simulation parameters 117
5.2 Vehicle and energy consumption model parameters used in this chapter (source [5]). 118
5.3 Comparison of the average performance **of fuel improvements** against baseline (ACC) for 1k episodes for distribution [40 6]. . . . 119

Acronyms

ACC	Adaptive Cruise Control
ACs	Access Categories
AEBS	Advanced Emergency Braking System
AIFSN	Arbitrary Inter Frame Space
BD	Bidirectional
BDL	Bidirectional-Leader
C-ITS	Cooperative Intelligent Transportation Systems
C-V2X	Cellular-V2X
CACC	Cooperative Adaptive Cruise Control
CAM	Cooperative Awareness Messages
CC	Cruise Control
CSMA/CA	Carrier Sense Multiple Access with Collision Avoidance
CTG	Constant time-gap
CW	Contention Window
DENM	Decentralized Environmental Notification Message
DNN	Deep Neural Network
DRL	Deep Reinforcement Learning
DSRC	Dedicated Short Range Communications
EDCA	Enhanced Distributed Channel Access

ETSI	European Telecommunications Standards Institute
FCC	Federal Communication Commission
FDM	Frequency Division Multiplexing
GCDC	Grand Cooperative Driving Challenge
GPS	Global Positioning System
HDV	Heavy-Duty Vehicle
ITS	Intelligent Transportation Systems
LDV	Light-Duty Vehicle
LiDAR	Light Detection And Ranging
LOS	Line-of-Sight
MAC	Media Access Control
MCS	Modulation Coding Scheme
MPC	Model Predictive Control
NCS	Networked Control Systems
NLOS	Non-Line-of-Sight
NN	Neural Network
OFDM	Orthogonal Frequency Division Multiplexing
OMNET++	Objective Modular Network Testbed in C++
PATH	Partners for Advanced Transportation Technology
PER	Packet Error Rate
PF	Predecessor-Following
PFL	Predecessor-Following-Leader
PHY	Physical layer
QPSK	Quadrature Phase Shift Keying

RL	Reinforcement Learning
RSU	Roadside Unit
SINR	Signal-to-Interference-plus-Noise Ratio
SNR	Signal Noise Ratio
SUMO	Simulation for Urban MObility
TDM	Time Division Multiplexing
V2V	Vehicle-to-Vehicle
V2X	Vehicle-to-Everything
VENTOS	VEhicular NeTwork Open Simulator
WAVE	Wireless Local Area Network
WHO	World Health Organization
WLAN	Wireless Local Area Network

Chapter 1

Introduction

This chapter introduces the problems investigated in this thesis by first addressing the background and motivation reasons behind its theme. We then highlight the main contributions of this thesis. Next, we present the overview and organization to facilitate the understanding and connection between chapters in an overall manner. Lastly, the list of published articles is presented.

1.1 Background and Motivation

Historically, the economic development consistently relied on the transportation system's expansion. Since the industrial revolution, transportation developments have been associated to growing economic opportunities due to the reduction of both cost and time of moving goods, people, and services [6]. In fact, transportation systems are crucial for society, as the persistent pace of economic growth and increase of demands are closely related to more transportation activity. In this framework, the field of Intelligent Transportation Systems (ITS) has emerged as a research trending topic to enhance and address new traffic-system challenges. In fact, it is one of the major component of smart cities [7], and its overall function is to improve the operation of the entire transport system, from the individual users till transport road and network operators. ITS deployment is feasible due to mutual interest of different sectors, such as commercial interest of private companies (automaker, technology provider, mobile network and road traffic operators) and public initiatives.

The ever-increasing number of connected mobile phones today allows users to share vast amount of information which leads to better decision-making, more efficient processes etc. A similar effect is expected when connected vehicles will be vastly deployed. In fact, it is reasonably to assume a massive increase of connected vehicular nodes in the network in the near future, which includes vehicles, buses,

trucks, roadside infrastructure, and other on-board devices sharing meaningful information about how, where and when they travel. Such initiative towards cooperative, connected and automated mobility leads to development of the Cooperative Intelligent Transport Systems (C-ITS) which aims to substantially improve road safety, traffic efficiency, environmental impact, and comfort of driving by exploiting communication systems. One promising C-ITS service is vehicle platooning, which encompasses the aforementioned assets, and is detailed next.

Vehicle platoon is a particular formation by a group of coordinated vehicles, in which a short inter-vehicle distance is maintained by virtue of automation and vehicular communication technologies. Platooning takes advantage of the special distribution of a convoy in order to increase road capacity and to decrease fuel consumption, by gathering vehicles close together in order to reduce the air resistance of the platoon's members. However, the feasibility and the deployment of platoons relies on the reliable and fast exchange of information between vehicles, as it allows taking control actions based on the most up-to-date information about the road and traffic status. Nevertheless, such an exchange of information occurs over an unreliable wireless communication channel subject to inherent characteristics such as latency and packet loss, which introduces additional challenges for deployment. The aforementioned constraints call for manifold solutions, which will be addressed in the following chapters of this thesis.

In the last decade, the research community experienced an exponential increase of platooning-related works, as exposed in Figure 1.1. It covers the volume of article citing "platoon vehicles" from 1990 until 2020 in the most two relevant library resources with technical science content. Such growth of platooning-related works demonstrates the interest in finding different solutions for ITS services up to now, and evidences the significance of platooning as one of them. In fact, vehicle platooning is one of the six major use case groups to enhance V2X services, including safety-related (e.g. vehicle platooning) and non-safety V2X services (also known as "comfort services") [8].

Vehicle platooning is expected to improve fuel efficiency [9–11] and reduce traffic congestion [12–14] by gathering vehicles close together, thus reducing the air resistance of the platoon's members. Experimental analysis have shown that with such particular convoy formation, a bus, following another one, is able to reduce 40% in aerodynamic drag at 80km/h when 10m of inter-vehicle distance is maintained [2, 15]. Therefore, it is reasonable to conclude that automotive manufacturers, chipset and communication system providers, mobile operators and infrastructure vendors are actively searching for solutions for future mobility and transportation services. In this context, platooning systems represent a relatively simple approach in terms of deployment towards fuel efficient solutions. Besides safety related advantages, platooning systems are very likely to reduce road con-

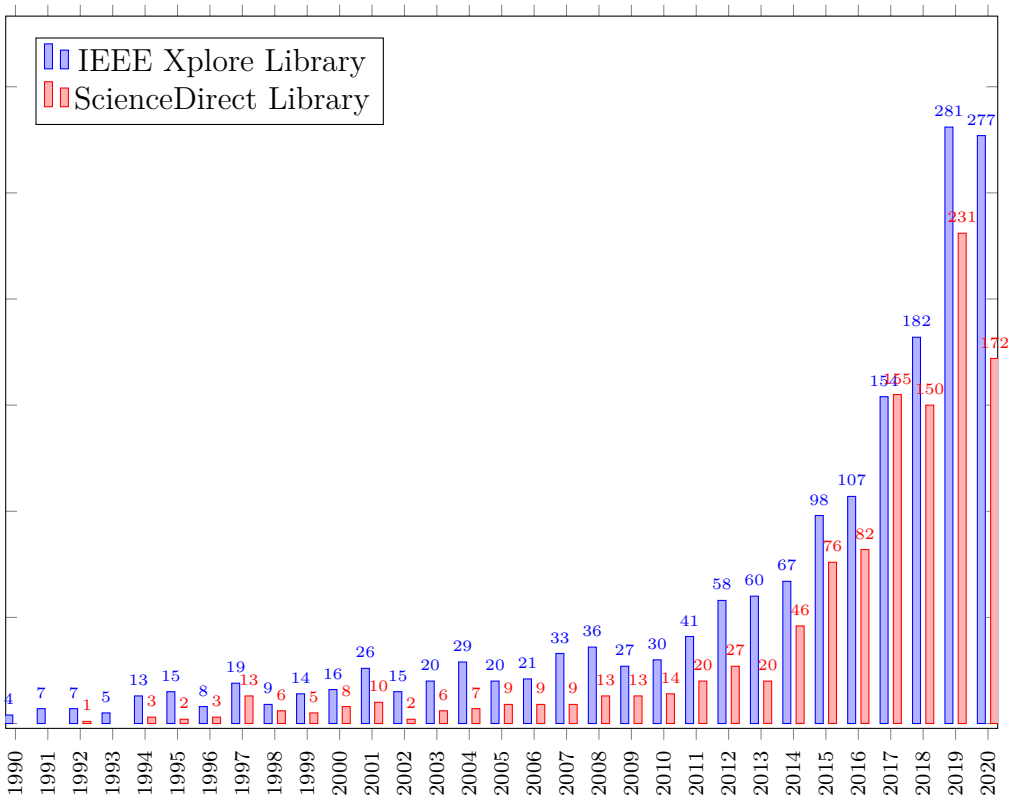

Figure 1.1 – Number of citations of "vehicle platoons" in the IEEE Xplore Digital Library, and in the ScienceDirect Library.

gestion [16] and raise the fuel efficiency while making travel faster and more efficient [9]. In fact, platooning systems are able to reduce fuel consumption of up to 10% [17, 18] depending on a series of factors such as the time gap, set speed and size of the platoon etc. Most of its gains are related to reduction of the overall air drag resistance and coordination of acceleration and deceleration of the platoon members.

In particular, the aforementioned advantages of platooning systems are feasible due to a couple of factors. First, the increasing level of automation possible due to fast and continuous improvement of decision-making computer systems and on-board sensors such as radars, cameras, LiDARs and GPS units that are responsible to monitor the environment and take intelligent actions. Second, the unprecedented cooperation and coordination needed to achieve such high level of automation are not possible without vehicular communications systems. In fact, wireless communication technologies are responsible to solve the Line Of Sight (LOS) problem, which is the largest limitation of sensor-based systems. Therefore, the advantages of platooning are enormous, and they are briefly described next in

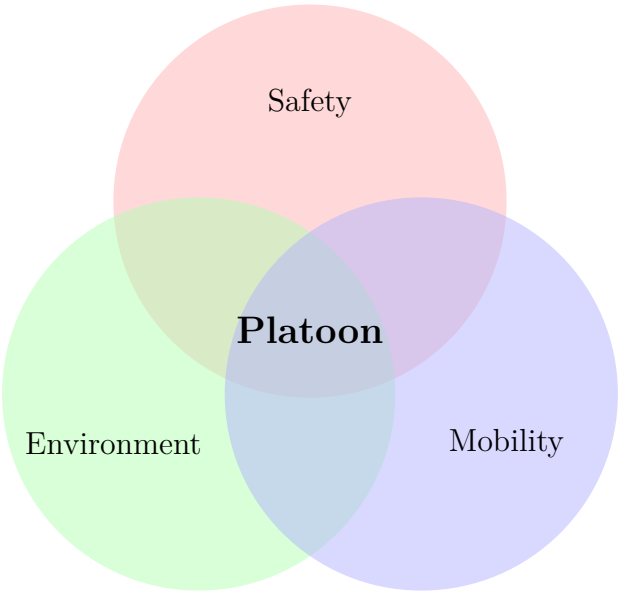

Figure 1.2 – Connected vehicle benefits.

three main categories: safety, environmental and mobility benefits as depicted in Figure 1.2.

Safety

According to the last status report from World Health Organization (WHO) [19], approximately 1.3 million people die every year as a result of road traffic crashes. In economic terms, road traffic crashes cost most countries 3% of their gross domestic product. In France, around 2780 people died due to road crash incidents in 2020 which is 21% lower than the previous year [20]. Undoubtedly, such historically lower statistic is due to the effects of the pandemic COVID-19 and the response measures adopted, such as lockdowns that have imposed restrictions on long-distance travels. Even though overall France achieved inferior occurrences when compared between $2010 - 2020$, the number of cyclist died in the road increase 26% which highlights the need for traffic-safety solutions. In 2020, the United Nations General Assembly adopted positive steps towards improving global road safety with the bold target of preventing at least 50% of road traffic deaths and injuries by 2030 [2]. Moreover, in such assembly they proclaimed the period $2021 - 2030$ as the Second Decade of Action for Road Safety (the first decade is refereed as the period of $2011 - 2020$) which puts in evidence that reducing road traffic deaths and injuries are still an economic and a social priority, especially for some countries, and that investment in road safety has a positive impact on public health and the economy.

A meaningful contribution of platoon systems is the improvement of safety for road users, as in traditional systems, about 90% of all accidents are caused by human error [21]. The two main factors of heavy truck accidents are failure to look properly and misjudgment of other user's path or speed. Similarly, in the research study of McKnight and Bahouth [22], the excessive speed of the driver is the biggest contributor to rollover type of crashes with 45% of the cases. Therefore, the human drivers clearly lose out when compared to automated driving systems mainly due to higher perception, reaction time and concentration required while driving, in addition to risk of fatigue, emotional factors and misuse of cellphones etc. In order to give an idea, since it vary greatly with the situation and from each person, the average human reaction is 1.5 s [23], whereas the reaction of a truck platoon under Vehicle-to-Vehicle (V2V) communication scheme is 0.1 s. At a first glance, such difference might sound minor, but it corresponds to maintain roughly 40 m of additional distance only due to higher perception and reaction time, when vehicles are at 100 km/h.

Mobility

Along with safety benefits, connected vehicles, specially platooning systems, are expected to improve traffic throughput. Due to possible better coordination in the transport layer, which addresses transport planning and vehicle routing. To highlight the potential savings of lowering traffic congestions, the particular pandemic year of 2020 allows interesting observations. Drivers of the United States and United Kingdom were responsible to save $980 and £613 million, respectively, due to the lack of congestion in 2020 [24]. It is clear that as the population increases, the traffic will naturally follow such tendency, and as a result, a complete congestion of urban streets will take place, which evidences the call for actions towards transport-solutions.

Undoubtedly, the most straightforward advantage is the improvement of traffic throughput. In fact, a tight coupling between vehicles in the platoon enables better traffic flow limits, as the lane capacity using platooning might significantly increase, as high as 300% against classical model as shown in [25]. Typically, according to recommendations, the safety gap between vehicles in a highway is around 2-3 s under good driving conditions, in France and in the United States, respectively. In other words, such safety rules, might be interpreted as keeping at least a distance of 55-83 meters from the preceding vehicle under cruising speed of 100 km/h, respectively. Whereas, platooning systems, equipped with V2V communication technologies, are able to maintain a gap of around 5-15 meters. This significant difference clearly shows that there is plenty of room for improvements in the actual traffic throughput.

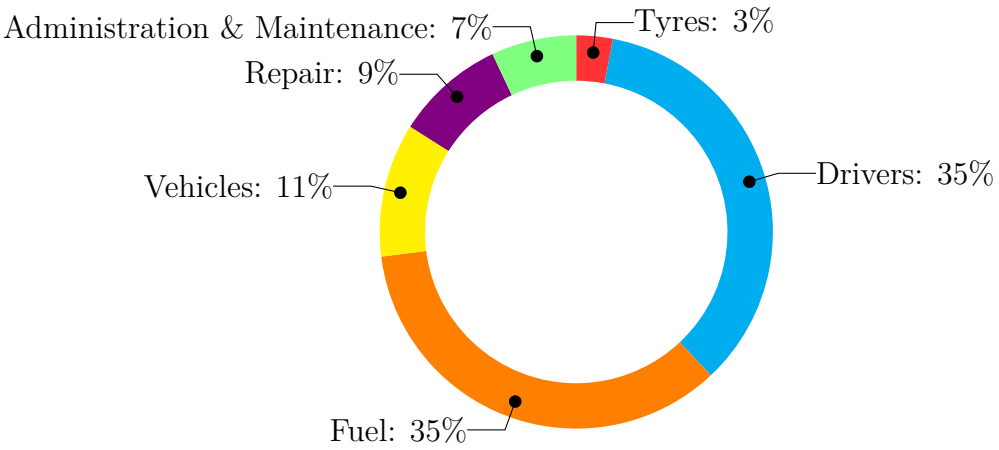

Figure 1.3 – Costumer operating costs for a European long haulage [1].

Environment

Fuel consumption is the number one factor for costumers buying a truck today [26] and together with driver's earnings they correspond up to 70% of the operating costs of a truck fleet owner as in Figure 1.3, with equal portion respectively. This motivates the research and development of improved platooning technology to reduce costs from both fuel and operator perspective, such as the adoption of platooning systems in their fleet. Furthermore, even though global initiatives such as the European Commission's Green Deal are stimulating the transition to a sustainable low-carbon economy, the transport sector is still one of the world's largest energy consuming sectors, responsible for around one-fifth (24%) of global carbon dioxide CO_2 emissions from fuel combustion [27]. More precisely, 74.5% of transport emissions come from *road* vehicles where truck carrying freight accounts for 29.4% and passenger vehicles (car and buses) contributes to 45.1%.

Despite many efforts towards sustainable transport solutions, by 2030 it is expected an increase of 8.2% of heavy trucks $CO2$ emissions in the Sustainable Development Scenario $2000 - 2030$ with respect to 2018 as reported in [28]. The unstoppable pace of economic growth and increase of demand goods are closely related to more trucking activity. Another main reason is that fuel economy standards for Heavy-Duty Vehicles (HDVs) are far behind Light-Duty Vehicles (LDVs) standards for many years. However, substantial progress by the public sector has been made, recently, towards vehicle efficiency and $CO2$ emissions standards for HDVs. Initiatives by European Union, India, and China have been introduced aiming to expand regulation to improve the efficiency of their HDV fleets.

1.2 Main contributions

This thesis addresses the problem of the joint design of the mobile communication system and the control scheme for enabling vehicle platooning applications. More precisely, we aim to design robust platooning systems in terms of an extremely low probability of emergency braking under arduous communication conditions, including bursts of packet losses. In other words, we assume that below certain inter-vehicular distance an Advanced Emergency Braking System (AEBS) is responsible to address the cases of abrupt changes due to emergency situations. Moreover, we propose a novel model for the channel access with the presence of relaying links through V2V and Roadside Unit (RSU) which aims to extend the coverage range of the platoon leader message. Lastly, we tackle the fuel consumption efficiency problem of two different control strategies for platoons. In this framework, we adopt Deep Reinforcement Learning (DRL) techniques to overcome the unpredicted platoon disturbances, and to learn appropriate transient shift times while minimizing the fuel consumption. The following are the main contributions of this thesis:

1. **Proposition of a new adaptive control scheme based on the offline optimization and online adaptation of the control gains according to the communication link qualities:**
   We design a dynamic control mechanism where some parameters of the evaluated controller are adapted based on information about V2V communication. In particular, we adapt the parameter that is responsible to weigh the influence of the leader's broadcasted messages in the control algorithm, as well as the target distance between vehicles, based on the communication links qualities. We evaluate the new approach in a highway scenario and show the improvements obtained by the dynamic adaptation of the control parameters over static control strategies.

2. **Development of a simulation platoon environment with Simulink and MATLAB:**
   We developed a simulation tool responsible to model platooning system environments with the control and communications interactions. The primary objective is to integrate all the necessary systems in one simulation environment and to ease the comparison of different platooning experiments. Therefore, we used Simulink and MATLAB WLAN Toolbox to model the mobility behavior of vehicles and the communication framework, respectively.

3. **Study of the impact of relaying on platooning performance:**
   In this contribution, we investigate the problem of the joint design of the

mobile communication system and the control scheme for relay-assisted platooning applications. We propose analytical models of a novel V2V relaying scheme, in addition to a study of the impact of RSU relaying. Moreover, extended performance analysis is presented, such as the impact of the platoon size and the RSU density. We demonstrate via simulations the benefit of the proposed relaying scheme, and that a joint design of application and communication systems is essential for enabling the integration of industrial applications in future generation networks.

4. **Fuel consumption improvement with classical control and deep reinforcement learning approach:**
   We aim at optimizing the fuel consumption by adopting two different control strategies while remaining within a safe and efficient platooning distance. More precisely, we exploit features for each of the controllers in order to improve fuel efficiency in platooning. We propose one enhanced controller responsible to mitigate undesired transient responses. Therefore, we first propose the optimal switching control logic for deterministic disturbance. Then, we include randomness in such disturbance and adopt Deep Reinforcement Learning (DRL) to determine the most appropriate action in terms of fuel efficiency and safety.

1.3 Thesis overview and Organization

In this section, we provide an overview of the thesis, which is structured into six chapters. In addition to the general introduction and motivations exhibited in Chapter 1, we introduce the main technology aspects related to communication and control field that allow platooning configuration as presented in Chapter 2. We aim to provide sufficient common information adopted along this thesis to facilitate the understanding flow before introducing the main contributions of each subsequent chapters. Then, the main results of the thesis are presented, which are exposed successively in Chapters 3-5. Figure 1.4 shows the thesis organization in a block diagram representation.

Chapter 3 presents the first contribution of the thesis, in which important communication and control aspects of platooning systems are addressed. It starts by introducing the related work for the control, communication and their joint framework. Then, the general simulation system is presented, followed by the proposed dynamic control scheme with the corresponding algorithm. Moreover, in addition to the propagation model, interference, and path-loss model for a platoon scenario, long bursts of packet losses are also considered. Finally, an evaluation of the concept of adapting the control of the platoon based on the V2V

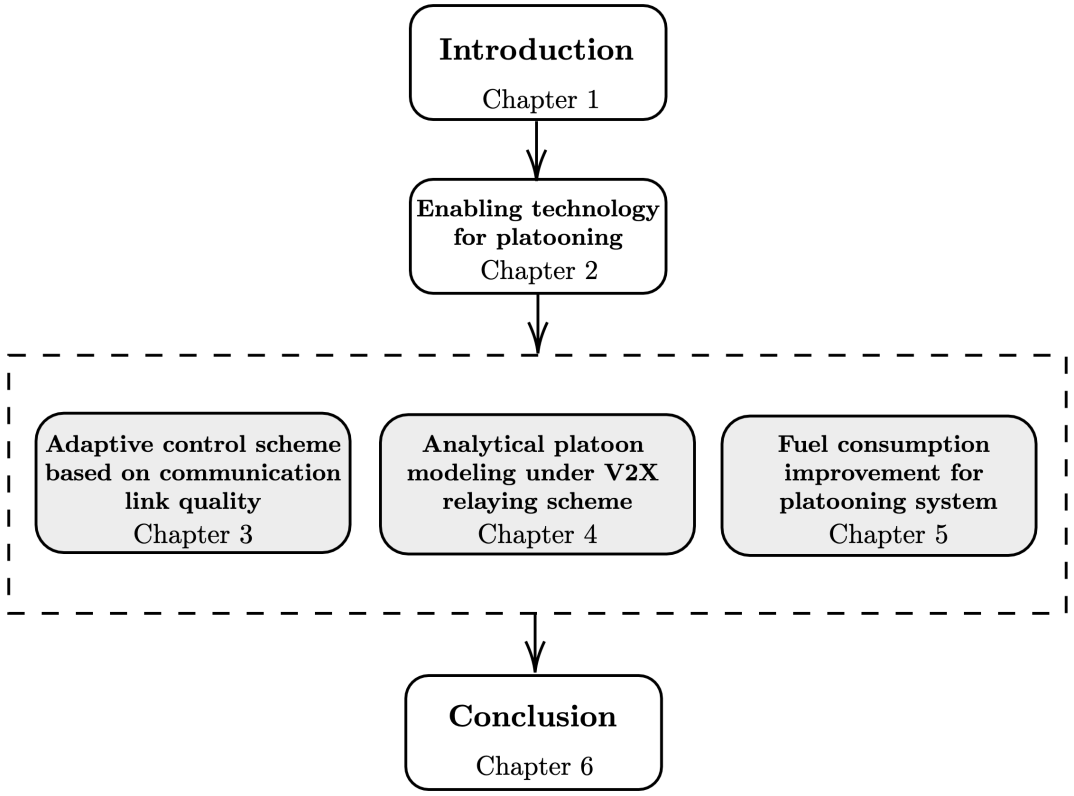

Figure 1.4 – Manuscript organization.

communication link under long bursts is carried out throughout this chapter.

At this point, we are able to conclude that the performance of the platooning system relies mostly on the quality of the communication V2V link. More precisely, in the quality status of the broadcast link of the platoon leader as its information is crucial for its followers to be able to properly apply the control action. In order to extend the coverage range of the leader message, we introduce in Chapter 4, relaying systems. Therefore, we adopt in this chapter relaying through V2V and RSU as solutions for the broadcast link, when the relaying vehicles in the platoon and RSU relay the packet received from the leader, in a broadcast manner to all other vehicles. Different from the previous chapter, this one consider more sophisticated radio link and system models in the presence of RSU relaying under unlicensed spectrum. Moreover, we propose a V2V relaying scheme which requires no extra infrastructure. Finally, we demonstrate via simulations the benefit of the proposed relaying scheme, and that a joint design of application and communication systems is essential for enabling the integration of industrial applications in future generation networks.

Once in a platoon formation, each vehicle benefits, in different levels, from the air-drag resistance reduction due to reducing the pressure on the front of the follower vehicle. Chapter 5 is dedicated to investigate the performance of the platoon in terms of fuel consumption and safety. It aims at optimizing the fuel consumption by adopting two different controllers. The chapter starts by modelling the platoon while considering external forces such as aerodynamics drag, rolling resistance and gravitation forces which were not treated in the previous chapters. Then, it introduces the optimal switch control for deterministic disturbances, whereas deep reinforcement learning techniques are used to achieve sub-optimal switch control outputs while under stochastic disturbances.

Finally, Chapter 6 includes considerations for future work and concludes the thesis.

1.4 List of publications

Conferences papers

- 1) T. R. Gonçalves, V. S. Varma, and S. E. Elayoubi, "**Vehicle platooning schemes considering V2V communications: a joint communication/control approach**," in *Proc. IEEE Wireless Communications and Networking Conf.* (WCNC), 2020, pp. 16.
- 2) T. R. Gonçalves, V. S. Varma, and S. E. Elayoubi, "**Performance and design of robust platoons under different communication technologies**," in *Proc. IEEE Vehicle Technology Conference 2021-Spring* (VTC), 2021, pp. 17.
- 3) T. R. Gonçalves, V. S. Varma, and S. E. Elayoubi, "**Performance of vehicle platooning under different V2X relaying methods**," in *Proc. IEEE International Symposium on Personal, Indoor and Mobile Radio Communications 2021* (PIMRC), 2021, pp. 16.

Journal papers

- 1) T. R. Gonçalves, V. S. Varma, and S. E. Elayoubi, "**Relay-assisted platooning in wireless networks: a joint communication and control approach**," submitted.
- 2) T. R. Gonçalves, R. F. Cunha, V. S. Varma, S. E. Elayoubi, and M. Cao, "**Fuel efficiency improvements for platooning systems with deep reinforcement learning approach**," submitted.

Chapter 2

Enabling technologies for platooning

This chapter describes the technologies required for the deployment of platoons, we focus on two main aspects: vehicular communication technologies and control systems for platooning. The interplay of both mechanisms is vital for platooning applications, but before addressing their complex interaction, we introduce their characteristics separately. We start by providing the main aspects related to wireless vehicular communication technology. Then, we introduce the vehicle dynamics, and the different vehicle controllers adopted along the thesis. Finally, past and ongoing projects of real platooning systems experiments are briefly described.

2.1 Vehicular Communication Technologies

We are currently experiencing unprecedented developments in the field of wireless communications. While a huge step towards mobile internet access and messaging to support consumer demands has been done, as today roughly 67% of the world population has a unique mobile [29], modest progress has been made in vehicular communications systems towards safety and non-safety applications. In fact, there are many challenges that start from tight communication and control requirements up to different legal frequency bands in some countries and regulatory barriers for the deployment of certain applications. The objective of such communication technologies are to increase driver safety and comfort, and to improve road efficiency. Note that such technologies are key to the deployment of vehicular safety and non-safety applications of Cooperative Intelligent Transportation Systems (C-ITS). Therefore, we aim to introduce one relevant radio access technology that enables Vehicle-to-Everything (V2X) communications known as Intelligent Transportation System (ITS)-G5 protocol developed by the European

Telecommunications Standards Institute (ETSI). In the United States, the same technology is referred to as Dedicated Short Range Communications (DSRC) standard proposed by the Federal Communication Commission (FCC). Other access technologies, such as the competing alternative which exploits the existing cellular infrastructure, named Cellular V2X (C-V2X), are not excluded, however are out of the scope of this thesis.

2.1.1 ITS-G5 protocol

The first decisive technology covered in this thesis is wireless communication vehicular technology. In fact, earlier version of automated vehicles did not include vehicular communication capabilities, and, therefore, they were limited to perceive its own surrounding to take decisions. Such vehicles are known as "autonomous" since they do not depend on wireless communication or even on cooperation among other vehicles to accomplish their task. In this case, all significant information is obtained through on-board sensors such as radar, camera or LiDARs placed in front, rear or on top of the vehicles. However, the performance limitation is evident, as such vehicles are limited to what their sensors can witness, i.e. Line-of-Sight (LOS), just like the human drivers as well. To significantly leverage its performance, vehicular communication technology is one appealing solution as it solves the LOS limitation through wireless exchange of information. The ITS-G5 defines two types of messages [30]: Cooperative Awareness Messages (CAM) that are periodically broadcast messages (or beaconing) that allow vehicles to coordinate their behavior even in complex traffic situations, and Decentralized Environmental Notification Message (DENM) that are event-triggered messages warning of a potential hazard. Such sophisticated approaches open room for innumerable C-ITS services such as: cooperative, sensing and awareness driving, however, in this thesis, we particularly focus on CAM messages for cooperation of platooning vehicles. Moreover, in order for such wireless technology to be reliable, communication latency and packet dropouts must achieve certain requirements. Otherwise, the application layer (control parameters) will fail to properly react under severe circumstances. So, a suitable understanding of the wireless vehicular protocol is fundamental to comprehend the synergy between communication and control aspects, introduced in the next chapter.

Among several vehicular communication protocols, we adopt, in this thesis, the Intelligent Transportation System (ITS)-G5 (which G5 stands for the 5 GHz frequency band) protocol, which is a medium/short wireless technology that allows vehicles to communicate with road users directly, without involving a cellular licensed carrier. This technology relies on an adaptation version of the IEEE 802.11 standard to allow dynamic vehicular application, and it uses the special allocated 5.9 GHz unlicensed band, which has been reserved in many countries for ITS ap-

plications. Before moving to technical definitions, we would like to introduce the main motivations behind creating a specific Wireless Local Area Network (WLAN) for vehicular application, commonly specified as Wireless Access in Vehicular Environments (WAVE).

First, notice that the IEEE 802.11 standard was initially released to meet wireless applications specifications with higher data rate and lower mobility, therefore, it is natural that new requirements would demand some adaptations. Moreover, the IEEE 802.11 standard includes very long authentication and association processes, which would be inappropriate for vehicular communication applications. Which call for a need of a faster message transmission in an ad-hoc manner. Second, many safety and non-safety applications rely on the support for long ranges operation up to 1 km, while the regular IEEE 802.11 range is about 20 to 90 meters depending on the standard version. Third, very high relative speeds of vehicles imposes a substantial challenge, as well as the extreme multi-path environment which causes reflections with long delays. Because of the multi-path reflections many different messages, that travel to distinct paths, arrive at the receiver slightly delayed which when all combined causes the delay spread.

In this context, researchers proposed the IEEE 802.11p protocol, which is an ad-hoc adjustment of the IEEE 802.11 to provide Wireless Access in Vehicular Environments (WAVE) with essential modifications in both physical (PHY) and medium access control (MAC) layers. In fact, in order to cope with the rapidly varying vehicular channels, the time domain parameters have been doubled, which translates to halve the frequency domain parameters, as shown in Table 2.1. The main reason for decreasing the bandwidth to 10MHz in 802.11p instead of 20MHz adopted by 802.11a devices is to mitigate the effect of delay spread in vehicular environments [31]. Moreover, this table highlights the main PHY layer parameters difference concerning the channel bandwidth. Concisely, one can describe that IEEE 802.11p reuses: the Orthogonal Frequency Division Multiplexing (OFDM) modulation of the IEEE 802.11a PHY layer, and the Enhanced Distributed Channel Access (EDCA) mechanism of the IEEE 802.11e MAC layer.

Note that in the literature, there is no clear consensus about the several terms such as IEEE 802.11p, DSRC, ITS-G5, and IEEE WAVE as all of them are often used arbitrarily. Even though, they are all related to wireless communication technology used for vehicular environments, we attempt to briefly delimit their main differences here. First, IEEE 802.11p is the standard that defined PHY and MAC layer, as they can be seen as the basis of the communication architecture. IEEE WAVE is a special stack of standards that comprises the IEEE 1609.x, which defines the Network and Transport layers for V2X communication, and the IEEE 802.11p standard. DSRC is the name of the 5.9 GHz band allocated for the ITS communication, and a DSRC device uses IEEE 802.11p, and WAVE standards.

Table 2.1 – Differences in PHY parameters between IEEE 802.11a and IEEE 802.11p (source [3]).

Parameters	**IEEE 802.11a**	**IEEE 802.11p**	**Changes**
Bitrate Mb/s	6, 9, 12, 18 36, 48, 54	3, 4.5, 6, 9 12, 18, 24, 27	Halved
Modulation type	BPSK,QPSK 16 QAM, 64 QAM	BPSK,QPSK 16 QAM, 64 QAM	No change
Code rate	1/2, 1/3, 1/4	1/2, 1/3, 1/4	No change
Number of subcarriers	52	52	No change
Symbol duration	4 μs	8 μs	Doubled
Guard time	0.8 μs	1.6 μs	Doubled
FFT Period	3.2 μs	6.4 μs	Doubled
Preamble Duration	16 μs	32 μs	Doubled
Subcarrier frequency spacing	312.5 kHz	156.25 kHz	Halved

Finally, ITS-G5 it also makes use of the IEEE 802.11p PHY layer, but it defines slightly different algorithms for medium access [32]. However, the full description of the abovementioned acronyms and their disparities are out of the scope of the present work. The reader is referred to [31–34] for additional detailed discussion.

EDCA and backoff procedure

Different levels of priority on vehicular environment is crucial in order to cope with distinct safety and non-safety applications. As, for instance, a collision risk warning message must have preference over traffic condition warning messages. Such feature is possible thanks to the medium access (MAC) layer that is responsible to address some of the wireless events that might happen and control the medium access of the node (vehicle) in order to reduce the number of collisions. Therefore, the contention based channel access method called Enhanced Distributed Channel Access (EDCA), which was first proposed in the IEEE 802.11e, is considered as the mandatory mode for Medium Access Control (MAC) in IEEE 802.11p. The EDCA mechanism defines four Access Categories (ACs) that provides different level of priorities as shown in Table 2.2. Therefore, the main advantage is the introduction of Quality of Service (QoS) support, which allows critical safety-messages to have higher priority and thus, a high chance of accessing the medium earlier due to shorter Arbitrary Inter Frame Space (AIFSN) and Contention Window (CW) values, as explained next.

One particular challenge is the multiple access feature of such protocol, which is aggravated by the vehicles' high mobility. Imagine rapid and important conversations between a lot of people that must understand each in order to avoid chaos.

Table 2.2 – EDCA parameters in IEEE 802.11p (source [4]).

Access Categories index	**AIFSN** [slots]	$\mathbf{CW}_{min}$ [slots]	$\mathbf{CW}_{max}$ [slots]
0 (lowest priority)	6	7	15
1	9	15	1023
2	3	3	7
3 (highest priority)	2	3	7

In addition, to that, all of them moves fast which makes their coordination even more complex. One practical solution is to make everybody quiet, while someone is talking. On top of that, there is a need for fast and efficient communication guidelines, in case of two people talk at the same time. This example illustrates the vehicular communication challenges and solutions proposed by the vehicular protocol. In fact, the IEEE 802.11p standard adopts the carrier sense multiple access with collision avoidance (CSMA/CA) with exponential backoff mechanism to control packet access to the medium. The vehicles are obliged to follow the Listen Before Talk (LBT) mechanism. This means that, before sending a packet, the transmitter has to sense the medium. If the medium is busy, it backs off for some interval calculated as a uniformly random number of slot times selected from [0,CW(AC)], which is a function of the access category (AC), as shown in Table 2.2. Each time slot, the transmitter decrements the timer if the channel is idle, until the timer reaches 0, the packet is then transmitted. If the packet is lost (no ACK), the same mechanism is repeated for a maximum of 7 stages [35].

2.2 Control aspects for platooning

After introducing the main radio communication technology commonly used to the deployment of platoons, we now focus on the longitudinal automation aspects of it. In fact, early prototypes of automated vehicular systems did not present any communication technologies. Nevertheless, a basic control mechanism responsible for adjusting the vehicle's parameters was necessary for early platoon formation. To ease the implementation and the mobility analysis of platooning, we adopt a similar approach of the two-layered control schemes from the California PATH [36] project.

Figure 2.1 illustrates the control loop block diagram of the system framework adopted along this thesis. It relies on the complex interplay among both on-board sensing and V2V communications signals, as depicted in blue and red, respectively. In particular, the upper controller is responsible to compute the desired acceleration for each vehicle, based on relative position and velocity from the preceding

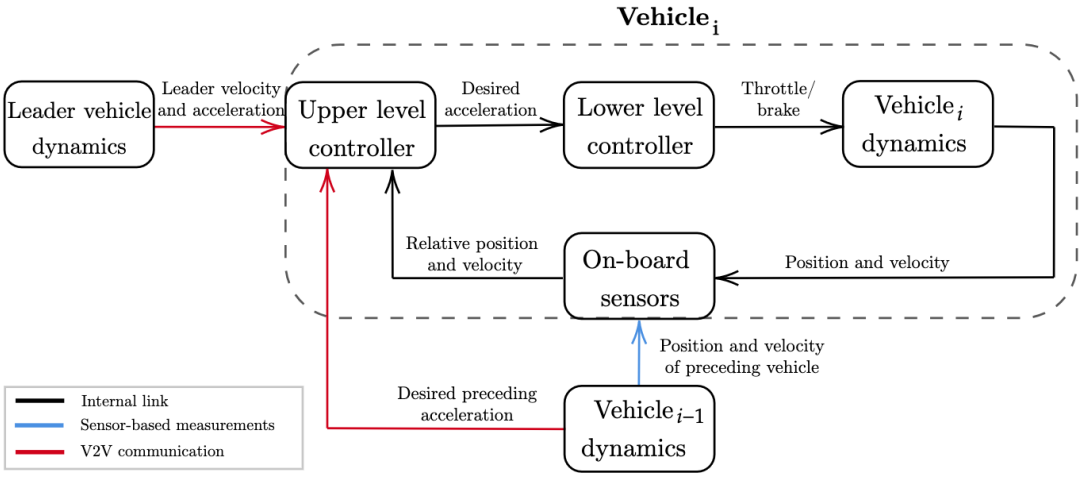

Figure 2.1 – Closed loop block diagram of the control system framework.

vehicle, obtained through radar, camera or LiDAR communication, and the desired acceleration from the leader and the preceding vehicle, achieved by V2V communication. On the other hand, the lower level controller determines the throttle and brake commands that are required to follow the desired acceleration from the upper controller. However, as detailed next, in this work we adopt a simplified approach of the systems' dynamics, which removes the lower level controller out of the control loop.

2.2.1 Vehicle dynamics

It is known that vehicle dynamics present nonlinear features due to wind drag, engine, gearbox, brake dynamics, etc. The inclusion of all the above characteristics in the control system framework would considerably increase its complexity, in addition to the challenges already imposed by the communication framework. Therefore, in this thesis, we embrace a common approach used in the literature that consists to eliminate the analysis of the lower level controller by simplifying the vehicle's dynamics. In other words, instead of considering complex driveline and engine dynamics that require throttle and brake signals as input, we assume the vehicle can be directly controlled by the acceleration signal. Therefore, we focus on the upper controller, so the vehicle dynamics are modeled as a first-order low pass filter due to the actuator lag, which has been widely adopted in the

literature [37–41] in the continuous-time dynamics as:

$$\dot{x}_i(t) = v_i(t) \tag{2.1}$$

$$\dot{v}_i(t) = a_i(t) \tag{2.2}$$

$$\dot{a}_i(t) = -\frac{1}{\tau}a_i(t) + \frac{1}{\tau}u_i(t) \tag{2.3}$$

with x_i, $\dot{x}_i = v_i$, and $\ddot{x}_i = a_i$ being the longitudinal position, velocity and acceleration of vehicle i, respectively. The subscript i is the vehicle platoon member index where $i \in \{1, \cdots, N-1\}$ for a platoon size of N vehicles, and 0 is the platoon leader's index. u_i is the control input of vehicle i, i.e., its desired acceleration. τ is the time constant of the first-order low pass filter. In other words, such parameter can be interpreted as the retarded behavior of the vehicle when performing the desired acceleration of the upper level controller. The idea is to approximate the dynamics of the vehicle in order to avoid instantaneous response. Furthermore, control input constrains were applied to avoid signals of little practical relevance

$$u_{min} \leq u_i(k) \leq u_{max} \tag{2.4}$$

where u_{min} and u_{max} are the minimum and maximum acceleration signal admitted that compass the control signal. Before introducing the control schemes, we present the two main control specifications that platooning vehicles are likely to satisfy. Then, we present the two main spacing policies that are also considered along this work.

- **Individual vehicle stability:** The main objective of a platoon control is to force all tracking errors to zero when no disturbance is applied, i.e. in constant speed. The vehicle is said to maintain individual vehicle stability if the spacing error is set to zero at constant speed, as in under transient time (accelerating or decelerating) nonzero error is expected. Therefore, the spacing error for the ith vehicle is described as:

  $$\epsilon_i = x_i - x_{i-1} + L_i + D_{des} \tag{2.5}$$

  where x_i is the position of vehicle i, L_i is the length of vehicle i, and D_{des} is the desired inter-vehicle distance to be set. Furthermore, a particular control law provides individual vehicle stability if

  $$\ddot{x}_i \to 0 \Rightarrow \epsilon_i \to 0 \tag{2.6}$$

  which means that once there is no disturbance in the acceleration of the preceding vehicle ($\ddot{x}_i = 0$), the spacing error of the designated vehicle converges to zero ($\epsilon_i = 0$). Moreover, in respect the spacing error policy and the definition of D_{des}, there are two main categories addressed in this thesis:

a) Constant spacing policy: In this particular case, the desired spacing between preceding vehicles is a simple constant, e.g. $D_{des} = 10$ m. The particular advantage is that with this policy, such constant is explicitly one of the control input parameters that can be designed for a particular purpose no matter the vehicle's velocity, which will be further investigated. For instance, note that smaller inter-vehicle distance in platoons benefits from better traffic flow, less congestion and higher fuel efficiency. Therefore, this policy is surprisingly appealing, as it leads to the highest road traffic efficiency and fuel savings.

b) Constant time-gap (CTG) spacing policy: In such a policy, the inter-vehicle distance between the vehicles is a linear function of the vehicle's velocity, or of the relative velocity [42], or even of road conditions and vehicle dynamics [43]. In this thesis, we assume the simpler case, in which the desired inter-vehicle under CTG policy is defined as:

$$D_{des} = d_{ss} + h\dot{x}_i \tag{2.7}$$

where d_{ss} is a constant term that establishes a nonzero spacing gap, in meters, between vehicles when at standstill, and h is the time-gap or time headway which is a constant, in seconds, greater than 1 s (meaning at least a distance of 28 m is required at 100 km/h). Note that under this policy, it is not possible to fix the inter-vehicle distance between the platoons and to profit utmost from the air-drag reduction, because of the dependency on the velocity. On the other hand, such policy ensures both individual vehicle stability and string stability as described next.

- **String stability:** While the individual vehicle stability focus on a singular vehicle, the string stability refers to the stability of an association of successive vehicles like a platoon. Indeed, there are many interpretations of string stability in the literature. Here, it implies that any acceleration or braking in the first vehicle is not going to cause an amplification of the error along the tail of the platoon. In other words, as long as the first vehicle is able to avoid a collision all others will be able too. More information about mathematical definitions and conditions to ensure the string stability can be found in [41, 44], but are out of the scope of this thesis.

In order to enable vehicular platooning, a sophisticated control system is required to cope with external disturbances on the road and traffic status. Before describing advanced control scheme that relies on cooperation strategy to exchange information, we start by describing the fundamental ones.

2.2.2 Cruise Control (CC)

Among some of the control technologies that were deployed to help the drivers safety and increase their driving experience, one can cite the Cruise Control (CC) as precursor of the autonomous cars. The main idea of CC is to control the velocity of the equipped car in a reference (also known as cruise speed) set by the driver, regardless of any disturbance or change of the road traffic. Notice that such system does not rely on radar or camera to measure any distance or velocity from preceding vehicles. Therefore, it is up to the driver to take control of the vehicle, if any disturbance occurs, in order to ensure a safe journey.

2.2.3 Adaptive Cruise Control (ACC)

Even though, the previous controller presented some benefits, its limitation is evident due to the lack of systems measuring the environment. Therefore, by the inclusion of on-board sensors such as camera, radar or LiDAR that are responsible to introduce awareness of the surroundings, greater autonomous performance is expected. In this framework, the Adaptive Cruise Control (ACC) scheme emerged, as it autonomously allows the equipped vehicle to keep a certain desired distance apart from the preceding vehicle. This is possible because of the adoption of on-board sensors that measure in real-time the preceding vehicle's position and velocity. Different spacing policies can be used, such as Constant Spacing (CS) and Constant Time-Gap (CTG) policy, as previously mentioned. However, generally ACC system exploits CTG policies, as for autonomous systems it corresponds to a safer approach due to string stability properties [41]. In this thesis, when not mentioned otherwise, the ACC controller exploits the CTG policy introduced by Ioannou and Chien [45] as

$$\ddot{x}_{i\_des} = -\frac{1}{h}(\dot{\varepsilon}_i + \lambda\delta_i) \tag{2.8}$$

where

$$\varepsilon_i = x_i - x_{i-1} + L_{i-1} \tag{2.9}$$
$$\delta_i = \varepsilon_i + h\dot{x}_i + d_{ss} \tag{2.10}$$

are the inter-vehicle spacing and the spacing error, respectively. The index i symbolizes the vehicle index, the leader vehicle being numbered 0. x_i denotes the position of vehicle i, L_i its length and a_i its acceleration. h is the time-gap parameter, λ is the design gain parameter, and d_{ss} is the standstill distance. The control input is calculated based on the difference of its own velocity and position with the preceding vehicle, $(\dot{x}_i,\ x_i)$ and $(\dot{x}_{i-1}, x_{i-1})$ respectively. For the rest of

the thesis, in platooning systems, we assume that the ACC control law is always adopted by the leader, since it is preceded by a vehicle that is not subject to the platooning controller.

2.2.4 Cooperative Adaptive Cruise Control (CACC)

A more sophisticated approach based on a coordinated exchange of information supported by wireless communication, in addition to on-board systems, was early provided by Rajamani *et al.* [40] and it is known as Cooperative Adaptive Cruise Control (CACC). Therefore, CACC takes advantages of V2V communications, like aforementioned ITS-G5 communication technology, to allow cooperation and intelligent exchange of information such as acceleration, velocity and position, between vehicles within a range. The breakthrough of such approach when compared to its ancestors is that it allows, for the first time, a large scale of distributed vehicles with small inter-vehicle distances, working in a cooperative manner to avoid collisions.

Different longitudinal controllers have been studied in the literature to address different subjects, along this thesis when not stated otherwise, we consider the CACC controller based on the sliding-surface CACC controller introduced by Rajamani *et al.* [40] as:

$$\begin{aligned}\ddot{x}_i = &(1-C)\ddot{x}_{(i-1)} + C\ddot{x}_0 \\ &- (\xi + \sqrt{\xi^2-1})\omega_n C(\dot{x}_i - \dot{x}_0) \\ &- (2\xi - C(\xi + \sqrt{\xi^2-1}))\omega_n \dot{\epsilon}_i - \omega_n^2 \epsilon_i \end{aligned} \tag{2.11}$$

where the spacing error (ϵ_i) is defined by (2.5) and, its derivative by $\dot{\epsilon}_i = \dot{x}_i - \dot{x}_{i-1}$, respectively. L_i is the length of the vehicle and D_{des} is the desired inter-vehicle distance that we want to minimize. The control parameters to be tuned are C, ξ and ω_n. The parameter C takes on values $0 \leq C < 1$ and is responsible to weigh the contribution of the leader's speed and acceleration. ξ is the controller damping ratio and ω_n is the controller bandwidth.

Taking into account the adopted controllers in this thesis, we highlight two main differences from the ACC controller previously introduced. First, the spacing error policies are entirely different. While ACC holds a constant-time gap policy defined in (2.10), CACC controller adopts a constant spacing policy, as can be seen in the spacing error defined in (2.5). Second, in addition to information that are provided by radars, cameras and LIDARs such as relative velocity and position, CACC controller requires acceleration signals from the preceding vehicle ($\ddot{x}_{(i-1)}$) and the leader vehicle ($\ddot{x}_0$) as seen in the first line of (2.11). Both aspects constitute the rationale behind which CACC controllers are considered the favorite choice over ACC for the deployment of cooperative platooning. Indeed, in platooning, we seek

to minimize the inter-vehicle distance to profit the most of the air-drag reduction while keeping safe and robust performance, which can not be done without wireless communication systems.

However, CACC technology has its drawbacks as it relies on the link quality of others vehicle information, which makes it vulnerable to inherent communication aspects such as packet loss and latency. In addition to wireless aspects, the CACC presents another disadvantage, which is related to the presence of the actuator lag effect in the control loop. A better explanation is given next, followed by a case comparison.

2.2.5 Predictive Cooperative Adaptive Cruise Control

Aiming at improvements, researchers introduced the PCACC controller [46], later called "modified CACC" [47]. In this framework, the PCACC control law requires the **desired** control effort, or the desired acceleration, of the leader and of the preceding vehicle and its control law is given by

$$\begin{aligned} u_i(t) = \ddot{x}_{i\_des} = (1-C)\ddot{x}_{(i-1)\_\mathbf{des}} + C\ddot{x}_{0\_\mathbf{des}} \\ - (2\xi - C(\xi + \sqrt{\xi^2-1}))\omega_n\dot{\epsilon}_i \\ - (\xi + \sqrt{\xi^2-1})\omega_n C(\dot{x}_i - \dot{x}_0) - \omega_n^2\epsilon_i \end{aligned} \tag{2.12}$$

The terms with subscript "des" in bold are introduced to highlight its fundamental difference with CACC control (2.11) as explained next. While the CACC control sends the actual acceleration, which is measured after the actuation lag, the PCACC is able to propagate the actual values that will become effective after the actuation lag. Therefore, PCACC is expected to be superior to CACC because the actuation lag of the system does not affect directly the control effort, which is a big limiting factor for achieving short inter-vehicle distances [46].

Along this thesis, the term PCACC is also referred as fully predictive cooperative control to avoid repetition. The main improvement of such control is due to the fact that it allows the communication between all the vehicles in the platoon including the leader while eliminating the actuation lag out of the control loop, as shown in Fig. 2.2. It also illustrates the input signals required by the PCACC controller and the respective segments V2V radio, vehicle dynamics, and radar equipment that provide them. Focus on vehicle i, the V2V radio component is responsible to receive the desired acceleration and velocity signal of the leader ($\ddot{x}_{0\_des}$,$\dot{x}_0$) and acceleration of preceding vehicle ($\ddot{x}_{(i-1)\_des}$) and to transmit its own desired acceleration ($\ddot{x}_{i\_des}$) backwards over a wireless channel. Note that in the case of ACC/CC controllers, such unit is not presented due to the lack of V2V communication requirement. Second, the vehicle dynamics computes the vehicle

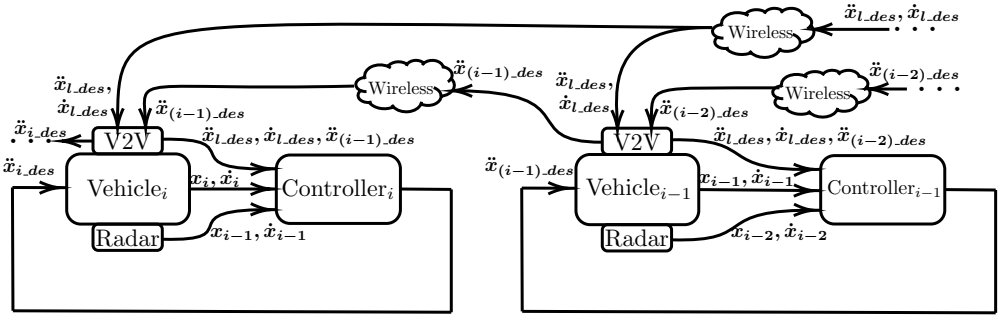

Figure 2.2 – Block diagram of the platoon system with a PCACC control between vehicle $i-1$ and vehicle i.

velocity and position $(\dot{x}_i, x_i)$ in the next time-step based on the desired acceleration $(\ddot{x}_{i\_des})$ value computed by the controller. Lastly, the radar module is in charge of measuring velocity and position of the preceding vehicle $(\dot{x}_{i-1}, x_{i-1})$.

2.2.6 Semi-Autonomous Control

This particular class of control is a light instance of the PCACC controller. In fact, it is named semi-autonomous because it still requires the acceleration information of the preceding vehicle, which has to be sent through some communication channel. The control strategy can be obtained with a simple change in one of the control parameters of the CACC control scheme, which is $C = 0$ that yields

$$u_i(t) = \ddot{x}_{i\_des} = \ddot{x}_{i-1} - 2\xi\omega_n\dot{\epsilon}_i - \omega_n^2\epsilon_i. \tag{2.13}$$

The control law is based on one vehicle look-ahead (or predecessor-follower) communication topology, which means that only preceding vehicle's information is required. In this case, its acceleration, velocity, and position $(\ddot{x}_{i-1}, \dot{x}_{i-1}, x_{i-1})$ are necessary, but without any information from the leader. As proven in [48], this particular control law is only string stable when the control of the preceding vehicle is immediately accessible, which means when there is no delay in the process.

Control schemes comparison

As above mentioned, each control scheme has its advantages by extending some features of earlier variants, but also drawbacks which are, in general, related to its practical deployment, as for instance undesired wireless effects. Figure 2.3 illustrates the impact on the platoon performance, in terms of inter-vehicle distance,

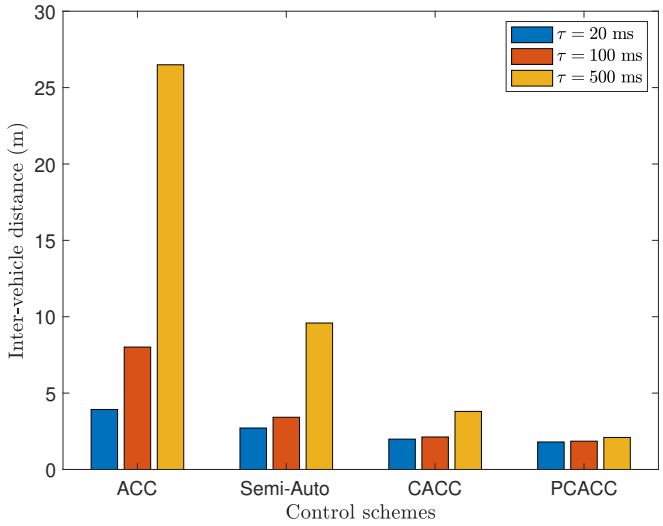

Figure 2.3 – Impact of actuator lag τ in the platoon performance for different control schemes under an average velocity of the leader of $18m/s$.

produced by the different aforementioned control schemes. The inter-vehicle distance is averaged over all pairs of consecutive platoon members and over time. The homogeneous platoon size was chosen to be $N = 11$ vehicles and the assumed message broadcast rate is 10 Hz, when applicable. Furthermore, the weight of the leader message is set to $C = 0.5$ for CACC and PCACC controller for seek of comparison. We used the MATLAB/Simulink environment to model the vehicle dynamics and to implement the control law. Whereas the WLAN Toolbox of MATLAB was used to implement the channel configuration for a 802.11p transmission, when applicable. We further discuss simulation aspects in the next chapters.

The impact of the actuator lag largely influences the platoon performance when the ACC controller is considered. Because the ACC adopts a constant time gap policy that is bounded by the actuator lag, more precisely $h \geq 2\tau$, in order to maintain string stability as proved by Swaroop [49]. Therefore, once the time-gap is lowered, the platoon achieves shorter inter-vehicle distances, and therefore, the lag plays a big role. The second largest impact can be observed for Semi-Autonomous and CACC approaches. In this case, a constant spacing policy is adopted, and the actuator lag plays an important aspect as large lags demand higher inter-vehicle distances.

Finally, as presented, the PCACC is the least sensitive to the change of the actuator lag. In fact, the platoon performance is roughly the same despite the variation of the actuator lag of a factor of 25 times. The reason, as mentioned

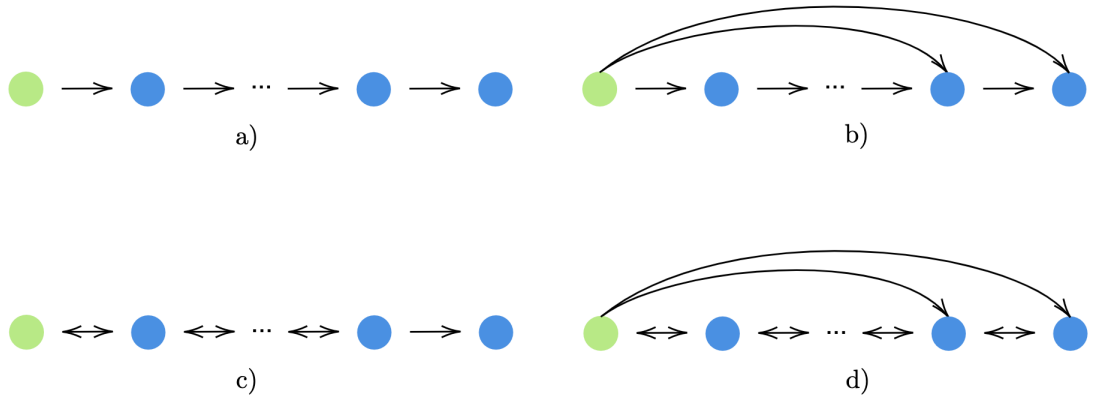

Figure 2.4 – Typical information flow topology of platooning systems. The vehicle in green is the leader, while the blue ones are the platoon members.

before, is that by considering the desired (instead of the instantaneous) acceleration of the leader and of the preceding vehicle, the actuation lag is removed from the control loop. Therefore, from this control schemes comparison, we can conclude that the PCACC is the best option as it is the less sensitive to the actuator lag, and it achieves shorter inter-vehicle distances among all. For such reasons, the PCACC controller is the one adopted in the subsequent chapters of this thesis.

2.3 Information flow topology

This section aims to define typical information flow topologies adopted on platooning systems, and to specify the one explored in this thesis. Based on the class of controllers and the wireless communication technologies, different information flow topologies are possible. As for instance, ACC controller relies on-board sensors it is limited to predecessor-following (PF) or bidirectional (BD) as shown in Figure 2.4a and Figure 2.4c, respectively. Whereas CACC controller, with the assistance of ITS-G5 communication technologies for instance, allows more alternatives since the leader information can be exploited by all platoon members. Two examples are shown in Figure 2.4b and 2.4d for the predecessor-following-leader (PFL) and bidirectional-leader (BDL) topologies, respectively. However, as we have mentioned before, many different combination from the above topologies can be adopted, and the reader is refereed to [50] for further discussions. In this thesis, we have adopted the schemes shown in Figure 2.4a and Figure 2.4b, for the ACC and CACC, respectively. The reason is that both controllers do not rely on successor information in order to compute the control law as seen in (2.8-2.13), i.e. there is no term with subscript $i+1$. As most human drivers do not require

information about following vehicles to control their own vehicle, so no bidirectional flow seems to be useful, which is in accordance with [51] that showed that bidirectional topology suffers fundamental limitations on string stability. However, the particular PFL topology for CACC is subjected to scalability issue due to the importance of the reliability of the leader communication message. We address such particular problem in Chapter 4.

2.4 Platooning research projects

In accordance with the significant increase of platooning related studies illustrated in Figure 1.1, a meaningful number of platooning research projects have been conducted in the world and the main relevant ones are described next. More detailed explanation regarding the technologies used, the number of vehicles, and achievements can be found in [52–60].

- **California PATH**
  The California Partners for Advanced Transportation Technology (PATH) Program was founded in 1986 with an initial plan aiming to identify solutions to increase the highway lane capacity, reduce congestion, and reduce pollution through platooning concept. A few years later, the project developed useful solutions by using the longitudinal CACC controller in an eight automated-car platoon arrangement in a real demonstration scenario in 1997. Even though DSRC technology was not yet matured, the PATH program managed to demonstrate the potential benefits of platooning with functional automation and preliminary V2V communication [54]. The PATH project is considered the first one on LDV platooning. However, HDV experiments only took place in the early 2000s, just a few years later than the CHAUFFEUR project in Europe described next.

- **CHAUFFEUR I**
  The first studies on truck automation, was the European research program CHAUFFEUR I, established in 1996 [55]. CHAUFFEUR project focused on a Tow-Bar approach, which consists of connecting two vehicles in a platoon through wireless communication with an infrared camera while keeping safe inter-vehicle distances. The experiments concluded that about 21% of fuel consumption reduction is attained when driving at 80 km/h and a spacing of 10 m [56].

- **Energy ITS**
  It was a national ITS project by Japanese government from 2008-2012, aiming at energy efficiency and global warming prevention with ITS technologies.

The project successfully accomplished truck platooning formation with four trucks operating with inter-vehicle distance of 4.7 m at speed of 80 km/h. The project adopted the DSRC technology as the V2V communication aspects and indicated an 15% of average fuel saving for the aforementioned gap and speed scenario.

- **SARTRE**
  The aim of Safe Road Trains for the Environment (SARTRE) was to mitigate environmental impact and traffic congestion. The three-year European project was formally launched in 2009, and two trials took place in Sweden and Spain, at 2011 and 2012, respectively [57]. The last demonstration, took place in public highways which they successfully demonstrated a three-car platoon following a lead truck running at a speed of 90 km/h with a gap between the platoon members of around 6 m.

- **GCDC**
  Different from the previous trials on platooning, the Grand Cooperative Driving Challenge 2011 (GCDC) focused on a heterogeneous platoon. In other words, the GCDC 2011 team combined both heavy trucks and passenger vehicles as platoon members to perform cooperatively while keeping short inter-vehicle distances through V2V technology. They identified some issues to be addressed in future tests, but one raised particular attention: the capacity to deal with missing data from other vehicles [58]. Five years later GCDC 2016 took place which aimed to demonstrate more realistic scenarios such as cooperative merge of platooning systems and cooperative intersection management [59].

- **ENSEMBLE**
  In the framework of a more recent effort, the ENabling SafE Multi-Brand pLatooning for Europe (ENSEMBLE) program is co-funded by the European Union under the Horizon research and innovation program (2018-2021). It focuses on the coordination of multi-brand specifications towards on standardization, and demonstration of multi-brand operation ability [60]. ENSEMBLE defined two platooning levels which the first one is the platooning as support function which the driver still responsible for the journey. While, the second level corresponds the platooning as autonomous function which the driver is out of the loop.

2.5 Summary

In this chapter, we have introduced the main technologies aspects responsible to admit platooning technologies. We have covered them according to two different aspects. First, we covered the vehicular communication aspect, which we aim to focus on the essential characteristics of the IEEE 802.1p protocol endorsed to cope with vehicular environment. Second, we provided fundamental awareness of the main control aspects for platooning, including classical control laws performance comparison in a platoon environment. Finally, we finished the chapter with the main platooning projects over the last decades.

From the above, we are able to identify that a full development of both control and communication aspects must be considered in order to properly handle platooning systems. So, once we have covered the main aspects involving both fields that enable platooning formation individually, we introduce in the next chapter a joint network and control design approach in order to properly evaluate platooning problems. Therefore, it includes the first two main contributions of this thesis. First, we propose a dynamic control mechanism that adapts some of the control parameters based on the communication link quality of the platoon vehicles. Second, we introduce our platoon simulator environment which encompasses platoon mobility, control laws, and communication features. With such a tool, we aim to evaluate the platoon performance including key performance indicators from communication point of view such as packet error rate and control feature such as inter-vehicle distance of the platoon.

Chapter 3

Adaptive control scheme based on communication link quality

In the previous chapter, we confirmed that in order to properly investigate platooning systems, the joint network and control design is imperative. Therefore, this chapter addresses communication and control aspects of platooning systems, with the related challenges introduced by the overlap of both areas. The main objective is to provide a dynamic control mechanism where the parameters of the well-known Predicted Cooperative Adaptive Cruise Control (PCACC) are adapted based on the observed quality of the V2V (Vehicle-to-Vehicle) communication links. Different from the state of the art, our main design goal is the minimization of inter-vehicular distances while being robust in terms of an extremely low probability of emergency braking. A new adaptive control scheme based on the offline optimization of the control gains is proposed. We evaluate the new approach in a highway scenario and show the improvements obtained by the dynamic adaptation of the control parameters over static control strategies.

3.1 Introduction

The chapter starts by providing an overview of the related work relevant for such platooning proposition problem in both control and communication perspectives. Next, we introduce the proposed controller scheme, responsible to readjust two control inputs accordingly to the communication link quality. Then, we present an overview of the simulation tool aspects achieved in this thesis, and we discuss the performance evaluation over static control strategies. Finally, we conclude the chapter by providing a general evaluation of our results, then we state the limitations of our analysis, which motivates the following chapter.

Related work

This chapter investigates one approach to address the lack of communication guarantees in fully cooperative platoon control problems. This proposition is based on the integrated design of vehicular communications protocol jointly with vehicle control loop. This section aims to review the related literature from both control and communication perspectives. In this framework, a coordinated group of vehicles shares state information, via V2V communication, of its surroundings in order to improve road efficiency and, more importantly, to accommodate vehicular safety applications and avoid collisions.

From the communication perspective, vehicles broadcasts packets (or beaconing) to other vehicles, which might fail at the receiver side and alter the quality of the cooperative controller. Furthermore, a proper design of a V2V protocol that accurately models the vehicular wireless communication behavior is of utmost importance due to the particular constraints introduced by the mobile environment. Regarding the control context, researches have focused on cooperative controllers, such as PCACC and CACC, that exploits the wireless information exchange capability. In particular, each vehicle with this controller is able to follow its predecessor while maintaining a desired distance. Additional requirement such as the string stability, as introduced in Chapter 2, is often considered in this framework.

Control framework

In the early stages of such a multidisciplinary approach, we could observe an unbalanced contribution from both fields, which translates to unrealistic assumptions towards the opposite most relevant domain. For instance, the effort in the control community has been for years to tackle the string stability problem while poorly addressing some communication effects. In fact, Hedrick *et al.* [61] provided early analysis of the effects of the communication delays on string stability in platooning. In addition, Seiler and Sengupta [62] adopt a simple packet-loss model in their feedback longitudinal control loop, but their model does not include the effect of delayed packets and focuses on the rather naive set up of the look-ahead communication topology. The authors extend their work in [63] by adopting an erasure model for a network, which translates to the unrealistic scheme that all vehicles either lose or receive their packets. Likewise, Rajamani *et al.* [64] demonstrated the CACC controller under limited wireless radio communication conditions in the PATH project framework. The superior focus on control aspects is evident as the authors in [64] concentrated their efforts in the longitudinal and lateral control of platooning systems, while no networking impairments are carefully treated.

As of the conception of control schemes in the presence of degraded radio link quality, Ploeg *et al.* [65] proposed a control strategy for graceful degradation based

on estimating the preceding vehicle's acceleration in case of packet losses, but it mainly deals with extreme cases like complete link failure or lack of a wireless device on one of the vehicles. More recently, in [66] the authors adopted a Smith predictor to compensate for the vehicle actuator delay in a homogeneous semi-autonomous control system. However, the Smith predictor can not compensate for the network communication delay, and therefore its gain is very limited in the conducted framework. Fernandes and Nunes [25] suggested different information management algorithms, including one with a dynamical control parameter, where they simply suggest a lower bound value for it. As experimentally reproduced in [67], the CACC approach inherently degrades to ACC when losing wireless communication for an extended period of time, which resulted in raising the time gap by a factor of roughly four times. Our proposed dynamic controller goes far beyond a simple performance assessment under errors or a graceful degradation framework that switches to a completely local controller, as it continuously adapts to the link quality while preserving the robustness. In fact, we propose a dynamic controller in which the quality of the communication link is continuously monitored, and the control parameters updated accordingly based on the results of an offline optimization as detailed in the next sections.

Communication framework

Regarding the communication framework, several works have focused on the requirements of vehicular communication technologies and their corresponding additional challenges regarding the significant mobility of the nodes in the network [68–70]. Over the last decade, an enormous number of studies concentrated on the evaluation of network performance in the platoon framework in terms of system throughput [71–73], the MAC access and queuing delay [74,75], the packet transmission delay [76,77], the probability of Packet Error Rate (PER) [46,78–81], and even under malicious cyberattacks [82–84], etc.

Similarly, in the communication community, there are many works which focus only on the minimization of the packet error rate while not concerning real demands of the control system. For instance, the authors in [78] investigated different beaconing solutions for platooning systems, but focusing mainly on the network performance in terms of channel busy ratio and packet collisions, while limited evaluation of static controller parameters is realized. In particular, Lyamin *et al.* [80] exposed a negative effect, specially for platooning applications, of the adaptive beaconing of the ITS-G5 standard, which is based on the kinematic-driven mechanism of the vehicle. The authors proposed either decreasing the sampling rate or the synchronicity between vehicles. The authors in [71] focused on the platoon management protocol, which through the use of open sources simulation platforms such as VEhicular NeTwork Open Simulator (VENTOS), Simulation

for Urban MObility (SUMO), and Objective Modular Network Testbed in C++ (OMNET++), they investigate the traffic flow throughput under different platoon maneuvers scenarios. Likewise, the authors in [85,86] also adopted aforementioned tools, however, different from them, we seek for flexibility instead of such black-box models, which motivates the adoption of our own simulation environment built from high-fidelity engine modeling Simulink and Matlab detailed in the next sections.

Molina and Gozalvez [87] conducted simulations to show a comprehensive analysis of the advantages of the performance of C-V2X Mode 4 over the 802.11p. Similarly, [88] used a simulation environment to compare the communications performance of both modes 3 and 4 of C-V2X with the 802.11p standards. More recently, [89] adopted an analytic approach to describe the C-V2X Mode 4 performance. However, these works were limited to the communication aspects of vehicular networks and did not consider the control aspects of the platooning problem. Another set of works considered the platooning scenario under different communication approaches. For instance, [90] used the 802.11p technology to evaluate the communication performance under a CACC controller in platoons. Likewise, [46] has adopted both wireless technologies (802.11p and C-V2X) and compared their performances in terms of the inter-vehicular distance of the platoon. More recently, Naik *et al.* [79] provide interesting thoughts about the next generation of both DSRC and C-V2X access technologies, namely IEEE 802.11bd and 5G NR V2X respectively, while highlighting their beneficial features in platooning applications. The authors conclude that is expected a significant improvement on performance metrics such as latency, reliability and the throughput in the advent of both evolutionary technologies. However, more importantly, they state that the successor of 802.11p will have backward compatibility, which is critical since a few countries already started deploying such technology [91], unlike the successor of C-V2X which is not backward compatible. Segata *et al.* [81] exploits static control parameters features to propose an adaptive control named "jerk beaconing" that sends beacons only when needed. The authors focus on network resource saving for platooning application.

Joint framework

In the last years, we have witnessed great improvements in such interdisciplinary problem, with researchers from both areas adopting more realistic assumptions, in addition to researchers performing real experiments to validate their approach. One of the first papers that performed experiments while considering a joint control/network analysis is the work in [37], where the authors perform a theoretical analysis of a CACC under different time headways and communication delays, which their results are validated in two CACC-equipped prototype vehicles. Even

though they adopted a more realistic modelling of the network behavior with respect to the one assumed in [67], the authors limit themselves to address a constant wireless communication delay, and no control adaptation is performed. Another interesting effort combining network performance to control theory is Xu *et al.* [92] which earlier concluded that driver's braking events contain very effective information for platooning, indicating some event-driven solutions instead of period beaconing transmissions. Moreover, the authors focused on the impact of communication delay in the system, which can diminish values of data communication in platoon control. Similarly, Dolk *et al.* [93] followed a more control-theoretical approach that restricts the communication to only the information that is absolutely required to establish a string-stable platoon. Similarly to [81], they consider an event-driven CACC control approach in order to reduce the communication resources, but focused on the opposite domain.

So far, although some interesting progress in both fields, none of them have considered the system under consecutive losses (burst) that despite being rare events, might occur and disturb significantly the system performance. Giordano *et al.* [94] was the first to assume burst of losses while deriving safety bounds on the inter-vehicle distance depending on network impairments. Likewise, we also consider a burst of packet losses, but different from them, we assume them with lower probability in order to derive superior robust outcomes. More recently, Sybis *et al.* [47] performed a string stability analysis for a CACC alternative control design, in this thesis called Predicted Cooperative Adaptive Cruise Control (PCACC). In particular, the authors resort to graphical solutions to verify that string stability is attained if the actuator lag is below 1.5 s. Different from the aforementioned articles, we propose an online adaptation of the control parameter based on the observed quality of the communication link determined by the distance to the transmitter and the level of interference caused by other vehicles.

Contributions

We investigate the joint design of the V2V network and the platooning control scheme, however, different from the aforementioned works, the novelty is the introduction of a dynamic control mechanism where some of the parameters of the PCACC controller are adapted based on information about V2V communication. In particular, we adapt the parameter that is responsible to weigh the influence of the leader's broadcasted messages in the control algorithm, as well as the target distance between vehicles, based on the communication links qualities. Keeping in mind the above discussion and the results available in the literature on cooperative platooning systems, the following are the main contributions of this chapter:

1) Evaluation of the robustness of the platooning mechanism under severe conditions for V2V communications, expressed in long bursts of losses and in

difficult traffic jamming conditions on the road.

2) Offline optimization of the platooning control parameters based on extensive simulations of a highway scenario.

3) Online adaptation of the control parameters based on the observed communication link quality and on the results of the offline optimization.

4) Adoption of safety as a primary performance metric, quantified in terms of avoiding emergency braking. This translates to robustness constraints, where the inter-vehicle distance in the platoon is set so that *emergency braking is avoided in 99,999% of the cases.*

3.2 General system outline

In this section, we aim to describe the high-level overview of the platoon scenario with the interaction of the control and communication aspects. As previously concluded in Chapter 2, the PCACC control incorporates many benefits when compared to earlier schemes such as ACC, and CACC, but room for improvements is still attainable. Although many works have tackled the platoon efficiency performance problem, only a few have considered a joint communication and control approach, and no one have presented a comprehensive study of the control parameters of the PCACC in respect of different communication link qualities.

Therefore, in order to present an entire perspective, Figure 3.1 illustrates a high-level platoon scenario for two vehicles which includes the V2V communication between them depicted in dashed lines over the wireless block, and the radar/camera/LiDAR measurement represented in the gray area. Moreover, the main functions are summarized inside each vehicle, and correspond to the vehicle dynamics, communication system, and the controller block, and will be further explained, as well as their interaction with the communication system.

In addition to sensor-based solutions such as radar/LiDARs, we adopt wireless communication illustrated by dashed lines in Figure 3.1. In particular, sensor-based systems, such as the ACC control, work only in LOS conditions, and therefore, are very limited due to the awareness of only its surroundings. Therefore, connected and cooperative vehicles that share information through a wireless link solves the LOS problem, and allows much broader understanding of its environment. Undoubtedly, such advantages come with a price as packet errors, interferences, and delays are inherent to all communication channels and may alter the quality of the cooperative controller. As discussed in Chapter 2, the vehicular environment introduces additional challenge on top of the aforementioned ones, and

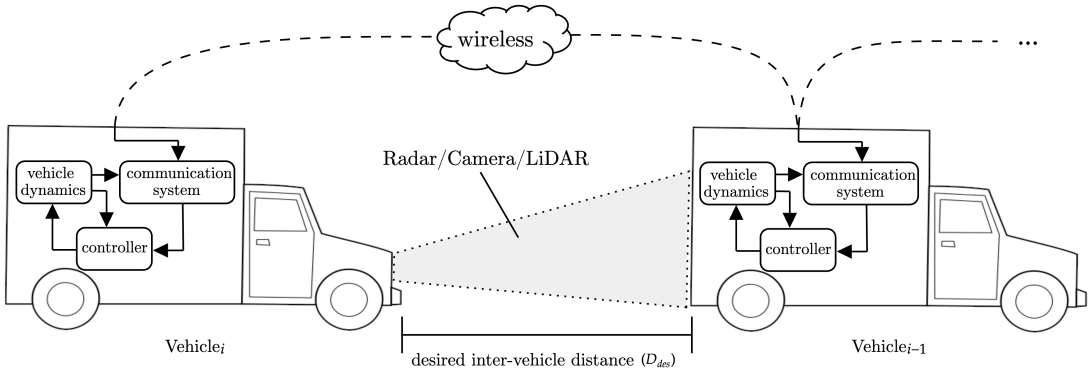

Figure 3.1 – General system outline for two platoon members only.

the overall operation of different V2X links together with platoon mobility should be taken into account.

Finally, Figure 3.2 illustrates the control and communication system interaction, for a certain vehicle i, in a more comprehensive aspect. In particular, inputs and outputs parameters are represented in each block diagram, and note that there are three different types of links to differentiate internal links, sensor measurements and V2V communication in black, blue and red lines, respectively. We highlight the relevance of the cooperation between both systems as each one captures different features, equally important. First, the control system block encompasses the initial conditions, the vehicle's dynamic and the controller block, which is the core component of the system. Such valuable unit is responsible to regulate the vehicle dynamics, in order to maintain certain velocity, and a desired inter-vehicle distance. Consequently, a careful analysis should be done in order to ensure safety operation despite surprising conditions. In fact, there are a myriad of external disturbances, a few examples are when a vehicle in front of the platoon leader suddenly breaks, or perform a lane change, or even a cut-in maneuver in one of the platoon members. In this thesis, we focus on the first example.

The controller obtains preceding vehicle dynamics through sensor measurements, in solid blue, but relies on the communication system to have access to all parameters needed to compute the control law, for instance, the leader information. In this context, the V2X block is the one responsible to compute the quality of the communication link since it overhears all other V2X links, which translates to a certain probability of packet received by the controller block. Moreover, it retrieves the acceleration signal of both leader and preceding vehicle and the velocity of the leader, note that we illustrate such uncertain nature by dashed red lines. Finally, the V2X block is responsible to provide the acceleration of vehicle i to the next vehicle in the platoon, which is the input of the V2X block of the next vehicle $i + 1$ (not shown), which closes the loop.

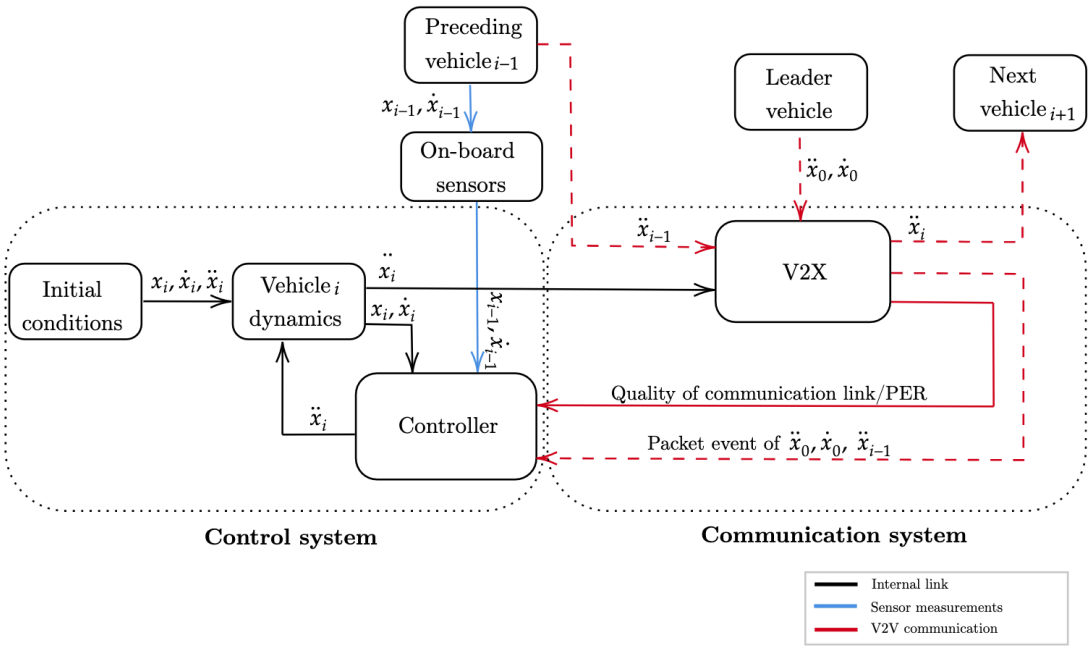

Figure 3.2 – Block diagram overview with control and communication system interaction.

Therefore, the communication system overall purpose is to grant the exchange of information between vehicles, not necessarily consecutive ones, in the platoon, which is done via a wireless medium. The reason behind such obligation is that we adopt a cooperative controller, which requires external control information of other platoon members, that can not be captured by on-board sensors. For instance, looking back at the control mechanism of equation (2.12), there are essentially three terms concerned. First, the desired acceleration of the preceding vehicle ($\ddot{x}_{(i-1)\_\mathbf{des}}$) weighted by parameter $(1 - C)$, the desired acceleration of the leader ($\ddot{x}_{(0)\_\mathbf{des}}$) vehicle weighted by parameter C, and the leader's velocity ($\dot{x}_0$).

In fact, we adopt sensor-based and communication-based solutions, which the corresponding information are later merged to allow better overall performance. Here, both fully cooperative control and semi-autonomous control strategies require relative position and longitudinal velocity of the preceding vehicle, so we assume that the measurements are exact sampled each 60 ms with 1 ms delay and done by a long-range radar as in [46].

Over the next sections, we aim to precisely describe the interplay between the communication system which relies on the wireless link quality, and the control and the vehicle dynamics. Along our thesis, we seek to minimize the desired-inter-vehicle distance (D_{des}) between the platoon members in order to boost the platoon

gains, while keeping safe and robust performance.

3.3 Control Platooning System

As discussed in Chapter 2, there are many controllers feasible for platooning schemes. In order to exploit the communication features, we adopt a scheme based on PCACC, which will be responsible to adapt the control parameters accordingly. Furthermore, the ACC controller defined in (2.8) is adopted by the leader since it is preceded by a vehicle that is outside the platoon formation. Nevertheless, when a complete failure of the leader information is observed, the proposed scheme remodel to the semi-autonomous as in (2.13).

Note that constant time gap policy recommends very high distance between vehicles, and therefore is not efficient for platoon formations. As a result, we adopt constant spacing policies in order to have fully control of the desired inter-vehicle distance between the platoon members. The objective of this section is to present the control schemes and their interaction with algorithms performance, and to introduce the proposed scheme based on PCACC.

3.3.1 Vehicle dynamics

As previously introduced in Chapter 2, the vehicle dynamics is modeled as first-order low pass filter due to the actuator lag. Moreover, such model has been experimentally verified to adequately describe the longitudinal dynamics of the system, as shown in [44, 93]. Looking back at the vehicle dynamics equations (2.1-2.3), we assume a lag of $\tau = 0.5$ s as in [41] in order to be conservative. The reader is referred to [95] and [47] for deeper discussion on different actuator lags values and its impact on the system performance. Moreover, a smooth behavior of a platoon is important, so to ensure the passenger comfort, the control input constrains introduced in equation (2.4) are bounded by $u_{min} = -3$ m/s^2 and $u_{max} = 2$ m/s^2 as in [46], [96]. Note that the maximum deceleration of -3 m/s^2 corresponds to the limit of brake capacity of cruise control systems imposed by the ISO 15622:2010 standard for the sake of passenger comfort.

3.3.2 Proposed dynamic scheme based on PCACC

In contrast to existing works that assume a fixed control strategy or consider only a lower bound parameter as in [25], we propose, as depicted in diagram scheme in Figure 3.3, an offline optimization of the control parameters based on the communication link quality characterized by the packet error rate from the leader to the last vehicle (defined as $\mathrm{PER}_{\mathrm{LLV}}$). In particular, among the control

inputs, extensive simulations demonstrate that this pair of parameters (C, D_{des}) has the most substantial impact on the performance of the system. As mentioned before, C is responsible to weigh the influence of the leader's message in the control algorithm while D_{des} is the desired inter-vehicular distance that we want to set, but due to actuator lag and delay in the process it does not correspond to the actual average inter-vehicular distance (D_{avg}). The following algorithm based on PCACC controller is proposed.

- **Step 1:** Update the traffic density range limits ($\mathrm{PER_{LLV}}$).
- **Step 2:** Vary the C parameter while minimizing D_{des} and register the average inter-vehicular distance D_{avg} for each $\mathrm{PER_{LLV}}$ inside the range of Step 1.
- **Step 3:** Consider the minimum D_{avg} result with no collision and identify its correspondent pair of $(C(PER_{LLV}), D_{des}(PER_{LLV}))$ to build the optimum lookup table $(C^*(PER_{LLV}), D^*_{des}(PER_{LLV}))$.
- **Step 4:** Observe the current communication link and adapt the control inputs (C, D_{des}) accordingly based on the optimum lookup table of Step 3.

Therefore, we conduct an offline heuristic optimization to determine the best control parameters (C, D_{des}), in terms of minimum inter-vehicular distance without collisions, for any given value of $\mathrm{PER_{LLV}}$ (which is the result of the traffic density and the resulting interference). We build a $(C^*(PER_{LLV}), D^*_{des}(PER_{LLV}))$ lookup table that will serve as an optimum reference for each $\mathrm{PER_{LLV}}$ value.

Many existing works on CACC and PCACC mention the minimum distance possible assuming a certain level of interference or traffic on parallel lanes, however, it is not clear what should be done in practice where these parameters will evolve over time in an unknown manner. We propose to apply an online adaptation of the parameters (C, D_{des}) based on the observed $\mathrm{PER_{LLV}}$ and on the results of the offline optimization. Note that due to actuator lag and delay the string stability is not guaranteed for all platoon sizes other than those evaluated.

Online adaptation of the control parameters

We now move to the online adaptation of the control parameters based on the observed communication link. To summarize, we perform an offline optimization of the control parameters, above-mentioned, followed by an online adaptation based on the communication link quality observed and the look-up table. We present two implementations of this controller: a centralized homogeneous control where the whole platoon adapts to the worst communication link, and a distributed

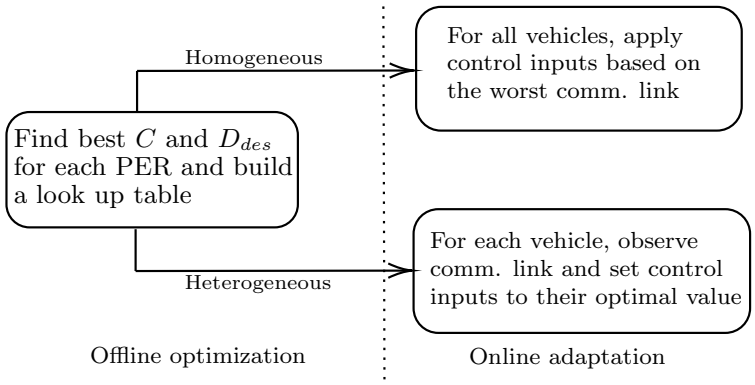

Figure 3.3 – Offline and online parameter election diagram.

controller where each vehicle adapts its own control parameters based on each communication link.

Homogeneous control

In this case, the whole platoon shares the same information that is transmitted by the leader vehicle to all members. We apply a local controller based on the packet loss observed on the communication link by the leader and the last vehicle (PER_{LLV}). The whole platoon adapts the control inputs corresponding to optimal values computed in the offline optimization for this PER. Thus, the whole platoon is subject to the same adaptive control procedure and we set both control parameters, weight of the leader's message and desired distance, according to its optimal values considering the worst communication link in the platoon.

Heterogeneous Control

An alternate approach corresponds to apply a local controller based on the packet loss observed on the communication link for each vehicle in the platoon. Therefore, based on the offline optimization mentioned before, for each vehicle, we set both control parameters according to their optimal values considering independent communication links. This implies that no additional communication resource is required for the whole platoon to exchanges the exact same information about the control law or communication conditions.

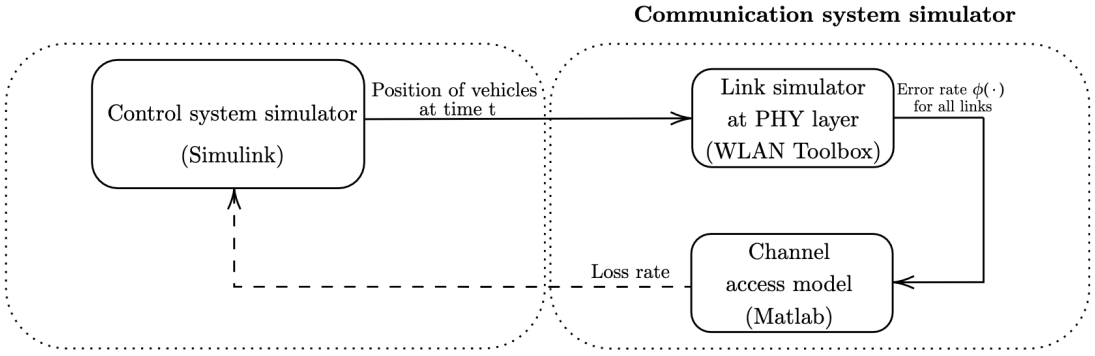

Figure 3.4 – Block diagram simulation overview.

3.4 Simulation system implementation

Now that the general system outline is introduced, we can concentrate on the general simulation tool of the platoon evaluated in this thesis. The idea is to specify the interaction in a simulation point of view, between each one of the general blocks introduced in Section 3.2. Thus, Figure 3.4 illustrates the top-level structure of the simulation platooning configuration implemented in this thesis in a block diagram arrangement. Moreover, a more detailed version of the communication system is also introduced, and the main output parameters for each block are also labeled.

From a simulation perspective, we have two different simulation components: the control system and communication system simulator. The former one is responsible to provide periodic information of the positions of the platoon vehicles to the communication system simulator. We have used the Simulink environment to model the vehicle dynamics and to implement the control law. The second essential part in our system is the communication system simulator, which includes the link simulator at PHY layer and the channel access model. The first one is responsible to compute the error rate for all links, i.e. the PER for each link, which we make use of the Matlab WLAN Toolbox for the simulation of the PHY layer of 802.11p standard. The second block models the interference with other links that also contend for the channel access, which is implemented in Matlab. Its output is the final loss rate of the communication links conveying the important parameters to the control system to compute the control law, which closes the loop.

3.4.1 Communication Platooning system

The wireless communication module concerns a significant element in the system, and the main blocks is particularized next. Indeed, platooning system has tight

Table 3.1 – Parameters for the MATLAB WLAN Toolbox PHY layer of 802.11p.

PHY layer	
Parameter	**Value**
Waveform Configuration	
MCS	QPSK, R=1/2
CAM size	500 bytes
Bandwidth (BW)	10 MHz
Channel Configuration	
Delay profile	Highway LOS Highway NLOS
Simulation Parameters	
SNR range	$\{-10, \ldots, 50\}$ dB
maxNumErrors	50
maxNumPackets	500

requirements on the wireless communication aspect. In fact, the triggering conditions of the update frequency CAM messages depend greatly on the use case scenario, and might vary between 1 Hz to 10 Hz. Therefore, along this thesis, we adopt the minimum time interval between CAM generations of 0.1 s, which is in conformity with speed limits notification use case as defined in the ETSI EN 302 637-2 standard [97]. Another factor, is the vast amount of V2V links coexisting to contend for the channel, which calls out for careful analysis of such interference links.

3.4.1.1 Link Simulator at PHY layer

The first block consists of link simulator at PHY layer, which address the lowest network layer. In this framework, the performance is characterized by the average Packet Error Rate (PER) versus Signal Noise Ratio (SNR), where PER is the probability that a particular transmission of a packet fails, due to fast fading and interferences from other links. In particular, we have adopted the MATLAB WLAN Toolbox for the simulation of the PHY later of IEEE 802.11p standard [98]. More precisely, with this toolbox, we are able to compute the PER of an 802.11p link between a transmitter and a receiver, considering a V2V fading channel and for a given link quality (SNR/SINR). However, it does not include the competition between links to access the channel. Therefore, we also develop a "Channel access" module which models interference with other links, including V2V, broadcast transmissions by relays and external interfering sources that contend for channel access, which will be further evaluated in the next subsection.

Table 3.1 encompasses the main parameters used in the WLAN Toolbox for the simulation of the PHY layer of IEEE 802.11p protocol. The first step of the simu-

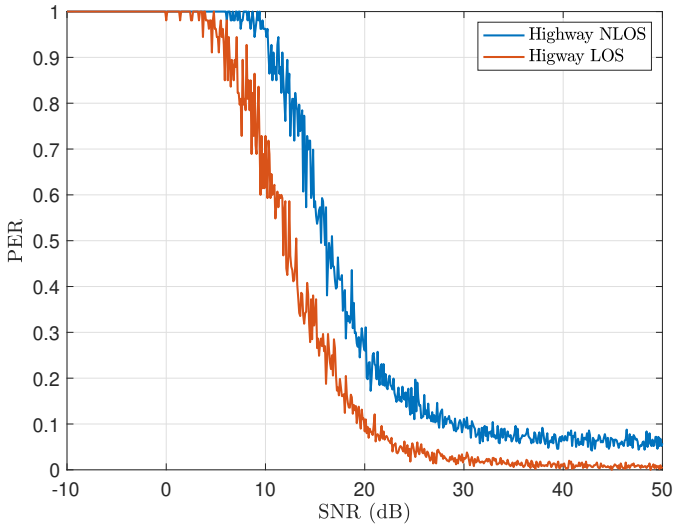

Figure 3.5 – Illustration of Highway NLOS and LOS profiles from WLAN Toolbox.

lation is to define the initialization procedure, i.e. detail the specific configuration format of the transmission. As a result, we define the packet waveform generation format that outlines the explicit layout of the cooperative awareness message to be sent, which includes its size of 500 bytes, the channel bandwidth of $BW = 10$ MHz, and, finally, the Modulation Coding Scheme (MCS) that designates two aspects: the modulation and the code rate, here adopted as Quadrature Phase Shift Keying (QPSK), and $R = 1/2$, respectively. Next, the channel configuration must be defined in order to obtain the delay and Doppler spread characteristics of the desired environment. Here, we have adopted two different environments: Highway LOS, and Highway Non-LOS (NLOS), whose respective delay and Doppler spread values can be found in Table 5 of [99]. Such a choice is motivated due to the endorsement of two different radio link models depending on the arrangement of vehicles in the platoon, about which a more precise discussion will be presented in the following subsections. Finally, the simulation parameters define the range of SNR points, here $\{-10, \ldots, 50\}$ dB. For each SNR value, a certain number of packets, limited to 500, are generated, passed through a channel and demodulated to establish the packet error rate as illustrated in Figure 3.5 for Highway NLOS and LOS environments, in blue and orange, respectively.

Path loss V2V link

Now the performance of the wireless environment for V2V transmissions is attained, which incorporates V2V fading channel aspects, the additive white Gaus-

sian noise, the packet errors. Therefore, we are able to associate each SNR level between -10 dB until 50 dB to a certain probability of packet error rate, which is precisely illustrated in Figure 3.5. However, we are interested to relate the packet error rate with the distance between the transmitter and receiver, instead of the SNR level. In order to do so, observe that message reception errors are evaluated through the computation of the Signal-to-Interference-plus-Noise Ratio (SINR). More precisely, the SINR of a packet transmitted between a transmitter (k) and a receiver (l) can be computed as

$$SINR_{(k,l)}(P_I) = P_{Tx} - P_{PL}(d_{(k,l)}) - 10 * log_{10}(10^{P_I/10} + 10^{P_N/10}) \tag{3.1}$$

where P_{Tx} is the transmission power in dBm, P_N denotes the noise floor in dBm, $P_{PL}(d_{(k,l)})$ consists the path loss in dB, and (P_I) corresponds the total interference. Accurately, the noise term is given by

$$P_N = -174 + 10 \cdot \log_{10}(BW) \tag{3.2}$$

where BW is the bandwidth allocated for the V2V channel. Then, the path attenuation component of the channel is responsible to include the distance as one parameter to be correlated to the power density, and afterward the packet error rate. Moreover, concentrating on the link (k, l) given by the distance $d_{(k,l)}$ in meters, the path loss power, in dB, corresponds to the Winner-II Path Loss Model (B1 scenario) from [100] computed by

$$P_{PL}(d_{(k,l)}) = 22.7 \cdot \log_{10}(d_{(k,l)}) + 41 + 20 \cdot \log_{10} \frac{f_c[GHz]}{5} \tag{3.3}$$

Finally, the last component (P_I) corresponds to the total interference coming from other vehicles outside the platoon and/or from within as well. Further explanation is given in the next section. Furthermore, we perform Monte-Carlo simulations to obtain the SINR for average relative distances of platoon vehicles in respect to the leader vehicle, as the latter transmits information of paramount importance to the stability of the platoon. For this, we need first to investigate the traffic interference, and determine how many and where are those vehicles accordingly to the platoon link.

Interference function

In practice, there are a large number of vehicles crossing and moving along the highway environment. Due to the mobility behavior of such wireless communication channel, it is infeasible to accurately reproduce flawlessly all the possible interferences caused by external vehicles in the platoon. In order to facilitate the analysis, consider Figure 3.6 that encompasses the highway traffic interference

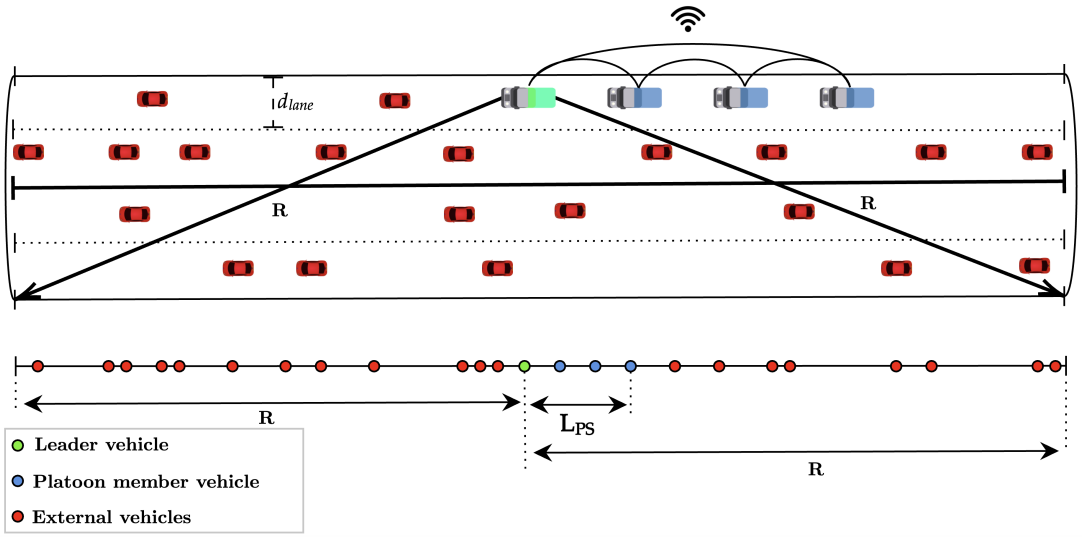

Figure 3.6 – Traffic interference in respect to the leader vehicle in green. The transmission range is denoted by R, and the length of the platoon size by L_{PS}. Platoon members and external vehicles are illustrated in blue and red, respectively.

considered here. Note that the leader vehicle, illustrated in green, is able to sense a certain number of vehicles within a certain R range. In fact, such distance is the transmission range, which delineates the vicinity of vehicles that might interfere when transmitting packets. In our model, we consider the transmission range R as much greater than the distance of the lane width d_{lane}, more formally $R \gg d_{lane}$. For simplicity, we assume a uniform distribution of 12 evenly spaced vehicles within $R = 500$ m, which translates to a maximum of 24 vehicles/km/lane. Furthermore, the hidden node problem on vehicular networks is not considered. In the next subsection, we aim to cover the channel access model, which defines the multiple access protocol adopted for the transmission of data via the shared network channel.

3.4.1.2 Channel access model

Briefly, the channel access model is responsible to control the access to the medium, and to define the rules in case packet collision happens. In fact, that are many ways of doing so such as by fixing allocation times to each station such as Time Division Multiplexing (TDM) and Frequency Division Multiplexing (FDM) techniques, which are not efficient in distributed resource allocation. A promising means is contention based protocols, which shares the medium just like in a conversation between two persons. If one is talking, the second must listen to not disturb the discussion. However, vehicle protocols, such as the IEEE 802.11p introduced in

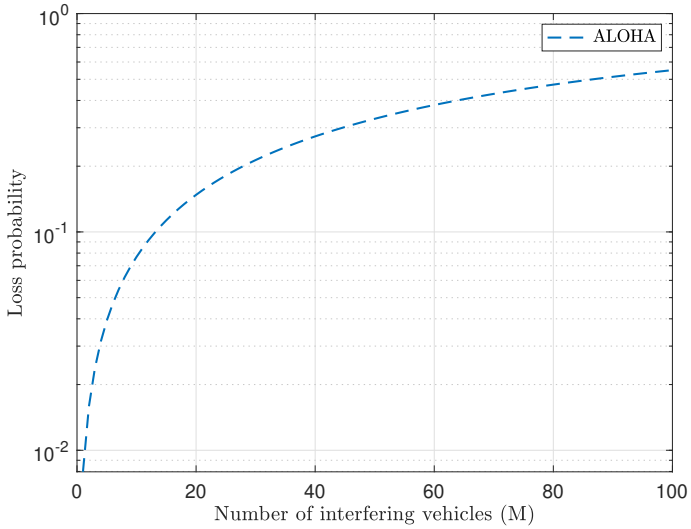

Figure 3.7 – Loss probability comparison for consecutive vehicles for ALOHA protocol in dashed blue.

Chapter 2, adopt enhanced contention protocols such as the Carrier Sense Multiple Access with Collision Avoidance (CSMA/CA) which will be further investigated and implemented in the next chapter.

ALOHA protocol

For simplicity, we have started by choosing the simplest contention-based protocol, namely ALOHA protocol. Concisely, in ALOHA protocol the transmitters are uncoordinated, as they are allowed to transmit as soon as they wish. The vulnerable time is defined as the time in which there is a chance of collision, for simplicity we assume fixed-length frames T_{fr}. In pure ALOHA the vulnerable time is $2T_{fr}$ since no rule defines when each station can send, so collisions might occur if a station contend for the medium shortly after another station has started or shortly before another station has finished to send a packet. To ease the performance computation, we assume that the intervals between transmissions have exponential distribution. Therefore, the probability of collision with each interfering vehicle can be computed as:

$$P_{Aloha} = 1 - e^{-\lambda 2 T_{fr}} \tag{3.4}$$

where λ is the mean packet arrival rate considered as 1 packet each 0.1 second, and T_{fr} is the packet length, here considered the size of the slot time for simplicity,

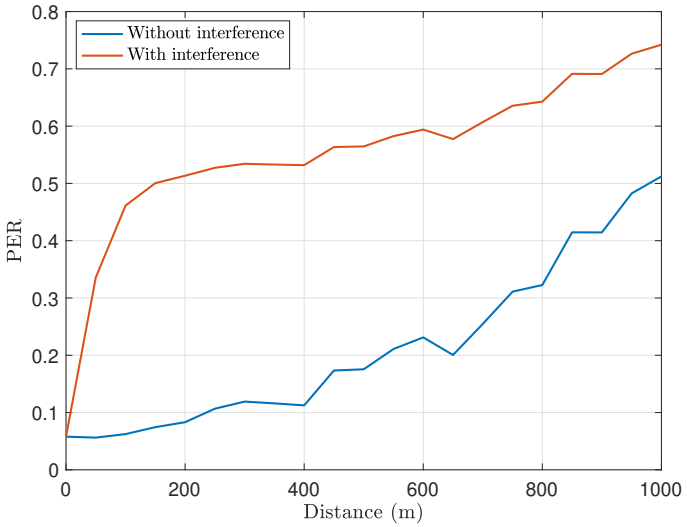

Figure 3.8 – PER of Highway environment with NLOS condition. Interferences are expressed in orange, while no interference conditions in blue.

computed by:

$$T_{fr} = \frac{CAMsize}{BW} = \frac{500 * 8}{10 * 10^6} = 0.4\ ms \tag{3.5}$$

For comparison purposes, Figure 3.7 illustrates the loss probability of the ALOHA protocol, considering an increasing number of interfering vehicles up to 100. In the next chapter, we present an improved access medium protocol that is compliant with the vehicular standards, i.e. the carrier-sense multiple access with collision avoidance (CSMA/CA) protocol.

Packet loss probability

Now that the channel access model and the interference computation is explained, we are able to evaluate the average PER for a given link quality (SNR/SINR) using the link performance, realized by the WLAN Toolbox of MATLAB as in Figure 3.5, and the interference computation function that stochastically calculates the SINR for each of the vehicles in the platoon considering the set of equations (3.1), (3.2), (3.3) and the interference from other vehicles as in Figure 3.6 with roughly $M = 70$ vehicles that contend for the medium according to the Aloha protocol (3.4). More precisely, in order to compute the total interference, we conduct an explicit computation for each of the interfering vehicles by taking the probability

of collision with this specific vehicle so

$$P_I = \sum_{k=1}^{M} \frac{P_{Tx,I}}{P_{PL,I}} \mathbb{1} \tag{3.6}$$

where $P_{Tx,I}$ is the transmission power of the interference vehicle in dBm, here considered the same as P_{Tx}, $P_{PL,I}$ is the path loss power in dB between the interference and the receiver vehicle as specified by the traffic interference, and $\mathbb{1}$ is the indicator function defined by

$$\mathbb{1} = \begin{cases} 1 & if\, \omega < P_{Aloha} \\ 0 & Otherwise \end{cases} \tag{3.7}$$

where ω is a random number following the standard uniform distribution on the interval $(0, 1)$, and P_{Aloha} is given by (3.4). Therefore, based on a random generation of event, we decide the collision episode for each interfering vehicle by taking the ALOHA probability of collision as in (3.4). Finally, the total interference P_I is the sum for all interfering vehicles, in which a collision took place as in (3.6).

Figure 3.8 illustrates the packet loss probability, with and without interference, for a V2V link in respect of the distance between the transmitter and receiver. Such loss probabilities are particularly important for the control framework, as certain parameters will arrive with different likelihood in the receiver side, and therefore alter the control performance. Moreover, as far as the control system input parameters are concerned, the relative distance between transmitter and receiver being a function of the loss probabilities, which are the output of the communication system, is sufficient to compute the control law.

3.4.2 Simulation Assumptions and Platoon Scenario

Now that the control and communication aspects of the respective platooning system were presented, the simulation assumptions and platoon traffic scenario can be defined. Therefore, in this section, we present the platoon scenario and the robustness criterion, the control and communication parameters employed, and the simulation tool adopted.

3.4.2.1 Platoon Scenario and Robustness Criterion

The system consists of a platoon of 10 automated vehicles following the leader, i.e. $N = 11$. The simulated scenario takes place in a four-lane highway, as illustrated in Figure 3.9, with a maximum traffic density of 24 interfering vehicles/km/lane, which translates to a total of $M = 72$ interfering vehicles when omitting the

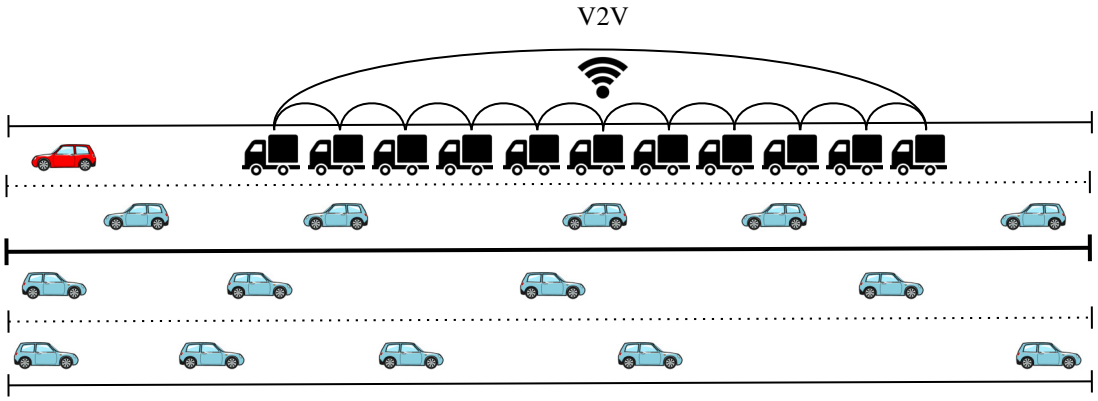

Figure 3.9 – Traffic scenario including a platoon with V2V communication approach.

platoon lane. The vehicles of all other lanes are not in platoons (blue vehicles) and a jammer (in red) precedes the platoon leader. In the offline optimization section, the speed of the jammer (vehicle outside of the platoon) follows a preset sequence, adapted to only two cycles from [46], as shown in Figure 3.10. The main reason for this jammer velocity profile is to study the capacity of the platoon system to avoid a collision in risky scenarios such as when the vehicle outside of the convoy suddenly applies the maximum brake capacity. Furthermore, different from the previous articles so far that just do Monte-Carlo simulations (100 or 1000 iterations of normal conditions), we have considered a burst of packet losses. While bursts are rare events, they may occur and impact the safety of the platoon, but are not well reflected in the numerical analysis of most previous works like [46,47,65,90,101]. In this sense, the robustness treated here is related to the following worst-case event: the jammer brakes at some time ($t = 60$ s in our simulation) and this braking coincides with a burst of packet losses (complete interruption of the transmitted signal) during the following interval $t + \Delta$ also illustrated in Figure 3.10.

Different from the literature, we aim to consider a robust platoon scenario under severe V2V conditions. Therefore, we consider long bursts of packet losses that occur with low probability, here described in powers of base 10 such as 10^{ν}, in order to be conservative, where $\nu \leq 0$ is the exponent power. Denoting by PER the probability of packet loss taking into account the channel model and packet collisions and T the time sampling interval for vehicle information, we have the following formula that relates to certain probability degree

$$PER^{\Delta \frac{1}{T}} = 10^{\nu} \tag{3.8}$$

From (3.8), we can obtain the burst size Δ (in seconds), which can be calculated from the expectation value of the packet error rate PER for a corresponding vehicle

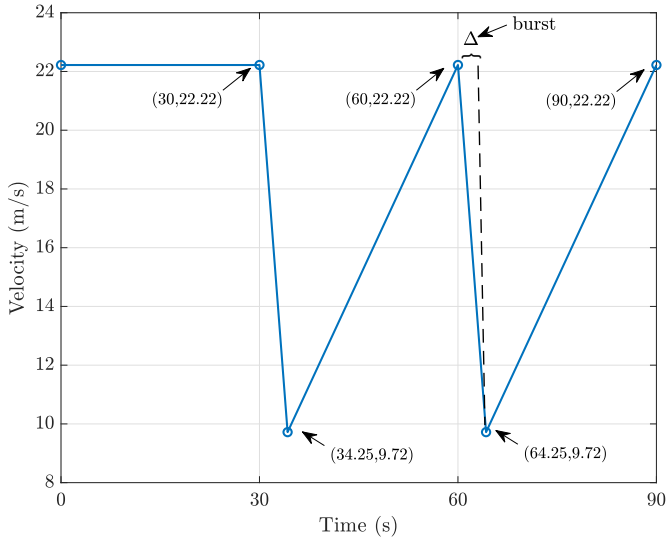

Figure 3.10 – Illustration of the jammer velocity profile adopted with 2 cycles.

in the platoon, and is given by:

$$\Delta = \frac{\nu \cdot T}{(log_{10}\text{PER})} \tag{3.9}$$

In our simulations, we have considered the sampling rate of $T = 100$ ms as advocated by the ETSI EN 302 637-2 standard. For illustrative comparison, Figure 3.11 illustrates the burst size Δ in seconds, which might occur with probabilities of 10^{-1}, 10^{-5}, and 10^{-10} in dashed blue, solid red, and dashed yellow, respectively, for certain probability of packet loss PER. We have adopted $\nu = -5$ as the exponent of the probability of burst to take place, as at a first glance it seems to be a reasonable choice due to moderate burst values and small enough likelihood. Such a choice translates to robustness constraints, in which the inter-vehicle distance in the platoon is set so the emergency braking is avoided in $99,999\%$ of the cases.

3.4.2.2 Simulation tool

We used the MATLAB/Simulink environment to model the vehicle dynamics and to implement the control law. Furthermore, we adopted the WLAN Toolbox of MATLAB to implement the channel configuration for a 802.11p transmission in order to obtain the Packet Error Rate (PER) taking into account the V2V fading channel aspects, the additive white Gaussian noise, the packet collisions, which corresponds to the block “link simulator at PHY layer" in the block diagram of the system as illustrated in Figure 3.4. The mobility behavior of vehicles is also

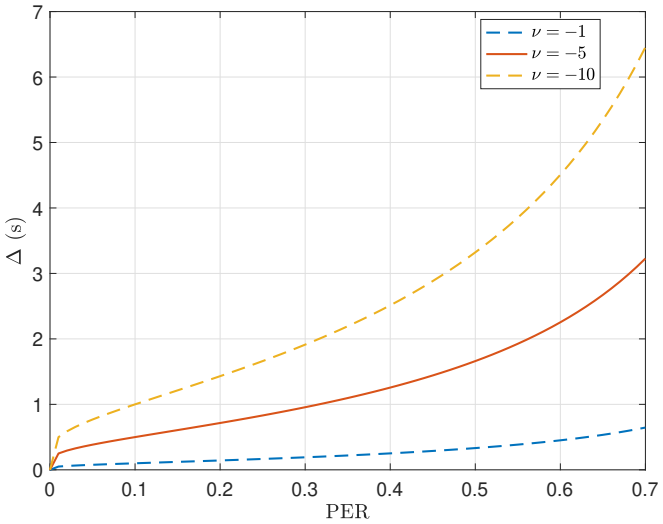

Figure 3.11 – Burst size with different probabilities to occur. The dashed blue, solid red, and dashed yellow corresponds to probabilities of burst to occur of 10^{-1},10^{-5}, and 10^{-10}, respectively. We have adopted the solid red line $\nu = -5$, while dash lines are shown for comparison purposes.

observed in the MATLAB/Simulink environment as we consider a traffic scenario as in Figure 3.9. So at the beginning of each simulation step, from the "preceding vehicle$_{i-1}$" module the "controller" is able to update the velocity and the position of the preceding vehicle $(\dot{x}_{i-1}, x_{i-1})$ as in Figure 3.4. Also, the block "vehicle$_i$ dynamics" provides the vehicle's dynamics, thus its own velocity and position $(\dot{x}_i, x_i)$, to the "controller" block and to the communication system which uses it to compute the loss probability of the control parameters. In particular, the controller obtains the leader's acceleration and velocity and the preceding vehicle acceleration $(\ddot{x}_0, \dot{x}_0, \ddot{x}_{i-1})$ from the communication system. Furthermore, the aforementioned algorithm in Section 3.3 is applied, where based on the quality of the leader link, the vehicle is able to adapt dynamically the pair of parameters (C, D_{des}). Recall that in the leader vehicle we implement an ACC controller, so the communication system is responsible only to broadcast its acceleration and velocity since the ACC controller does not require any other inputs as those provided by the blocks "preceding vehicle$_{i-1}$" and "vehicle$_i$ dynamics". Based on the inputs mentioned, the "controller" module is able to calculate the desired acceleration $(\ddot{x}_{i\_des})$ in order to keep a certain desired distance (D_{des}) from the preceding vehicle. Thus, the "vehicle$_i$ dynamics" block, applies the desired acceleration and provides as output the vehicle's position and velocity at the next simulation step.

Table 3.2 – Communication and Controller Parameters

Communication		**Controller**	
Parameter	**Value**	**Parameter**	**Value**
Simulation		**PCACC (Followers)**	
Duration (T_{sim})	1200 s	Weight of the leader (C)	Adaptive
Jammer profile	Check Fig. 3.10	Desired distance (D_{des})	Adaptive
Application		Damping ratio (ξ)	2
CAM size	500 bytes	Bandwidth (ω_n)	0.5 Hz
CAM interval (T)	100 ms	**ACC (Leader)**	
PHY layer		Time gap (h)	1.4 s
Path loss	Winner+B1 LOS	**Vehicle & Highway**	
Noise power	-174 dBm/Hz	Actuator lag (τ)	0.5 s
Tx power	22.5 dBm	Vehicle length (L)	16.5 m
MCS	QPSK, R=1/2	Max. acceleration	$+2\text{m/s}^2$
Channel	Highway NLOS	Min. acceleration	-3m/s^2
Frequency (f_c)	5.9 GHz	Radar interval	60 ms
Bandwidth (BW)	10 MHz	Lanes per direction	2
Process delay	1 ms	Lane width	5 m
		Traffic density (M)	72 vehicles

The WLAN Toolbox is used to simulate the wireless condition for a 802.11p transmission. We adopted two different packet error rate parameters that depend on the arrangement of vehicles in the platoon. The first one is related to the packet error rate between two successive vehicles and defined as $\text{PER}_{\text{i,i+1}}$ along the thesis. We adopted a Highway Line-of-Sight (LOS) profile, as vehicles in the platoon are close enough to justify the usage. The second one is the packet error rate between the leader to the last vehicle that was defined as PER_{LLV}. In this case, we used the Highway Non-Line-of-Sight (NLOS) profile in the toolbox since in this case the leader is less likely to be in the LOS with the last vehicle in the platoon. Consequently, we have considered both environments Highway NLOS and LOS in the WLAN toolbox simulation as illustrated in Figure 3.5 in blue and orange, respectively.

Furthermore, we stochastically calculated the SINR (Signal to Interference and Noise Ratio) for each of the vehicles, as in (3.1) with (k, l) being the link between the leader and each platoon member, considering Winner-II Path Loss Model (B1 scenario) as in (3.3) and the interference from other vehicles. Finally, Table 3.2 encompasses all the communication and controller parameters adopted in this chapter.

3.5 Performance Evaluation

The leader is equipped with an ACC control to be in accordance with the recommended safety time interval gap of the respective local law while the platoon is equipped with fully predictive cooperative control. The focus is to apply a longitu-

dinal control in the platoon through V2V communication technology and analyze the system stability by means of vehicle collisions in some robust and worst-case scenarios. We considered the zero-order hold mechanism as the holding strategy for the control signal during the periods of packet losses. Furthermore, in all simulations, we focus on obtaining the minimum feasible inter-vehicular distance in the platoon with a emergency breaking probability no more than 10^{-5}. Note that we implemented a safety gap distance of 0.5 m for the emergency braking actuation to avoid collisions in practical settings.

The control strategy demands relative position and longitudinal velocity of the preceding vehicle so we assumed that the measurements are sampled each 60 ms with 1 ms delay and done by a long-range radar as in [46]. All the vehicles in the platoon broadcast a 500 bytes message on a 10 MHz channel bandwidth. Neighboring vehicles are subject to a Highway LOS channel model [99] and our simulations provide a $\mathrm{PER}_{\mathrm{i,i+1}} \in \{0.006, 0.0245\}$ for the cases without interference and with interference, respectively. We have computed $\mathrm{PER}_{\mathrm{i,i+1}} = 0.0245$ as the default value. As of the leader communication, the leader broadcasts a message to all other vehicles that is subject to a Highway NLOS channel [99] with roughly a $\mathrm{PER}_{\mathrm{LLV}} \in \{0.1, \ldots, 0.7\}$, depending on the interference conditions as shown in Figure 3.8.

3.5.1 Offline optimization

We start by performing an offline optimization of the control parameters (C, D_{des}) as described by the proposed algorithm. Figure 3.12 illustrates the substantial impact of C parameter on the average inter-vehicular distance (D_{avg}) for different $\mathrm{PER}_{\mathrm{LLV}}$ values, which corresponds to steps 1 and 2 of the algorithm. Thus, from Figure 3.12 we can retrieve the C^* optimum that minimizes the inter-vehicular distance for each $\mathrm{PER}_{\mathrm{LLV}}$ evaluated, which is illustrated in Figure 3.13 on the left (step 3). Similarly, the optimum D_{des} values were established as shown in Figure 3.13 on the right. In this figure, $C = 0.3$ represents the best alternative in the robust scenario for low $\mathrm{PER}_{\mathrm{LLV}}$ values. While, $C = 0.2$ indicates to be the best value for mid-range values as $0.2 \leq \mathrm{PER}_{\mathrm{LLV}} \leq 0.4$. For higher $\mathrm{PER}_{\mathrm{LLV}} \geq 0.5$ the best parameter values is $C = 0$ which is the case of semi-autonomous control.

3.5.2 Online adaptation of the control parameters

We now move to the online adaptation of the control parameters that corresponds to step 4 of the proposed algorithm, where the whole platoon adapts the control inputs (C, D_{des}) corresponding to the optimal values computed in the offline optimization based on the packet loss observed on the communication link by the leader

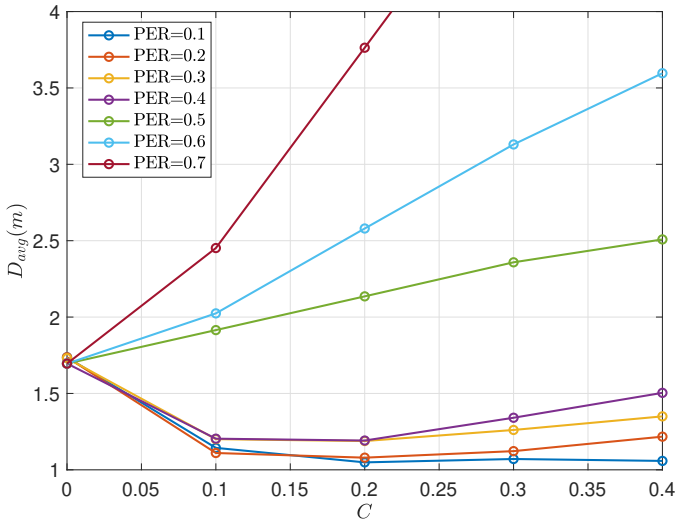

Figure 3.12 – Illustration of the average inter-vehicular distance with $\text{PER}_{i,i+1} = 0.0245$ for different C values. Several cases of PER_{LLV} are considered.

and the last vehicle (PER_{LLV}). In fact, we present two implementations of this controller: a centralized homogeneous control where the whole platoon adapts to the worst communication link, i.e. (PER_{LLV}), and a distributed controller where each vehicle adapts its own control parameters based on each communication link. For comparison purposes, we also simulated cases with fixed control parameters. The idea is to inspect the occurrence of collisions and to compare the inter-vehicular distance of the platoon in a long simulation of 25 minutes in four different cases defined as follows:

- Case 1 - Static PCACC with weight of leader corresponding to $C = 0.2$. We apply the desired distance corresponding to the PER between the leader and the middle car in the platoon obtained under average traffic conditions.
- Case 2 - Semi-autonomous (weight of leader set to zero, i.e., $C = 0$).
- Case 3 - Homogeneous adaptive approach. We apply a uniform control in all the vehicles based on the PER between the leader and the end of the platoon (PER_{LLV}).
- Case 4 - Heterogeneous adaptive approach. We apply a distributed controller that is based on the observed PER for each vehicle.

In all cases, we consider the jammer profile as the pattern in Figure 3.10, but repeated 50 times. Another important factor is the traffic density that generates

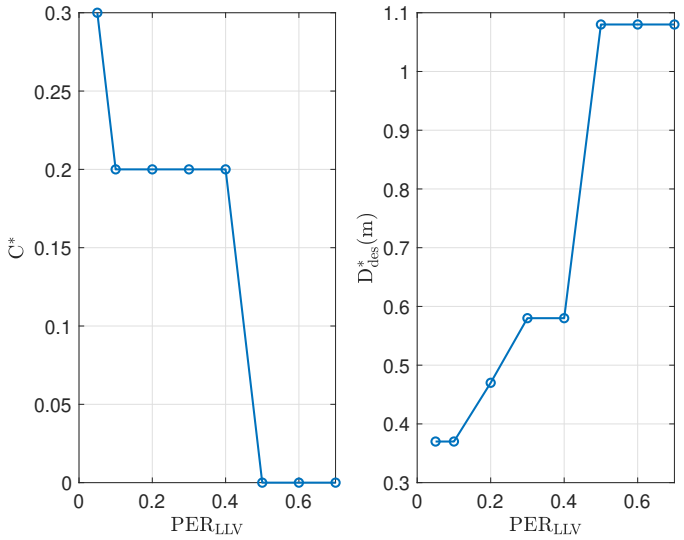

Figure 3.13 – Illustration of the optimum C and D_{des} parameters for different $\mathrm{PER_{LLV}}$ values.

Table 3.3 – Case comparison for the online implementation.

	Parameters	Case 1	Case 2	Case 3	Case 4
Controller	Weight of the leader	0.2	0	Dynamic	Dynamic
	Desired dist. (m)	0.5847	1.0375	Dynamic	Dynamic
Outputs	Average dist. (m)	1.2103	1.6785	1.3823	1.26
	Minimum dist. (m)	0.2537	0.6297	0.5233	0.51
	Collisions	8	0	0	0

interference and changes the PER for each vehicle. The traffic density varies in the range $\{0,\ 20\}$ vehicle/km, with the packet error rate between leader to first vehicle set in the interval $\{0.1,\ 0.2\}$ and from the leader to last vehicle set in the interval $\{0.2,\ 0.6\}$ as shown in Figure 3.14. Similarly, the traffic density is generated for the other vehicles in the platoon. Every 2 minutes (4 cycles), the predefined traffic density increases up to its maximum and then decreases to its minimum, and 25 minutes of traffic are simulated overall. We also apply radio error bursts as defined in (3.9) every 6 min of simulation in the $i = 9^{\text{th}}$ vehicle in the platoon to simulate the burst of packet losses in the most critical moment.

From Table 3.3, we notice that Case 1 exhibited 8 collisions while cases 2, 3 and 4 had none. In the first case, the system is assumed to operate in an average traffic condition. However, it can be seen that this is not a safe approach, since

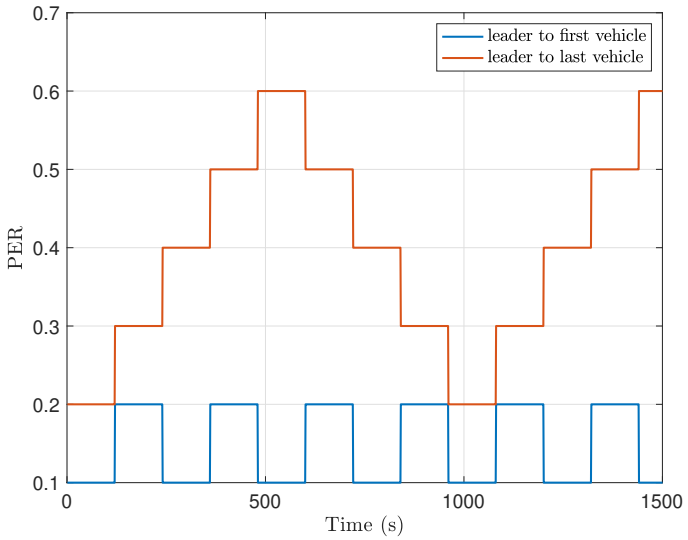

Figure 3.14 – Traffic density pattern adopted for the best and the worst communication link with the leader, illustrated in blue and orange, respectively.

it does not guarantee a secure operation. In case 2, despite no collisions, there is an increase of 21% and 33% in the inter-vehicular distance when compared to cases 3 and 4, respectively. Case 4 is capable to improve approximately 10% in the inter-vehicular distance when compared to Case 3. Furthermore, it demands fewer communication resources since it adopts a distributed control approach, while Case 3 uses homogeneous control that requires an exchange of the same information in the whole platoon.

To give more insights about the platoon dynamics, Figure 3.15 illustrates the average inter-vehicular distance for the heterogeneous approach. It can be noticed that vehicles at the beginning are closer, while vehicles at the end tend to keep larger distances due to poor communication conditions with the leader. Therefore, the proposed heterogeneous approach is demonstrated to be the best option, so that platoon formation remains robust while reducing the average inter-vehicular distance.

3.6 Concluding Remarks

This chapter studies the design of the platoon control algorithm based on the V2V communication quality. We started by devising the optimal parameters of the controller for different communication qualities, namely the weight given to the information broadcast by the platoon leader (C parameter), and the desired

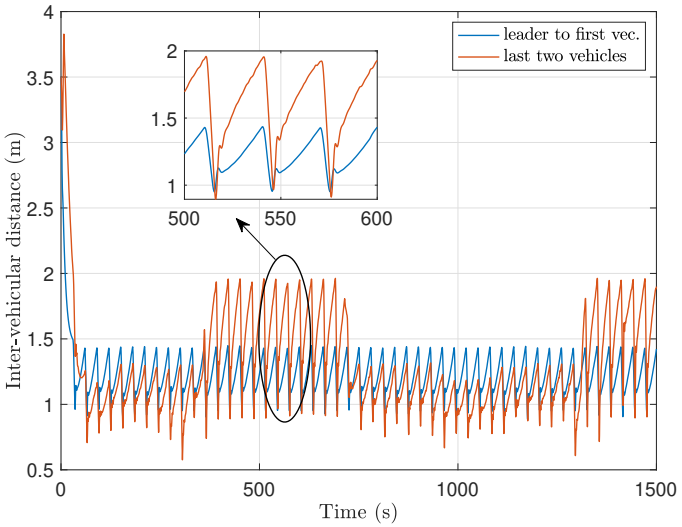

Figure 3.15 – Illustration of the average inter-vehicular distance for the first two and last two vehicles considering the Case 4 simulation.

distance (D_{des}) between vehicles. We then proposed a new dynamic approach based on the offline optimization of the control parameters (C, D_{des}). In this dynamic scheme, the quality of the communication link is continuously monitored and the control parameters updated accordingly based on the results of the offline optimization. Our simulation results show that, if the control parameters *are not adapted to the channel quality*, the *semi-autonomous control* performs best. However, with the *proposed adaptive heterogeneous control, using leader information results in a better performance.*

A careful design of fundamental platooning performance is investigated through the built simulator. From Matlab WLAN toolbox and the Simulink environment, we are able to implement the platoon V2V communication channel and the platooning longitudinal mobility. Moreover, due to proper development of both systems in one overall simulation scheme, we are able to perform the first contribution of this thesis that resides in the dynamic scheme based on PCACC controller previous mentioned. In particular, the flexibility to improve the system design with additional consideration of certain control and communication aspects motivates the argument to develop our own. For instance, in the next chapter, a slightly different control law that incorporates the wireless delay is examined jointly with improved network design of the channel access.

Finally, as we have shown, the quality of the communication link is a key parameter for the performance of a platoon formation. In fact, the link between

the leader and other vehicles in the platoon quickly deteriorates based on the distance due to path loss, and other interfering links that also contend for the medium. Moreover, for even larger platoon sizes or more congested channel, such a decay phenomenon is expected to worsen the communication quality even more the system performance, putting at stake the safety of whole platoon formation. In order to work around, different approaches are possible. One promising method will be further investigated in the next chapter. It consists of relaying the leader's most updated information to the following platoon members by the usage of V2V and/or RSU infrastructure. Furthermore, a comprehensive performance analysis is provided such as the platoon performance, observed in terms of inter-vehicle distance, and an evaluation of the impact of network QoS carried out in terms of packet error rates and delays.

Chapter 4

Analytical modeling of platoon under V2X relaying scheme

So far, we have presented the main motivations that drives us to find better transport solutions, in which one promising alternative is platooning systems. Then, fundamental aspects of the combined effort to its deployment is covered in Chapter 2. In the previous chapter, a careful design of network and control teamwork is introduced, and we conclude that large platoon sizes and channel congestion might alter the platoon performance, which calls out for solutions that are able to improve the reliability of the leader message. In addition to an improved design of the network communication system and the control scheme, this chapter addresses the relaying systems as a solution to extend the communication range of the leader. Vehicles communicate essential information for platooning control through multi-hop vehicle-to-vehicle (V2V) communications and are assisted in this task by Roadside Units (RSU), when available. While classical approaches, adopted in previous and current mobile systems, consider the application needs solely as requirements for the communication network, we advocate a bi-directional interaction of application and communication network. We first study the impact of different communication strategies on the application-level performance, namely the inter-vehicle distance in the platoon. Such schemes introduce a trade-off between the packet delivery rate and the additional delay introduced by relaying. In order to assess the impact of both metrics, we start by developing a Markov model for the different communication links (inter-vehicle and vehicle-to-RSU). We then propose a cross-layer approach that adapts the application layer (platoon control parameters) to the observed Medium Access Control (MAC) layer performance. We demonstrate via simulations the benefit of the proposed relaying scheme, and that a joint design of application and communication systems is essential for enabling the integration of industrial applications in future generation networks.

4.1 Introduction

In this chapter, we investigate the joint design of the Vehicle to Everything (V2X) network and the platooning control scheme. We specifically consider relay-assisted vehicle-to-vehicle (V2V) communications for conveying essential platooning information. When a vehicle (platoon leader or member) sends a packet, it is overheard by the other vehicles and the Roadside Units (RSU) that may relay the packet, increasing thus the packet delivery ratio but introducing an additional delay. We propose analytical models for the network and application sides and then use them for joint optimization.

On the network side, we propose a novel model for the channel access schemes with the presence of relaying links through V2V and the RSU. In particular, we model the presence of a large number of point-to-point V2V links, coexisting with a broadcast relaying link that conveys the leader's packets to the rest of the platoon. Our model also integrates the impact of radio errors resulting from the physical layer (link performance) within the Medium Access Control (MAC) layer model (packet collision estimation).

For the application layer, we consider the Predictive Cooperative Adaptive Cruise Control (PCACC) controller [47] and extend it by introducing a dynamic control mechanism where some of the parameters of the controller are adapted based on the expected quality of the radio system, as exposed in Chapter 3. We assess the performance of this proposed control scheme under the different relaying strategies. We specifically integrate the resulting packet error rate and delay distribution and evaluate their impact on the platoon performance. To the best of our knowledge, no prior studies addressed the analysis of the network performance with a comprehensive comparison between different relaying schemes while considering the coexistence of communication and control aspects.

In such a framework, the main contributions of this chapter are summarized as follows.

- Proposition and analytical modelling of a novel V2V relaying scheme and a study of the impact of RSU relaying. These models integrate the impacts of link and system levels.
- Evaluation of the impact of network QoS (errors and delay) on the controller performance.
- Offline optimization of the platoon control parameters for a given communication scenario.
- Joint optimization of the network and application as we show that the communication performance is impacted by the control performance and vice

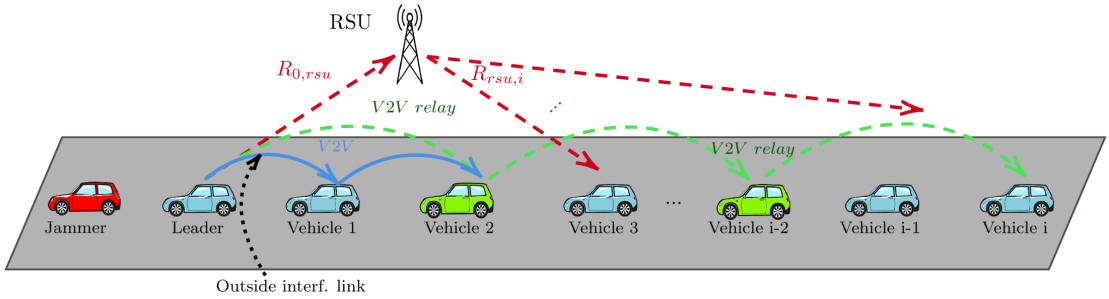

Figure 4.1 – Arrangement of a platoon with V2V and V2I relaying communication technologies. The solid blue lines are the vehicle to neighbour links, the dashed green and red lines are the broadcast links for V2V and RSU relaying, respectively, and the dotted black lines are the outside interference links from outside the platoon.

versa leading to behaviour that can not be easily predicted by a "silo-based" approach.

Related work

Many research works look at platooning formation, of which several have proposed different approaches in order to extend the coverage range of the leader message to other platoon members using relaying systems [73, 102–108]. In particular, two main factors are the motivation behind relaying in platooning systems: (i) large path loss fading caused by extensive platooning; (ii) external interference that substantially reduce the probability to decode the signal correctly. A recent evaluation on side-link relay for platooning was done by [102] where the authors proposed two relay schemes that use geographic location information. In [103], a disturbance adaptive platoon architecture is proposed where they adopt V2V relaying to mitigate negative effects of traffic disturbance such as uncomfortable passenger experience and increased exhaust emission. Inspired by Bianchi's 2-D Markov chain [104], the authors in [73] proposed a platoon-based cooperative retransmission scheme by formulating a 4-D Markov chain so that one sender can retransmit blocks to its neighbors within the same platoon in case of a previous transmission error. However, they consider the RSU as the only destination receiving data from all vehicles, which may not be the case in real applications. Instead of a highway scenario, the scheme proposed in [105] focused on the performance of safety message broadcasting for the road-intersection scenario. The authors in [105] adopted different antennas configurations for the RSU relaying.

Different from this work, the vehicle dynamics are neglected and no V2V relaying is evaluated. The authors in [106] proposed a centralized method of jointing power control and V2V relay selection. They assume a C-V2X communication where the leader performs the intra-platoon resource allocation for the platoon members after interacting with the eNB. However, the evaluation of the platoon performance is left for future work. In [107], a relaying policy for platooning applications using a TDMA-based scheme is proposed. The authors focus on enhancing the probability of receiving event-driven messages, which translates to focus on hazardous environmental events message over periodic vehicle awareness message. In opposition to these works, we do not aim at proposing new relaying schemes for platooning but use the existing relaying methods through V2V relaying and RSU to study the performance from an end-user perspective.

Another important contribution of this chapter is associated with the heterogeneous communication delays analysis and its impact on the control and networking performance. The design of control systems that explicitly takes into account network and vehicle performance is proposed in [94] where theoretical bounds on the minimum inter-vehicular distance are derived considering a network subject to packet losses. A few works evaluate the performance of platooning systems under heterogeneous wireless communication delays. The authors in [109] evaluated the effect of communication delay by considering packet dropout as a time delay chosen as multiple of the sampling period and upper bounded. Similarly, the authors in [110] proposed a robust distributed control based on Lyapunov-Krasovskii theorem and H_∞ control that ensures decent operation under stochastic wind and wireless communication delays. All aforementioned works have evaluated low time-delay values of wireless communication such as 20-40 ms while IEEE 802.11p presents no fixed upper bound delays for a contention-oriented MAC scheme [111]. Furthermore, the authors in [111] have investigated the MAC access delay distribution by proposing an exponential distribution as a reasonable approximation for it. However, no multi-hop broadcast is evaluated. Di Bernardo *et al.* [112] proposed a platooning control scheme based on the solution of a high-order consensus problem in the presence of heterogeneous time-varying delays. Despite interesting results, the authors assume that the leader vehicle is globally reachable, which might not be the case in real high dense scenarios and extensive platoons. Peng *et al.* [113] presented an IEEE 802.11p distributed coordination function (DCF) based communication model for multi-platooning where they present a probabilistic analysis of the communication performance considering intra and inter-platoon communications. However, the impact of relay-assisted platooning schemes is not explored in these studies.

In this chapter, we study a joint system of periodic platooning communication and control to reduce inter-vehicular spacing while maintaining platoon safety.

Several works evaluate the performance of platooning under different communication approaches [25, 38, 46, 65, 90, 114–116]. For instance, [90] used the 802.11p technology to evaluate the communication performance under a CACC controller in platoons. Likewise, [46] has adopted both 802.11p and C-V2X wireless technologies, and compared their performances in terms of the inter-vehicular distance of the platoon. Jia and Ngoduy [115] developed an enhanced cooperative traffic model considering V2V and V2I communications in order to improve the traffic flow and smooth shock waves. Ploeg *et al.* [65] proposed a control strategy for graceful degradation based on estimating the preceding vehicle's acceleration in case of packet losses, but it mainly deals with extreme cases like complete link failure or lack of a wireless device on one of the vehicles. Fernandes and Nunes [25] suggested different information management algorithms including one with a dynamical control parameter where they simply suggest a lower bound value for it. In [38], certain control parameters and the radio resource allocation are jointly considered. However, they do not consider the impact of state variables (position, velocity, and acceleration) on the platooning control while the impact of vehicle mobility on reliability is considered in our model. In fact, we aim at adapting the inter-vehicular distance of the platoon while observing the communication link quality. Note that in Chapter 3, we proposed a homogeneous and heterogeneous design of the controller under a simple radio model based on V2V only, while in this chapter we develop a joint communication/control model that considers sophisticated radio link and system models in the presence of V2V and RSU relaying methods.

The remainder of the chapter is organized as follows. Section II presents the platooning control system model. Section III presents the communication solutions considered in the platooning scenario, and introduces the proposed relaying algorithms. Section IV develops an analytical model for the performance of the communication network with the different relaying techniques. Section V presents simulation results for the platoon performance and an analysis of the impact of the different communication parameters on the platoon performance. While the main features of our system are captured by the analysis of Section V, we present in Section VI an extended performance analysis for exploring the impact of different RSU density, different platoon sizes and for comparing our scheme with the state of the art. Finally, we draw conclusions in Section VII.

4.2 Platooning control system

As in the previous chapter, we consider a longitudinal platoon of N vehicles, arranged as 1 platoon leader and $N-1$ platoon members. However, in addition to it, here the platoon members are distributed as non-relaying and $N_r - 1$ relaying

vehicles as depicted in Figure 4.1 in blue and green colors, respectively. The vehicles in all other lanes are not necessarily in platoons, and a jammer precedes (in red) the platoon leader. In order to stabilize the platoon under the presence of the jammer, while reducing the distance between the platoon members, the platoon leader communicates data about its acceleration and velocity to all the members of the platoon, as does also each vehicle to its following one. If packets are lost or delayed, the platoon performance may be adversely affected. Therefore, the communication link reliability is imperative to the deployment of controlled platoons. We introduce in this section a brief overview of the system with the proposed dynamic control, and the considered communication scenarios specific to platooning.

4.2.1 Vehicle dynamics and objective of platoon control

As already specified in the previous two chapters, the vehicle dynamics are equivalent in this chapter. Therefore, we adopt an actuator lag of $\tau = 0.5$ s, and to avoid recurrence, the reader is kindly invited to check Section 2.2.1 of Chapter 2 and Section 3.3.1 of Chapter 3 for further discussions. The objective of platoon control is to allow the platoon members to track the leader's speed, while maintaining a desired constant distance gap D_{des} between preceding vehicles in the absence of any disturbance in the leader's vehicle, i.e, no acceleration nor braking. The constant spacing condition being satisfied can be written as

1) $\lim_{t\to\infty} |\dot{x}_i(t) - \dot{x}_0(t)| = 0$

2) $\lim_{t\to\infty} |x_i(t) - x_{i-1}(t) + L_i + D_{des}| = 0$

where the first limit aims to mimic the leader's speed while the second aims to keep a desired distance D_{des} between preceding vehicles in the platoon where L_i is the length of vehicle i.

4.2.2 Platoon controller with delay factor

We describe briefly the application level control schemes for the platooning scenario. A thorough understanding of the dynamics of the controller is indeed essential for the design of relevant communication schemes. Contrasting the previous chapter, we adopt a modification version of the PCACC controller to incorporate packet delays. Such scheme implies that the control effort, i.e. the desired acceleration, of the leader ($\ddot{x}_{0\_des}$) and of the preceding vehicle ($\ddot{x}_{(i-1)\_des}$) are available

to the following vehicle under certain delay time, and its control law is given by

$$\begin{aligned}\ddot{x}_{i\_des}(t) = (1-C)\ddot{x}_{(i-1)\_des}(t-\boldsymbol{\zeta}) + C\ddot{x}_{0\_des}(t-\boldsymbol{\varphi}) \\ - (2\xi - C(\xi+\sqrt{\xi^2-1}))\omega_n\dot{\epsilon}_i(t-\boldsymbol{\rho}) \\ - (\xi+\sqrt{\xi^2-1})\omega_n C(\dot{x}_i-\dot{x}_0)(t-\boldsymbol{\varphi}) - \omega_n^2\epsilon_i(t-\boldsymbol{\rho}) \end{aligned} \tag{4.1}$$

Note that the bold terms are brought in to highlight the variation from the former PCACC controller in the previous chapters. Such terms are the miscellaneous type of delays considered, allowing the evaluation of the impact of network delay on the controller performance, as explained next. The spacing error ϵ_i is defined in (2.5), and as we adopt a constant spacing policy, the spacing error derivative is the relative velocity between vehicles, defined by $\dot{\epsilon}_i = \dot{x}_i - \dot{x}_{i-1}$. The control parameters to be tuned are C, ξ and ω_n. As already mentioned, the parameter C takes on values $0 \leq C < 1$ and is responsible to weigh the contribution of the leader's speed and acceleration. ξ is the controller damping ratio and ω_n is the controller bandwidth. Therefore, the most up-to-date values of the $(\ddot{x}_{0\_des}, \dot{x}_0, \ddot{x}_{(i-1)\_des})$ in (4.1) are subject to wireless inherent characteristics such as packet dropouts or delay, as follows. ρ consists the delay in sensor measurement and disturbs preceding radar information of position and velocity as in (2.5) and its derivative, respectively. ζ is the delay in V2V wireless communication from $(i, i+1)$ vehicles, and affects the preceding vehicle acceleration $(\ddot{x}_{(i-1)\_des})$. Lastly, φ describes the delay in wireless communication from $(0, i)$ link, and it affects the acceleration and velocity of the leader $(\ddot{x}_{0\_des}, \dot{x}_{0\_des})$. Broader explanation of different types of communication links are explained in the next sections.

4.3 Communication mechanisms for platooning

In order for the platoon control to be efficient, there is a need for a reliable exchange of information between neighboring vehicles and from the leader to the rest of the platoon. We introduce in this section the communication solutions considered along this chapter, which are significantly different from the ones adopted in the Chapter 3.

4.3.1 Baseline scheme with V2V communications only

In this baseline, vehicles use direct communication links. Without loss of generality, we consider an IEEE 802.11p-like access on the unlicensed spectrum. The model can be easily extended to other contention-based mechanisms. There are three types of links, as follows:

- Vehicle to neighbor links, where each vehicle conveys its acceleration and velocity to its preceding one. For a platoon of N vehicles, there are $N-1$ such links. We denote by $(i, i+1)$ the link between vehicle number i and its preceding. Following the CSMA/CA mechanism, a packet on this link is repeatedly transmitted until an ACK is received from vehicle $i+1$, or the maximum number of transmissions, say m is reached. Such links are displayed in (blue) solid lines in Figure 4.1 for the first two and omitted for the rest for simplicity.

- Broadcast links, where the platoon leader or the assigned relaying vehicles communicates its information to the rest of the platoon. As there is no native broadcast channel design in CSMA/CA, it cannot be expected that an ACK is received from each vehicle. The leader, therefore, does not wait for an ACK to retransmit but attempts a fixed number of repeated transmissions denoted by m_l. We denote the broadcast link from the leader to vehicle i as $(0, i)$.

- Outside links, that correspond to signals from an interfering source that does not belong to the platoon. We consider M such links and model them as interference as shown in (black) dotted lines in Figure 4.1.

4.3.2 Relaying of the leader's packets

Looking back at the control mechanism defined in (4.1), the $(i, i+1)$ links convey local control information that is weighted by parameter $(1-C)$, while link $(0, i)$ is responsible for carrying information of the leader, weighted by parameter C. Knowing that the distance on link $(0, i)$ is generally large and that it is subject to larger shadowing (because of the existence of cars in-between the leader and the vehicle i), it is of utmost importance to enhance its quality. Therefore, we adopt relaying through V2V and RSU as solutions for the broadcast channel, where the relaying vehicles in the platoon and RSU relay the packet received from the leader, in a broadcast manner to all other vehicles. We consider two flavors of relaying as follows.

4.3.2.1 V2V relaying

This scheme has the advantage of not employing extra infrastructure. Certain vehicles in the platoon are able to relay the leader's message, namely relaying vehicles, which act like additional contending nodes in the channel. Furthermore, this introduces delays in the system that can not be neglected, and its impact is evaluated in the next section. We use N_r to denote the total number of broadcast links. Such links are arranged as $N_r - 1$ for relaying vehicles and one for the leader

with m_r and m_l fixed number of transmissions, respectively (without waiting for an ACK). This communication can be received by any other vehicle in the platoon but the control packet may be outdated due to the delay induced by the relaying. We denote the broadcast link from selected relays V2V vehicles r_z, $z \in \{0, \cdots, N_r - 1\}$ to vehicle i by (r_z, i). Such links are visible in dashed lines in Figure 4.1.

We propose a novel system of relaying the leader packets by exploiting the V2V communications already used in the baseline scheme to vehicle-to-neighbor communication. The main idea is that the assigned relaying vehicles will communicate with their neighbors only after receiving information from the leader, either directly from the leader or via another relay. Since the schedule of the leader's packet generation is fixed, the only variable is the delay to transmit due to the access delay caused by the CSMA protocol. Let's denote the mean access delay by ζ, which is computed later in Section 4.4.1. Therefore, each relay node waits for a maximum time of twice this delay multiplied by the relay index before generating its own packet so that it can receive the leader information from the leader or a previous relay. Then, it will include the information from the leader on the vehicle-to-neighbor communication packet. This implies that the relaying is done *without excessive addition of packets into the network*, and therefore not increasing the network load or generating interference for the other vehicles. This procedure is detailed in Algorithm 1.

We will next describe the information management of the presented V2V relaying scheme. Algorithm 1 is based on a round-robin scheduling or a token based protocol, in which a relay waits for a packet from the previous relay or leader before communication. This type of a sequential relay is useful to minimize the delay induced by the relay. The delay here refers to the time between the measurement of the leader information (velocity and acceleration) to the time at which this information is received by a vehicle in the platoon. If all the relays communicate randomly, the average delay induced per hop can be of the order of 50 ms plus the waiting time in the CSMA/CA queue. However, when the relays communicate sequentially, this delay can be reduced to just the waiting time.

In the V2V relaying information scheme, described in Algorithm 1, the leader of the platoon broadcast m_l times its desired acceleration and velocity to the rest of the platoon at each cycling period t_c. Then, each vehicle in the sequence transmits its data to the corresponding follower one. Moreover, if a particular vehicle is a relaying vehicle that successfully decoded the leader's signal, it will incorporate the latest leader packet it has and broadcast its own data with m_r retransmission attempts. Observe that we look at the expected or average delay, and we set the maximum waiting time by a relay to be twice of this value in Algorithm 1.

Remark 4.1. *The sequential scheme and the waiting time proportional to z is utilized to ensure that the latest leader information is propagated with minimal*

Algorithm 1: V2V relaying information scheme

for all t_c **do**
Leader broadcasts m_l times its acceleration and velocity ($\ddot{x}_{0\_des}$, $\dot{x}_0$);
for all non relaying vehicles i **do**
Vehicle i receives the acceleration and velocity ($\ddot{x}_{0\_des}$, $\dot{x}_0$) from leader or overhears it from certain relay, if any;
Vehicle i transmits its desired acceleration and velocity to its successor vehicle;
for all V2V relays r_z **do**
Vehicle r_z receives the leader acceleration and velocity ($\ddot{x}_{0\_des}$, $\dot{x}_0$) from the leader or another previous relay;
After the max. waiting time of $2z\zeta$, vehicle r_z broadcast m_r times its acceleration jointly with leader's acceleration and velocity ($\ddot{x}_{r_z\_des}$,$\ddot{x}_{0\_des}$,$\dot{x}_0$);
end for
end for
end for

delay. This implies that relay r_z communicates before relay r_{z+1}, and therefore can not listen to the message of r_{z+1}. We are thus able to estimate the packet error rates and delays of the leader packet at each relay by causality checks. For non-relaying vehicles, no extra information management logic is enforced since such vehicles can overhear any broadcast messages from the leader or relaying vehicles without a directional distinction.

4.3.2.2 RSU relaying

The second form is the RSU relaying, where the RSU is considered as an additional node in the system; it overhears the packet sent by the leader to vehicle 1 (let $(0, RSU)$ be this link), and then retransmits it in a broadcast manner, without expecting feedback. We denote the broadcast link from the RSU to vehicle i by (RSU, i). Note that since the RSU acts as a broadcast relay, it does not expect or receive any feedback, and therefore, does not attempt re-transmissions even if its packets are lost. The main advantage of the RSU is having a direct line of sight link with both the leader and all the other vehicles in the platoon and introducing minor delays when compared to the V2V relaying approach.

Algorithm 2 details the information handling agreement needed for the appropriate management under RSU relaying with unlicensed spectrum. In such a case, the leader broadcast m_l times its data to the rest of the platoon where each vehicle member, in sequence, transmits its information to their respective follower. How-

Algorithm 2: RSU relaying information scheme

for all t_c **do**
Leader broadcast m_l times its acceleration and velocity ($\ddot{x}_{0\_des}$, $\dot{x}_0$);
for all vehicles i **do**
Vehicle i receives the acceleration and velocity ($\ddot{x}_{0\_des}$, $\dot{x}_0$) from leader or RSU relay;
Vehicle i transmits its desired acceleration and velocity to its successor vehicle;
for closest RSU relay from leader do
RSU receives the acceleration and velocity ($\ddot{x}_{0\_des}$, $\dot{x}_0$) from leader;
After the delay ζ, the RSU broadcast only once leader's acceleration and velocity ($\ddot{x}_{0\_des}$,$\dot{x}_0$);
end for
end for
end for

ever, after having correctly decoded the leader's data, the closest RSU from the leader will also contend for the medium by broadcasting it only once to the rest of the platoon. Note that the RSU relaying must wait the mean access delay (ζ) before transmitting which is due to consider it as an additional contending node. Therefore, when comparing with the previous algorithm, the RSU relaying takes advantage by not demanding a special agreement between vehicles in the platoon. Moreover, it is installed sufficiently high for ensuring a LOS link with vehicles on the highway, and it introduces a much smaller delay when compared to the delay from the V2V relaying approach.

4.4 Communication performance analysis

In this section, we identify the main performance metrics on the different links and we introduce the mean access delay computation. Then, we propose an analytical model adapted to different platooning scenarios, and integrating both link and channel access levels. We first devise a Markov chain to model the CSMA/CA protocol with retransmissions for point-to-point V2V links. Next, we introduce the broadcast channel analysis and derive the probability that a given vehicle, numbered i, receives the packets of the leader. We finally extend the model to consider the V2V and RSU relaying cases for unlicensed spectrum.

Regarding the main performance metrics, we differentiate between link and system levels. At the link level, performance is characterized by the average Packet

Error Rate (PER), i.e. the probability that a particular transmission of a packet fails, due to fast fading and interference from other links. This PER takes two different values when the packet is conveyed alone, compared to the collision case when it is transmitted on an occupied channel. Let $f_{0,(k,l)}$ and $f_{c,(k,l)}$ be the PER for the collision-free and collision case, respectively, for links (k, l) defined above (k and $l \in \{RSU, 0, ..., N-1\}$. At the system level, the main performance metric is the packet loss, which incorporates the PER on the link level but also takes into account the m possible retransmissions and the CSMA/CA mechanism. We develop in the next section a performance model on the system level (channel access) that takes into account the link-level metrics.

4.4.1 Mean access delay

In the proposed V2V relaying scheme, a heterogeneous delay rises as each relaying vehicle waits a certain maximum time for the preceding relay's packet, after which it generates a packet to broadcast including the latest leader information it has. Once this packet is generated, it must wait for the contention window to expire before transmitting this packet. Note that different contention window sizes are possible, e.g. using the four access categories (AC) in IEEE 802.11p as shown in Table 2.2 (AC0 indicates the lowest priority with the highest contention window whereas AC3 indicates the highest priority with the lowest contention window). Therefore, we aim at evaluating its impact over the control performances in addition to the network performance. Such an evaluation is achievable due to the inclusion of the estimated average delay caused by different access categories in the dynamic control scheme, as in (4.1), for V2V relaying approach. More precisely, we evaluate the mean access delay (ζ) basing on the estimation of an average time interval between consecutive successful channel access attempts given by

$$\zeta = \frac{W \cdot T}{2 \cdot (1 - p_c)} \tag{4.2}$$

where $W/2$ is the average contention window, T is the packet period in the channel access, and p_c is the probability that the channel is busy during a slot. Note that we assume that the length of the packet is constant which is reasonable when the data frame is short in contrast to the protocol overhead. The backoff interval is calculated as a random number of slot times uniformly selected from [0,$W-1$]. As for the introduced delay by each approach, we have considered the following.

- Baseline introduces minimal delay in the system as we assume that once certain node is ready to transmit in the queue, it will send its most updated information measured just before transmitting. Also, due to the lack of relaying mechanism information, we assume a maximum link delay of 1 ms.

- In the presence of V2V relaying systems we have considered the following delay computation for each active relaying vehicle

$$\varphi_z = \zeta \cdot z \qquad \forall z \in \{1, \cdots, N_r - 1\} \tag{4.3}$$

  where ζ is the delay coefficient introduced by each relaying hop whose value corresponds to the average waiting time for a certain contention window size introduced in (4.2). z is the vehicle index of the effective selected relay vehicle that forwards the leader's message in the platoon.

- The RSU is considered as an additional node that contends with the medium by broadcasting only once, and therefore, the delay is computed as in (4.2).

4.4.2 Packet loss probability for V2V links

Before focusing on the analytical modeling of the proposed V2V relaying scheme, notice that vehicle to neighbor links, i.e. the link between a vehicle i and its preceding one $(i+1)$, are modelled as unicast transmission following the CSMA/CA protocol described next. Differently, for broadcast transmissions there is no acknowledgment frame, thus, we consider a simpler systematic retransmission.

We model the CSMA/CA channel access procedure using a discrete time Markov chain, as illustrated in Figure 4.2. Similarly to the authors in [73], [117,118], we adapt the Bianchi [104] model to unsaturated sources to better cope with vehicular networks. However, different from them, we consider, in addition to losses due to collisions between packets, losses that are due to imperfections on the radio channel.

Radio transmission errors are modeled using the function that maps the Signal to Interference plus Noise Ratio (SINR) to the packet error rate (PER) as previously shown in Figure 3.5. As in the previous chapter, the SINR is computed as (3.1) and we assume the Winner-II Scenario B1 as the propagation loss model as in [46, 87, 119]. The last component of (3.1) is the total interference coming from other vehicles that likewise contend for the medium, defined by P_I. Next, we aim to introduce how we compute the probability of loss for V2V links, taking in mind possible external interferences.

4.4.2.1 Vehicle to neighbor channel

At each transmission attempt, and focusing on link (k, l), the packet is correctly decoded with probability

$$\alpha_{(k,l)} = (1 - p_c) \cdot (1 - f_{0,(k,l)}) + p_c \cdot (1 - f_{c,(k,l)}) \tag{4.4}$$

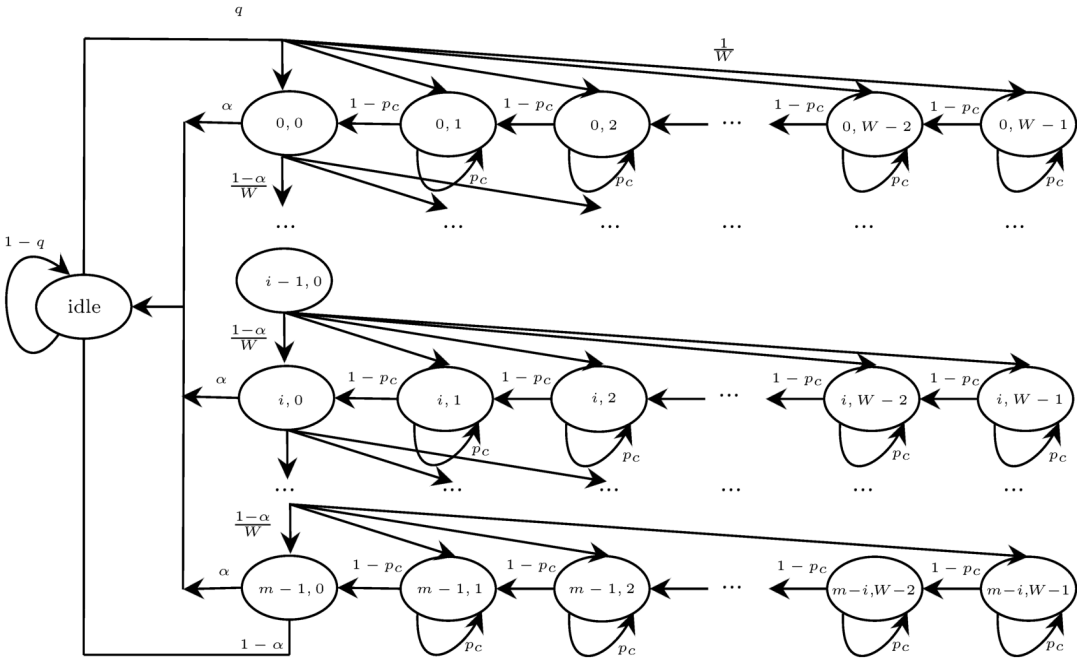

Figure 4.2 – Proposed Markov chain for baseline scheme.

p_c is the probability that the channel is busy during a slot (collision probability), f_0 is the probability of loss without collision, and f_c is the probability of loss with collision, introduced previously and computed in the numerical applications under a vehicular channel environment given by (3.1). We drop in the following the link identification (k, l) for convenience, except when needed. The evaluation of the detailed impact of packet collision due to interference in the system is of enormous complexity due to the vehicle's mobility. Nevertheless, it can not be neglected and we consider the following to be true.

Assumption 4.1 (**Probability of loss with collision**). *Regarding the probability of loss with collision between link* (k, l)*, we assume the following influence on the reliability of the model.*

$$f_{c,(k,l)} = \mathbb{E}_{P_I}[\phi(SINR_{(k,l)}(P_I))] \tag{4.5}$$

where $\phi(\cdot)$ *is a function that models the quality of the link* (k, l) *based on* $SINR_{(k,l)}$*.*

Note that such probability fluctuates over the distance between link (k, l) and the considered external interference. In fact, concerning the latter, we consider a uniform distribution where certain external vehicle contend for the medium with equal probability. Moreover, we may introduce the probability of loss without

collision over the same function that models the quality of the link (k, l) based on $SINR_{(k,l)}$ that yields

$$f_{0,(k,l)} = \phi(SINR_{(k,l)}(0)) \tag{4.6}$$

Assumption 4.2 (**Poisson process for packet arrival**). *In order to capture, the bursty nature of the traffic where small packets are generated by each vehicle following a Poisson process of intensity λ, we have included one inactive state in the Markov chain to model the probability to remain idle on a slot, taken equal to a packet duration T. For small T, this is approximated by $1 - q = e^{-\lambda T}$.*

In order to attain the probability of loss for point-to-point V2V links we establish the following. Define the Backoff Timer (BOT) as a randomly number chosen in the range $(0, W - 1)$ where W is the contention window (CW) size[1] for a generic access category. Next, define the Backoff Stage (BOS), as the stage attempt to transmit the packet. Let $s(t)$ be the stochastic process representing the BOS $\{0, \ldots, m - 1\}$ and $\Pi(t)$ representing BOT at time t. Let $\Pi_{k,j} = \lim_{t\to\infty} P\{s(t) = k, \Pi(t) = j\},\ k \in \{0, m - 1\},\ j \in \{0, W - 1\}$ be the stationary distribution of the chain.

Proposition 4.1. *The steady-state probabilities of the proposed Markov chain shown in Figure 4.2 are computed by:*

$$\Pi_{idle} = \left[1 + \frac{q(1 - (1 - \alpha)^m)}{\alpha} \cdot \left(1 + \frac{W - 1}{2(1 - p_c)}\right)\right]^{-1}. \tag{4.7}$$

Proof. To calculate the loss, we have to calculate the stationary probabilities of the states. Given the BOS and BOT defined above, we can recursively calculate the probability of states for the first backoff stage $k = 0$ and for any timer $2 \leq j \leq W - 1$, given by

$$\Pi_{0,W-j} = \frac{jq}{(1 - p_c)W}\Pi_{idle}. \tag{4.8}$$

Now, evaluating the last state (timer expiration $j = W$) for the first stage ($k = 0$), we have the following

$$\Pi_{0,0} = \frac{q}{W}\Pi_{idle} + (1 - p_c)\Pi_{0,1} = q\Pi_{idle}. \tag{4.9}$$

Therefore, taking into account the probability of success transmission introduced in (4.4), we can define the following

$$\Pi_{1,W-1} = \frac{(1 - \alpha)}{W}\Pi_{0,0} + p_c\Pi_{1,W-1} = \frac{(1 - \alpha)q}{(1 - p_c)W}\Pi_{idle}. \tag{4.10}$$

[1]The CW may change from one stage to another, but we adopt here, without loss of generality, a constant CW, as advocated for delay-sensitive services using LBT cat3.

Recursively, we can calculate the last states probabilities ($j = W$) for any backoff stage as

$$\Pi_{k,0} = (1-\alpha)^k q \Pi_{idle}, \tag{4.11}$$

for $0 < k < m-1$. Therefore, the probability of stationary states are given by

$$\Pi_{k,W-j} = \frac{jq(1-\alpha)^k}{(1-p_c)W}\Pi_{idle}, \tag{4.12}$$

for $0 \leq k \leq m-1$ and $1 \leq j \leq W-1$. Moreover, the steady-state probabilities must satisfy the normalization condition $\Pi'\Pi = 1$, that yields to (4.7) which concludes thus the proof. □

The loss depends on the probability of finding the channel occupied during a slot. For the broadcast channel, the transmission attempt probability for a packet generated from the leader and the relaying vehicles is given by

$$\tau_{\#} = q \cdot m_{\#} \tag{4.13}$$

where $\# \in \{l, r\}$ for leader and relaying, respectively as they attempt a constant number of transmissions. However, for the other V2V communications, the number of transmissions depend on the ACK and we will compute this using a fixed point approach as follows.

Proposition 4.2. *The channel occupation probability p_c is given by*

$$p_c = 1 - (1-\tau_p)^{N-1}(1-\tau_e)^M(1-\tau_r)^{N_r-1}(1-\tau_l). \tag{4.14}$$

where the following transmission attempt probabilities are investigated, when different nodes contend for the medium to transmit a packet. First, the probability of trying to transmit for intraplatoon link is calculated by:

$$\tau_p = \sum_{k=0}^{m-1} \Pi_{k,0} = \frac{(1-(1-\alpha_{i,i+1})^m)}{\alpha_{i,i+1}} q \Pi_{idle} \tag{4.15}$$

while for external link is given by

$$\tau_e = \sum_{k=0}^{m-1} \Pi_{k,0} = \frac{(1-(1-\alpha_{ext})^m)}{\alpha_{ext}} q \Pi_{idle} \tag{4.16}$$

Proof. The probability of a slot being busy is computed as the probability that at least one of the competing transmitters is active. More precisely, it encompasses the contribution for the neighbor, the interference from other vehicles, and the broadcast links to contend for the channel. For the first and second components,

we consider $N-1$ links within the platoon, and M external vehicles that do not belong to the platoon but generate nevertheless packets, respectively. For the broadcast component, we consider the leader and $N_r - 1$ relaying vehicles with distinct possible retransmissions. Therefore, we can thus compute the channel occupation probability as in (4.14) where τ_p (rep. τ_e) is the probability of trying to transmit for platoon and external vehicles, respectively, with the corresponding link decoding probability α precised as follows. For platoon vehicles, $\alpha_{(i,i+1)}$ is used, while for external vehicles, the same proposed Markov chain model can be used, replacing the PER in (4.4) by the PER corresponding to a typical distance on a non-platoon link (α_{ext}).

While for the broadcast component, the probability of trying to transmit the packet for the leader and relaying vehicles is computed as in (4.13) where $\# \in \{l, r\}$ for leader and relaying, respectively. While q is the probability of generating a packet, i.e. probability to not remain idle on a slot, while m_l and m_r are the broadcast retransmissions attempts for the leader and relaying vehicles for the broadcast component, respectively.

The channel occupation probability p_c can thus be obtained using a fixed point analysis that solves the set of equations (4.7, 4.14, 4.15, 4.16, 4.13). □

Note that we have modeled the capture effect by assuming that only collisions from a certain distance lead to a loss, so only devices within a distance are taken in the analysis. Interference that comes from far vehicles does not account. Therefore, the probability that a packet is lost on link $(i, i+1)$, i.e. neighbor link, despite the m possible retransmissions, is computed by:

$$L_{i,i+1} = (1 - \alpha_{(i,i+1)})^m, \quad i \in \{0, ..., N-1\} \tag{4.17}$$

Now that the final probability of packet error is defined for a vehicle to neighbor channel, we are able to compare the CSMA/CA performance, which includes the radio channel conditions as in equation (4.17), against the simpler contention-based Aloha protocol considered in Chapter 3. Figure 4.3 illustrates the final probability of loss for consecutive vehicles considering both CSMA/CA and Aloha protocol. In addition to lower probability of losses compared to Aloha, the CSMA/CA protocol considered here is less sensitive to the increase of interfering vehicles, as it can be seen from the flat curve shape for 60 interfering vehicles and beyond. The main reason is the consideration of losses that are due to imperfections on the radio channel in the final loss probability, which allows the system to assess packets even if a collision occurred evaluated based on the SINR level.

4.4.2.2 Broadcast channel

The broadcast mode is introduced and detailed here. In addition to outside links and vehicle to neighbor links, certain vehicles such as the leader and relaying

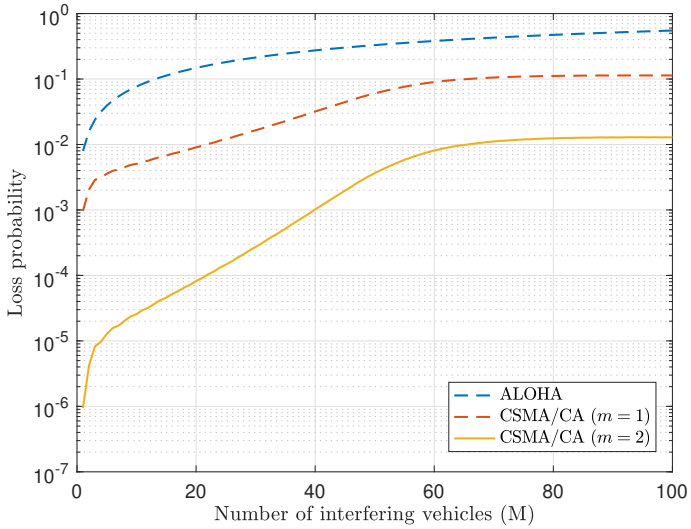

Figure 4.3 – Loss probability comparison, for consecutive vehicles, of CSMA/CA with no retransmission ($m = 1$), and one retransmission ($m = 2$) in dashed orange and solid yellow lines, respectively. Aloha is kept for comparison purposes in dashed blue.

vehicles contend for the shared channel with broadcasting messages as in (4.14). In fact, we assume different transmissions attempt for leader and relaying vehicles as m_l and m_r, respectively. Such particular vehicles periodically broadcast critical safety messages containing its acceleration and velocity, for instance. Therefore, the probability of loss of the broadcast link $(0, i)$ is given by

$$L_{(0,i)} = (1 - \alpha_{(0,i)} \cdot \sigma_0)^{m_l} \tag{4.18}$$

$\forall i \in \{1, \cdots, N-1\}$ where σ_0 is the probability that the packet is correctly decoded by the leader which is one by default and $\alpha_{(0,i)}$ is the probability for the leader message to be successfully decoded by the receiver vehicle i, considering packet collisions and path loss, as in (4.4). Moreover, note that vehicle mobility has not been neglected as the probability of loss with and without collision on a vehicular channel is taken into account. Furthermore, we assume m_l retransmission attempts, and due to the inherent feature of broadcast, no acknowledgement is possible. Finally, note that for broadcast channel, we consider a simpler broadcast chain with m_l systematic retransmissions (no backoff and no retransmission due to loss).

4.4.3 Performance analysis for V2V relaying

In Section 3.4 we have introduced a novel V2V relaying scheme in which we propose that certain platoon members are selected as relays, namely relaying vehicles r_z where $z \in \{0, \cdots, N_r - 1\}$. These relays are capable to forward the packets of the platoon leader along with their regular vehicle-to-neighbor communication as a decoded-forward relay in order to preserve the quality of platooning communication with no extra infrastructure or additional packet generation needed. In this subsection, we study the performance of such a relay.

Proposition 4.3. *The probability that the packet is correctly decoded by relaying vehicle r_z, where $z \in \{0, \cdots, N_r - 1\}$, is given by*

$$\sigma_z = \begin{cases} 1 & z = 0 \\ 1 - (1 - \alpha_{r_0,r_1} \cdot \sigma_0)^{m_l} & z = 1 \\ 1 - (1 - \alpha_{r_0,r_z} \cdot \sigma_0)^{m_l} \prod_{k=1}^{z-1} (1 - \alpha_{r_k,r_z} \cdot \sigma_k)^{m_r} & \\ & \forall z \in \{2, \cdots, N_r - 1\} \end{cases} \tag{4.19}$$

*The final probability of loss between the leader and a particular **non** relaying vehicle i in the presence of V2V relaying is thus calculated as*

$$L_i = (1 - \alpha_{r_0,i} \cdot \sigma_0)^{m_l} \prod_{z=1}^{N_r - 1} (1 - \alpha_{r_z,i} \cdot \sigma_z)^{m_r} \tag{4.20}$$

$\forall i \in \{1, \cdots, N-1\} \wedge i \neq r_z$. *While, the final probability of loss between the leader and certain relaying vehicle r_z is*

$$L_{r_z} = 1 - \sigma_z \qquad \forall z \in \{0, \cdots, N_r - 1\} \tag{4.21}$$

Proof. In broadcast transmission, the leader sends packets to all platoon members simultaneously as in (4.18). Note that relaying vehicles communicate only after receiving information from the leader either directly from it or from another previous relay. Once correctly decoded, they are able to hand over the information as a broadcast with m_r possible retransmissions to the posterior platoon members. For the V2V relaying link, we define the probability that the packet is correctly decoded by each relaying vehicle as (4.19). The reasoning for each line is as follows:

- $\sigma_0 = 1$ because leader always has packet;
- $\sigma_1 = 1 - (1 - \alpha_{r_0,r_1} \cdot \sigma_0)^{m_l}$ corresponds to the hop from the leader to the first relaying vehicle which is broadcasted m_l times, i.e. it can be seen as the complement of (4.18) for link $(0, r_1)$ instead;

□ $\sigma_z = 1-(1-\alpha_{r_0,r_z}\cdot\sigma_0)^{m_l}\prod_{k=1}^{z-1}(1-\alpha_{r_k,r_z}\cdot\sigma_k)^{m_r}$ as now we have the influence of $z-1$ hops of the previous relaying vehicles that are broadcasted m_r times and calculated recursively for each $z \in \{2,\cdots,N_r-1\}$.

where $\alpha_{(r_0,r_z)}$ is the probability for the leader message to be successfully decoded by the receiver selected relaying vehicle r_z, considering packet collisions and path loss, as in (4.4). Note that Algorithm 1 is required to guarantee the functional operation of the V2V relaying approach. More precisely, such specific order token ring alike between relays is essential to preserve causality, which explains the upper bound limit of the product operator in (4.19). In other words, it prevents that certain relay vehicle σ_{z+1} to handle and forward a message before relaying vehicle σ_z, where $z \in \{0,\cdots,N_r-1\}$, by assuring certain maximum waiting time as described in Section 4.3.2.1. Moreover, for each hop we consider independent events in which the product rules can be applied. Therefore, the final probability of loss between the leader and a particular *non* relaying vehicle i in the presence of V2V relaying is then computed by (4.20). However, note that no specific order is considered as any *non* relaying vehicle is able to overhear the broadcast relayed transmission which explains the upper bound limit of the product operator in (4.20) that accounts for all possible N_r-1 relaying vehicles in the platoon. Furthermore, the final probability of loss between the leader and certain relaying vehicle is given by (4.21) where with (4.19) we confirm that for relaying vehicles the causality constrain was imposed. This completes the proof. □

4.4.4 Performance with RSU relaying

In addition to the V2V relaying scheme, we aim to extend the Markov model to the RSU relaying case. Whenever the leader sends a packet to its platoon, this packet can be also received by the RSU closest to the leader, which then relays the packet as a broadcast.

Proposition 4.4. *The final probability of loss between the leader and the vehicle i in the presence of RSU is*

$$L_i = L_{(0,i)} \cdot \left(L_{(0,RSU)} + L_{(RSU,i)} - L_{(0,RSU)} \cdot L_{(RSU,i)}\right) \tag{4.22}$$

where the loss on the downlink is thus given by

$$L_{(RSU,i)} = p_c f_{c,(RSU,i)} + (1-p_c) f_{0,(RSU,i)}, \tag{4.23}$$

while the uplink is given by the probability of loss of (4.18) considering the link $(0, RSU)$ accordingly.

Proof. A loss for a broadcast channel occurs here only if both the direct $(0, i)$ link and the relaying link fail, increasing the robustness of the system. In other words, we consider independent events in which the product rule applies. As for the relaying link, it is composed of two links $(0, RSU)$ and (RSU, i) as shown in Figure 4.1. Accordingly, with a simple additive rule of probability we are able to compute the relaying factor through RSU. Therefore, the final probability of loss between the leader and the vehicle i in the presence of RSU is given by (4.22).

To ease the comparison with the previous V2V relaying approach, we consider in this work the RSU relay link under unlicensed spectrum. The RSU in this case is a node like the others in the IEEE 802.11p system. The RSU here overhears the transmission on the leader-follower link, and its probability of loss is computed as in (4.18), taking into consideration in $\alpha_{(0,RSU)}$ the PER on the uplink of the relay.

If the packet is correctly decoded, the RSU is able to broadcast it, only once, to the other platoon members. We model this downlink of the relay by a one-stage Markov chain (like the one in Figure 4.2, with $m = 1$) where the loss on the downlink is thus given by (4.23), which concludes the proof. Such results are in line with Algorithm 2 that describes the information handling agreement when adopting RSU as the relaying scheme. □

4.5 Simulation results

In this section, we present our numerical results which compare the performance of the baseline scheme, the proposed V2V relay and an RSU relay. We also illustrate the interaction between the proposed dynamic controller and the communication schemes in a realistic platooning simulation.

4.5.1 Simulation environment description

In our simulations, vehicles in the platoon move along a highway with 2 lanes per direction with 4 m width each. An overview of the system diagram is given in Figure 4.4. Although similar to Figure 3.4, we provide the delay component as input to the control system simulator, in addition to the loss rate. Moreover, the channel access mode is completely redesigned to address the CSMA/CA mechanism. Therefore, as previously, we used the Simulink environment to model the vehicle dynamics and to implement the control law, which corresponds to the "Platoon simulator". Therefore, it is responsible to give periodic snapshots of the positions of the platoon vehicles to the communication simulator. As shown in Figure 4.4, the communication framework is implemented with Matlab and its WLAN Toolbox and some main parameters are highlighted as input/output. The first one is the ("Link simulator") which computes the PER for a given link quality based

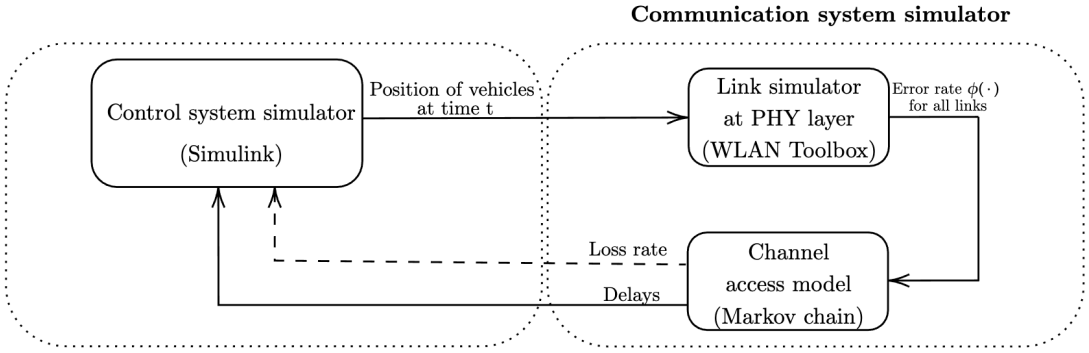

Figure 4.4 – Block diagram of system simulator with control and communication interaction.

on the positions of vehicles obtained from the platoon simulator system. Finally, the ("Channel access model") is responsible to model the channel access, which is implemented as modeled using the Markovian model presented above, considering that vehicles broadcast a 500 bytes message under baseline, V2V, and RSU relaying conditions, if applicable. In the simulation analysis, we use the 10 MHz channel with a 100 ms scheduling period that corresponds to the 10 Hz CAM message generation frequency, as advocated by the ETSI EN 302 637-2 standard [97]. The system parameters for both communication and control-traffic model are specified in Table 4.1.

Remark 4.2. *We make use of the MATLAB WLAN Toolbox^{TM} for the simulation of the PHY layer of IEEE 802.11p standard. More precisely, with this toolbox, we are able to compute the PER of an 802.11p link between a transmitter and a receiver, considering a V2V fading channel and for a given link quality (SNR/SINR), i.e., $\phi(\cdot)$ from Assumption 1. However, it does not include the competition between links to access the channel. Therefore, we also develop a "Channel access" module which models interference with other links, including V2V, broadcast transmissions by relays and external interfering sources that contend for channel access.*

When not stated otherwise, we have adopted the following framework. For the link $(0, i)$, we assume a shadowing that increases linearly with the number of vehicles in the platoon (2 dB per intermediate vehicle). As for the CSMA parameters, we have adopted $W = 32$ and $m = m_l = m_r = 2$ as the contention window size and the retransmission attempts for the neighbor, leader, and V2V relay link, respectively. Furthermore, for the RSU relay scheme, we have implemented one RSU each one kilometer.

As for the control parameters, the platoon members are equipped with the dynamic proposed controller. Different from the literature, we evaluate the system

Table 4.1 – Communication and control and traffic simulation parameters

Communication		**Control and Traffic**	
Parameter	**Value**	**Parameter**	**Value**
MAC protocol	802.11p	Leader factor (C)	0.5
Path loss	Winner+B1 LOS	Desired dist. (D_{des})	Adaptive
Noise power	-174 dBm/Hz	Damping ratio (ξ)	2
Tx power	22.5 dBm	Bandwidth (ω_n)	0.5 Hz
Shadowing	2dB/vechicle	Actuator lag (τ)	0.5 s
MCS	QPSK, R=1/2	Vehicle length (L)	16.5 m
Data rate	6 Mb/s	Max. acc. (u_{max})	+2m/s^2
Channel	Highway LOS	Min. acc. (u_{min})	-3m/s^2
Carrier frequency	5.9 GHz	Radar interval	60 ms
Bandwidth	10 MHz	Lanes per direction	2
CAM size	500 bytes	Lane width	5 m
CAM interval	100 ms	Max. traffic density (M)	Fig. 4.5b
BOT (W)	32	Simulation duration	1200 s
BOS (m)	2	Jammer profile	Fig. 4.5a
BOS leader (m_l)	2		
BOS relays (m_r)	2		

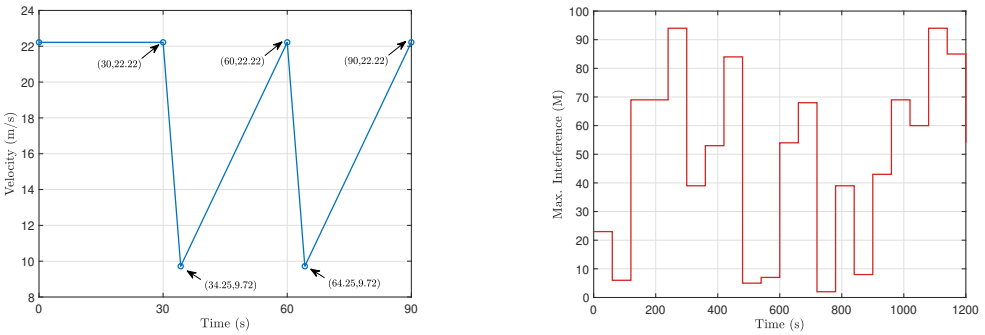

(a) Jammer velocity profile.

(b) Traffic density profile.

Figure 4.5 – Illustration of different profiles adopted over time.

performance under a strongly perturbed scenario as shown by the jammer profile in Figure 4.5a, but repeated 50 times to seek robustness. The control strategy demands relative position and longitudinal velocity of the preceding vehicle so we assumed that the measurements are sampled each 60 ms with a delay of $\rho = 1$ ms and done by a long-range radar. Simulations are performed with a platoon size of $N = 21$.

Another important simulation aspect is the traffic density profile. The maximum road traffic density that generates external interference to the platoon was considered as $M = 100$ cars/km/lane and its profile is shown in Figure 4.5b. We have implemented it as a uniformly distributed random parameter with a period of 60 s. Notice that the traffic density period is doubled when compared to the jammer incidents that occur each 30 s.

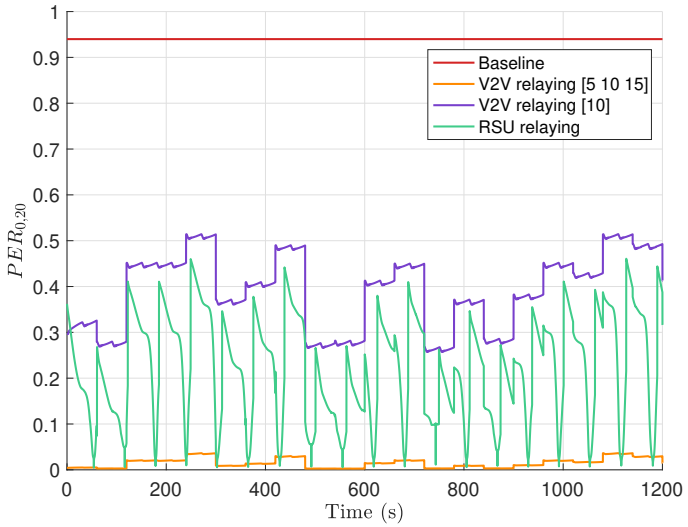

Figure 4.6 – PER for 20th vehicle for the different communication scenarios with $m = m_l = m_r = 2$ retransmission attempts.

In order to cope with the information handling algorithm presented in the previous section, a simpler way is to consider the delay as a linear uniformly distributed random function for each V2V relaying vehicle. So, by each relaying vehicle's index, the delay increases linearly and, therefore, the causality imposition in the proposed handling algorithm is attended. From (4.2), the correspondent delay value for $W = 32$ is $\zeta = 9.8$ ms for each relaying vehicle hop.

4.5.2 Communication system performance

We next describe the performance from a communication perspective with platoon sizes of $N = 21$. Note that the reliability of the system-level performance is measured by the packet loss as defined in (4.18), (4.20)-(4.21) and (4.22) for baseline, V2V relaying and RSU relaying, respectively. We present a communication radio link comparison as shown in Figure 4.6 for 21 vehicles, where we present the average probability of loss between the leader and the last vehicle over time for each communication approach considered. We observe from Figure 4.6 that V2V scenario without any V2I results in a very high loss rate when compared to RSU relaying scheme and V2V relaying vehicles. This loss is expected to be even higher for larger platoons. Due to the very large inter-vehicular distance required to avoid a vehicular collision, the path loss and shadowing play a substantial role comparing to the number of external interference vehicles which explains the rough behavior of a straight line for the baseline in Figure 4.6. While relay schemes exhibit a more

Table 4.2 – Performance metrics over different communication schemes for platoon size N=21, $m = m_l = m_r = 1$.

Outputs	Baseline	V2V Relay		RSU Relay
		r = [5 10 15]	r = [10]	1RSU/1km
Avg. Dist. (m)	32.6280	2.2476	21.4118	2.1350
Min. Obs. Dist. (m)	1.1163	1.4125	1.8963	1.2991
Max. Obs. Dist. (m)	63.2088	2.6910	34.2947	2.5584
Avg. PER (10th car)	0.9579	0.1779	0.8666	0.1033
Avg. PER (20th car)	0.9695	0.2088	0.9534	0.2222

Table 4.3 – Performance metrics over different communication schemes for platoon size N=21, $m = m_l = m_r = 2$.

Outputs	Baseline	V2V Relay		RSU Relay
		r = [5 10 15]	r = [10]	1RSU/1km
Avg. Dist. (m)	32.4961	2.2455	2.6458	2.1357
Min. Obs. Dist. (m)	1.3476	1.4884	1.9203	1.3837
Max. Obs. Dist. (m)	60.9268	2.6045	3.1339	2.5501
Avg. PER (10th car)	0.9196	0.0184	0.2642	0.0555
Avg. PER (20th car)	0.9399	0.0150	0.3903	0.2227

cyclic behavior with respect to the closest RSU from the leader vehicle (recall that an RSU is deployed every 1 Km).

4.5.3 Platoon performance: inter-vehicle distance

We now move to the evaluation of the robustness of our dynamic control scheme under different communication links. To this aim, we have adopted the inter-vehicle distance as the end-service performance metric. We apply the zero-order hold mechanism as the holding strategy for the control signal during the periods of packet losses. In all simulations, we focus on minimizing the inter-vehicular distance with respect to a fixed value of all the other control parameters while ensuring that zero vehicle collisions occur. Note that we implemented a safety gap distance of 1 m for the emergency braking actuation to avoid collisions in practical settings.

4.5.3.1 Platoon performance for different network configurations

We first start by evaluating the performance of the platoon under different network configurations. We present in Table 4.2 and 4.3 the average inter-vehicular distance for 21 vehicle platoon over all the communication approaches considered for retransmission attempts $m = m_l = m_r = 1$ and $m = m_l = m_r = 2$, respectively. A baseline without relaying is also considered but will be discussed later in section 4.6.1. From the former table, we can observe large inter-vehicular distance

for V2V relaying with only one relaying member vehicle i.e. vehicle 10 as the selected relay $r = [10]$. However, when the retransmission attempts increase better platooning performances are obtained for the relaying vehicle $r = [10]$ as shown in Table 4.3. That is due to substantial improvements on communication performances of around 70% for the average packet error rate for the 10th vehicle under V2V relaying $r = [10]$ produced by boosting m_l and m_r that allows forwarding the leader's message more reliably. Clearly, regardless of the retransmission attempts, the baseline scheme imposes higher inter-vehicular distances in the platoon, as much as 32 m, when compared to relayed schemes where the average distance is around 2 m. We also illustrate in Table 4.2 and 4.3 the minimum observed distance during the simulation (that must not go below 1 m to avoid emergency braking) and the maximal observed distance for their respective platoon size. When looking at the platoon performance with relaying, similar performances are observed for both relay schemes, despite the large difference in the loss rates, as recalled in the last rows of Table 4.3. This similarity raises a question related to the necessity or not of RSU relaying and its additional infrastructure for platooning systems when compared with V2V relaying that shows slightly larger inter-vehicular distances but with no extra cost required while satisfactory retransmission attempts are observed.

4.5.3.2 Optimization of the communication protocol for the platoon

We have observed above that the platoon performance highly depends on the parameters of the network, and that there is no systematic correlation between the degradation of the packet success rate and the platoon performance. This indicates a certain robustness towards the packet loss rate. As control systems are known to be sensitive to packet delays and not only to packet losses, we investigate in this section the impact of delay on the platoon performance for a fixed number of retransmission attempts of $m = m_l = m_r = 1$. The network parameter that influences most the delay is the backoff parameter (waiting time before retransmissison that is a random number of slot times uniformly selected from $[0, W - 1]$). The results are shown in Figure 4.7. We can observe that increasing W leads to considerable improvement of the average packet error rate in the platoon as displayed in solid blue and red lines for the 10th and 20th vehicle, respectively. This is because increasing the backoff times reduces the collision probability p_c. However, considerable access delay is proportionally introduced as in (4.3) by each selected relaying vehicle. Therefore, regarding the control performance, the results in the right axis of Figure 4.7 show that more than doubled inter-vehicular distance is now required to avoid collision when considering the correspondent extremes contention window values (8 and 1024, resp.), leading to an inter-vehicle distance of 2.24 m and 4.65 m, respectively. Therefore, the best

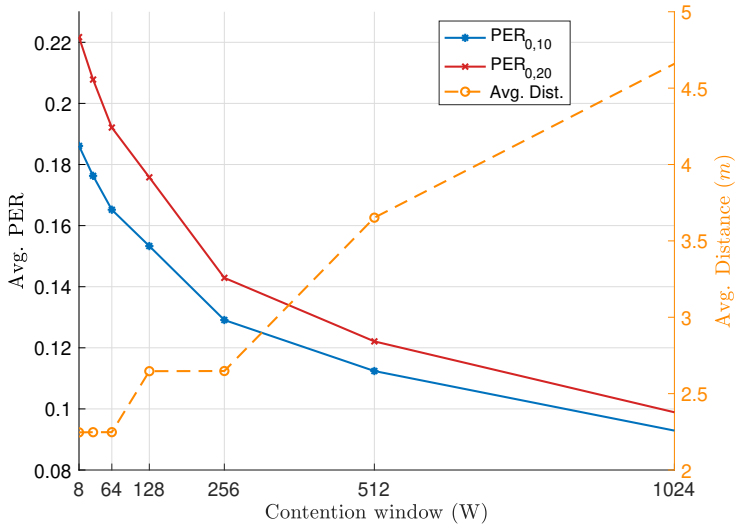

Figure 4.7 – Average packet error rate for 10th and 20th vehicle under V2V relay $r = [5\ 10\ 15]$ approach in solid blue and red lines, and average inter-vehicular distance of the platoon for different contention window sizes in dashed yellow line, respectively.

trade-off is observed for $W = 64$ which significantly improves the average inter-vehicular distance of the platoon while achieving a lower average packet error rate (and therefore a lower retransmission probability and a lower interference to other systems).

4.6 Extended performance analysis

While the above performance analysis captures the essential features of the joint communication/control design, there is a myriad of parameters that impact the performance and there are schemes in the literature that consider communication network for platooning. We first compare in this section our scheme to the state of the art. We then explore the impact of these parameters, including the road-side unity density, and the size of the platoon.

4.6.1 Comparison with classical approaches

We now compare our scheme against the classical approaches [102], [111], [38], [120], that simply fix an inter-vehicular distance for the platoon and do not consider the bi-directional interaction between control and communication parameters. We present the following comparison with our baseline approach with $N = 21$ vehicles

presented in Table 4.3. We have set a fixed distance of $D_{des} = 5$ m between vehicles, and we can indeed observe moderate packet errors rate as $PER_{0,10} = 0.34$ and $PER_{0,20} = 0.89$ for the 10th vehicle and 20th vehicle in average, respectively. Note that such high values for the 20th vehicle are achieved due to the significant length of each vehicle as $L = 16.5$ m and the extensive size of the platoon with $N = 21$ vehicles. However, such a scenario does not guarantee a secure outcome as 9 collisions are detected. In fact, due to the interplay of control and communication system, the PER and distance blow up and the safe distance becomes 32 m with $PER_{0,10} = 0.92$ and $PER_{0,20} = 0.94$ for the 10th vehicle and 20th vehicle in average, respectively, as shown in Table 4.3. As it can be seen, a joint approach eliminates collisions and requires higher distances that result in a higher PER, which requires the vehicles to be even further apart and so on in a recursive loop. Therefore, a joint analysis is especially important as the communication performance is impacted by the control performance and vice versa leading to behavior that can not be easily predicted by a singular approach.

4.6.2 Impact of the RSU density

The ability of vehicles in a platoon to communicate with the infrastructure relies on the amount and radio coverage for the RSU relaying approach. The best (minimal) amount of RSUs that allows safety operation (short inter-vehicular distance with no collision) of the platoon is a critical design choice factor. Therefore, the trade-off between cost deployment and safety operation is analyzed as indicated as follows. We assume a uniform mesh deployment policy that consists of distributing RSUs uniformly on the road, regardless of the roadmap topology or the traffic density. Table 4.4 encompasses three different cases evaluated in this work and the correspondent control performance. For each case, we adopt the Algorithm 2 aforementioned to assure the correct information handling protocol and to properly select the RSU to communicate with. As shown in Table 4.4, when the density becomes larger (1RSU/5km) much higher inter-vehicular distances as 26.61 m are required to avoid a collision. This is due to the fact that the packet error rate is incredibly large (close to 1) at certain moments in the time simulation as shown (in green) in Figure 4.8, where we present the average probability of loss between the leader and the last vehicle ($i = 20$) over time for each RSU density treated. A good compromising between cost deployment and safe operation of the platoon is reached with 1 RSU per 2km as it allows to severely reduce the cost of deploying the infrastructure, without losing performance when compared to a shorter density as of 1RSU/1km. Different deployment policies are indeed an interesting subject for future research.

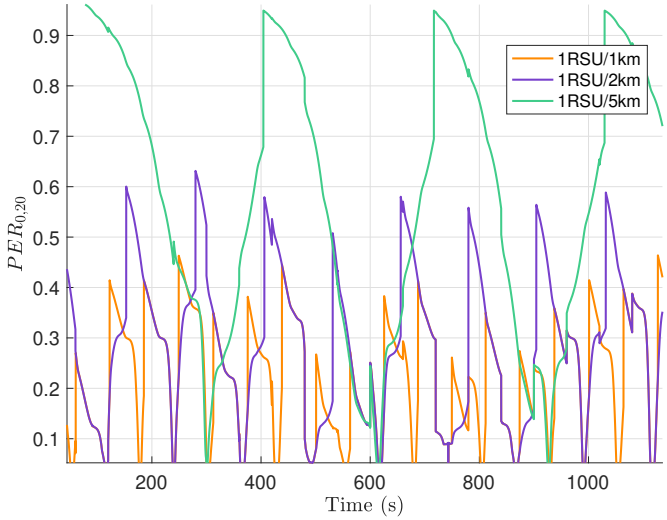

Figure 4.8 – PER for between leader and last vehicle for different RSU densities.

Table 4.4 – Performance metrics over different RSU relaying densities for platoon size N=21 with 0 db shadowing.

Outputs	RSU density		
	1RSU/1km	1RSU/2km	1RSU/5km
Avg. Dist. (m)	2.1350	2.7313	26.6127
Min. Obs. Dist. (m)	1.2991	1.6223	1.5270
Max. Obs. Dist. (m)	2.5584	3.2624	36.0392
Avg. PER (10th car)	0.1033	0.1497	0.5289
Avg. PER (20th car)	0.2222	0.3050	0.5923

4.6.3 Impact of the platoon size

The system performance has been evaluated in the previous section for a platoon of 21 vehicles. However, one question we would like to answer in this section is if relaying schemes are useful when the platoons are much smaller. For this purpose, we consider a platoon of $N = 11$ vehicles and study its need in terms of system design. We observe in Figure 4.9 substantially lower packet error rates for the last vehicle. Due to shorter platoon size, larger coverage, and consequently shorter inter-vehicular distances, the baseline approach varies accordingly with the external interference as the channel path loss plays a limited role now. Even though relaying approaches have smaller loss rates, similar control performances are obtained which raises a question of relaying approach's requirement for smaller platoon sizes as shown in Section 4.5.3. However, it is important to note that despite what the simulation results on the system-level performances indicate,

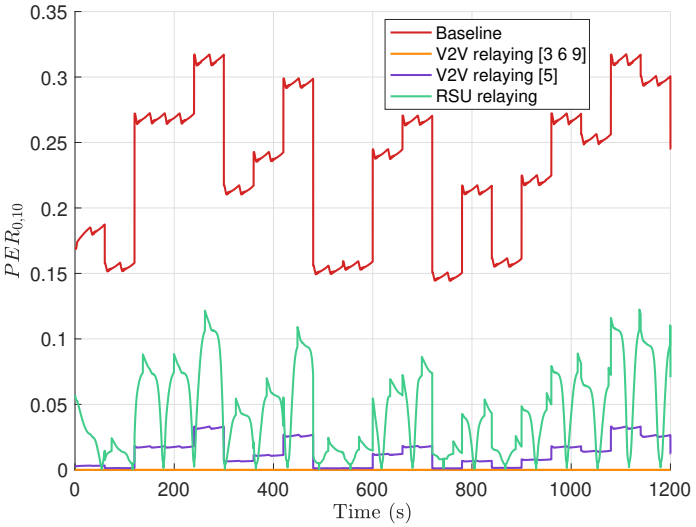

Figure 4.9 – PER for 10th vehicle for the different communication scenarios with $m = m_l = m_r = 2$ retransmission attempts.

Table 4.5 – Performance metrics over different communication schemes for platoon size N=11, $m = m_l = m_r = 1$.

Outputs	Baseline	V2V Relay		RSU Relay
		$r = [3\ 6\ 9]$	$r = [5]$	
Avg. Dist. (m)	3.1058	1.7112	2.2104	1.6896
Min. Obs. Dist. (m)	2.1928	1.0758	1.5719	1.0355
Max. Obs. Dist. (m)	3.4987	2.0638	2.5826	2.0493
Avg. PER (5th car)	0.1706	0.0003	0.1666	0.0330
Avg. PER (10th car)	0.4979	0.0011	0.1494	0.0872

these simulations have been run for a limited time, and the impact of packet bursts and improbable effects have not been studied. A lower packet error rate will result in a safer and more robust system-level performance due to smaller randomness in the dynamics.

On the other hand, for platoon size of $N = 11$ similar control performances are obtained regardless of the communication approach adopted as shown in Table 4.5 and 4.6 for $m = m_l = m_r = 1$ and $m = m_l = m_r = 2$, respectively. Which indicates that for smaller platoons no extra relaying approach is mandatory as even for the baseline a satisfactory outcome is observed. This fact can be explained by the robustness of the dynamic PCACC control for a sampling rate of 100 ms under moderate packet losses due to limited path loss effect. Finally, Figure 4.10 shows the average inter-vehicular distance of the platoon size $N = 11$ with the respective interference number of vehicles over time. We can observe that, the

Table 4.6 – Performance metrics over different communication schemes for platoon size N=11, $m = m_l = m_r = 2$.

Outputs	Baseline	V2V Relay		RSU Relay
		$r = [3\ 6\ 9]$	$r = [5]$	
Avg. Dist. (m)	2.2124	2.2143	2.2122	1.6896
Min. Obs. Dist. (m)	1.5622	1.5099	1.5640	1.0714
Max. Obs. Dist. (m)	2.577	2.5635	2.5635	2.0318
Avg. PER (5th car)	0.0328	≈ 0	0.0343	0.0071
Avg. PER (10th car)	0.2313	≈ 0	0.0126	0.0443

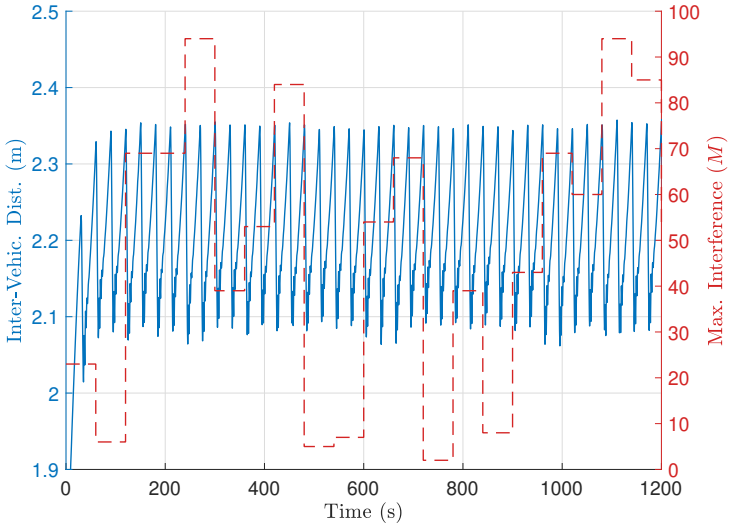

Figure 4.10 – Average inter-vehicular distance for platoon size of $N = 11$ under baseline approach in solid blue, and traffic density profile over time in dashed red lines.

average inter-vehicular decreases slightly for higher interference, and a smooth control performance and spacing is observed overall.

4.7 Concluding Remarks

In this chapter, we have proposed an integrated design of control and communication systems for future V2X networks, focusing on the platooning use case. We advocate that such integrated control is essential for enabling industrial applications in highly contended networks. We propose a novel analytical model to compute the probability of packet loss in a platoon with and without a relay support, through RSU or V2V relaying. An offline optimization of the control parameter,

inter-vehicular distance, is then presented based on the computed loss rate. The numerical results show that the joint communication-control optimization scheme with V2V relaying can significantly reduce the inter-vehicular distance while guaranteeing the control and communication requirements. However, the best platoon performance is achieved when the contention window is optimized so that the channel access delay is reduced without excessively increasing the packet error rate; this ensures a lower inter-vehicular distance while maintaining robustness of the proposed control scheme to moderate communication errors.

Additionally, we have evaluated the impact of the RSU density, the platoon size and demonstrated a comparison over classical static control strategies in terms of platoon and network performance. Even though substantial improvements in the communication platooning system has been done with the development of relaying systems techniques, the fuel efficiency problem has received limited attention so far. In fact, as exposed in Chapter 1, fuel corresponds to 35% of the total operating cost of the business model of certain enterprise [1], and, therefore, cut down such expense is the main financial motivation behind platoon systems. The results presented in chapters 3 and 4 indeed focus on the minimization of the inter-vehicle distance between the platoon members. However, no analysis has been done yet in order to quantify the fuel gain under platoon operation. Therefore, in the next chapter we intend to tackle the fuel efficiency problem in a substantial unique approach with the use of classical control schemes and recent deep reinforcement learning techniques.

Chapter 5

Fuel efficiency improvements to platooning systems

Until now, this thesis concentrated in the joint design of the network and control system for platooning. More precisely, we have focused on the minimization of the desired distance (D_{des}) that determines the inter-vehicle distance between the platoon members, regardless the control effort and fuel performance. However, this chapter is primarily concerned with the impact of vehicle platooning on the fuel consumption. The wide appeal of fuel-efficient transport solutions is constantly increasing, due to the major impact of the transportation industry on the environment. Platooning systems represent a relatively simple approach in terms of deployment towards fuel-efficient solutions. This chapter addresses the reduction of the fuel consumption attainable by dynamically switching between two control policies, Adaptive Cruise Control (ACC) and Cooperative Adaptive Cruise Control (CACC), in platooning systems. We propose one enhanced controller responsible to mitigate undesired transient responses. The main objective is to find the set of controllers that is a combination of both under challenging disturbances. In this framework, we adopt Deep Reinforcement Learning (DRL) techniques to overcome unpredicted platoon disturbances, and to learn appropriate transient shift times while minimizing the fuel consumption. However, due to safety and convergence issues of DRL, our algorithm establishes transition times and minimum periods of operation of ACC and CACC controllers, instead of directly controlling vehicles. Numerical experiments show that the model-based DRL agent outperforms both static ACC and CACC versions, and the threshold control in terms of fuel-efficiency, while also keeping a robust and safe approach.

5.1 Introduction

The efficient operation of platooning systems is meaningful due to its substantial economic and environmental impact. This chapter's focus is on the suitability of switching controllers in order to improve the fuel efficiency in platooning systems. For simplicity, this chapter is divided in two parts. First, we adopt a deterministic approach to evaluate the platoon fuel efficiency. We identify that based upon the disturbances caused by the vehicle that precedes the platoon, namely jammer, a specific controller might be more appropriate than other, in terms of fuel efficiency. In particular, we evaluate such disturbances in a platoon under Adaptive Cruise Control (ACC) or Cooperative ACC (CACC). The former one is pertinent due to the relative low complexity of the controller, which does not rely on the communication system, and, therefore, might boost the deployment of platooning systems in the near future. Moreover, it is generally adopted as back up strategy in case of losing the communication system link [65, 67]. Whereas the second controller allows shorter inter-vehicle distances, which translates to substantial improvements in the fuel performance due to the air-drag reduction. However, the control effort for each alternative plays an important role in the fuel efficiency [121, 122], and must be carefully evaluated. As an additional remark, we would like to point out that the switch between both controllers is motivated by possible problematic scenarios, for instance when a long burst of losses in the communication network is observed, or by the requirement of extra inter-vehicle distances imposed by merging and splitting maneuvers, and when aggressive jammer behavior is detected for some period, which the ACC acts as the appropriate support technology. Subsequently, we propose an enhanced switch control to reduce the burden caused by switching controllers.

In the second part, we extend the previous analysis, but focusing on stochastic disturbances, and their effect on the platoon fuel efficiency. We start by modeling such disturbances with Markov chains that adequately cope with the required randomness of the profiles. In particular, we consider two opposite operating modes, a steady and an aggressive condition, to impose robust outcomes. In addition to the switching operating modes, we introduce troublesome conditions to mislead the system, and increase robustness. We propose two different controllers to determine the best switching moment. The former one is a threshold control, while the latter adopts a Deep Reinforcement Learning (DRL) approach. We assess their performance by performing several simulations to obtain a reliable amount of samples.

The main contributions of this chapter is to demonstrate the feasibility of switching controls to coordinate a platooning in terms of safety and fuel efficiency. Firstly, we identify the burden caused by switching controllers under determin-

istic disturbances, and thus, we propose an enhanced controller to mitigate such transition losses. Secondly, we model such disturbances as a random process and reformulate the vehicle platoon fuel efficiency problem in a DRL framework. To the best of our knowledge, the present study is the first to propose a method to reduce fuel consumption, while accounting for stochastic traffic conditions that determines the switching control scheme.

Related work

In the literature, many works have addresses external forces such as aerodynamics drag, rolling resistance and gravitation forces, which indeed are imperative to investigate the fuel consumption problem of platooning system [9, 10, 18, 121, 123]. Alam *et al.* [18] conducted an experimental study on the fuel reduction potential for platooning systems under CC and ACC control with different time-gaps. Unlike this work, the authors in [18] surprisingly conclude that when a platoon is under a more stringent control effort, the overall fuel consumption does not increase. On the other hand, we demonstrate that a more stringent control, in our case the CACC, is actually more fuel demanding when compared to a less stringent control, in our case the ACC, as naturally expected. Liang *et al.* [123] proposed a parameter called the platooning incentive factor responsible to indicate whenever is beneficial to form a platoon. However, their approach is only valid under no traffic conditions, which has limited practical purposes. More recently, the same authors proposed in [9] an extension scheme that addresses that all vehicles in the platoon (including the leader) must participate in the platoon formation, and not only the platoon members. Their algorithm guarantees fuel improvements for the whole platoon, instead of individual vehicles progress. De Hoef *et al.* [10] proposes a centralized platoon coordinator explicitly considering the effect of speed and the fuel consumption for a large number of vehicles. The authors focus on a path planning approach to be assigned by a subset of vehicles called coordination leaders to which other platoon members adapt. Turri *et al.* [121] exploits the road topography information to predict the behavior of vehicles to improve fuel efficiency in the platoon. Unlike this work, the authors in [121] assume that external disturbances, as traffic ahead, are handled manually by the drivers.

Another meaningful contribution of our study is related to the deep reinforcement learning approach, adopted to learn from trial and error the most suitable action, in order to reduce the fuel consumption of the platoon when under stochastic disturbances. In this context, researchers try to find solutions using such machine learning techniques [124–128]. Yu and Sethi [124] were one of the first to adopt Reinforcement Learning techniques to generate steering control signal to maintain the vehicle moving within road boundaries. In a platoon framework, Ng

et al. [125] proposed a gain schedule control to be learned by a RL technique. The authors show that when under platooning they approach performs better than a simple linearization of the longitudinal model. The first attempt to use RL for controlling CACC was done by Desjardins and Chaib-draa [126]. Different from this work, the authors in [126] adopt a policy-based algorithm, which allows them to handle continuous-state variables and directly attempt to achieve the longitudinal control, as output of the neural network. However, they faced oscillatory behavior of the RL approach, which is overcome in our work, as we do not attempt to control directly the platoon with such framework. Li *et al.* [129] applied RL to the development of an ACC control that aims to maximize the expected time before system constraints, such as the acceleration and velocity, are violated. Therefore, the authors weakly address the fuel efficiency problem, as they just attempt to constraint the velocity and acceleration, which indirectly limits the fuel consumption. They adopt a hybrid Markov process to model the lead vehicle dynamics, while we adopt continuous Markov chains with two opposites modes to produce robust outcomes. Ling *et al.* [127] considered a platoon in which the future velocity profile of the preceding vehicle is predicted by Artificial Neural Networks (ANNs) techniques that uses a topographic map of the road as input. Such velocity prediction system is used together with a Model Predictive Control (MPC) that controls the platoon. More recently, [128] adopted neural networks for the estimation of the aerodynamic drag coefficient for platooning, which under performed traditional approaches due to limited availability of data.

Lately, Deep Neural Networks (DNNs) have been successfully applied to improve the learning ability of RL techniques, which lead to the development of the Deep Reinforcement Learning (DRL) framework. In this context, Chu and Kalabi [130] proposed a model-based DRL approach that learns the best headway signals for CACC in a platoon. Unlike this work, they simply investigate a catch up maneuver to the leader vehicle, which does not justify the DRL framework. Whereas in this work, our platooning system is under severe traffic condition imposed by stochastic disturbances that pose an enormous challenge to maintain the platoon within the system's constraints, which clearly motivates the adopted framework. Li *et al.* [131] also adopted a DRL framework, but they used a deterministic policy gradient algorithm, which it is trained to perform appropriate overtaking maneuver for autonomous vehicles. However, no attention was made towards the fuel consumption problem and platooning operation. Chen *et al.* [132] focus on a path planning point of view that attempts to determine the best path strategy for the platoon through the employment of DRL techniques. The authors make a restrictive assumption by selecting a mild road selected area for the path alternatives that the vehicles are able to choose. Different from the aforementioned works, we aim at optimizing the fuel consumption by adopting two different control

switching strategies while remaining within a safe and fuel efficient distance.

The rest of the chapter is organized as follows. Section 5.2 presents the system dynamics, the fuel consumption model, and the treated controllers including an enhanced proposed switching control. In Section 5.3, we introduce analysis for optimal switching when constant disturbances are considered. Section 5.4 addresses the disturbances as a random processes. In Section 5.5, we present two proposed switching controllers strategies to improve the fuel efficiency of the platoon. In Section 5.6, we perform a performance comparison over static control approaches. Finally, Section 5.7 concludes the chapter.

The notation used throughout is standard. For real vectors or matrices, $(')$ refers to their transpose. The symbols $\mathbb{R}$, $\mathbb{R}_+$, $\mathbb{N}$, $\mathbb{K}$, and Γ denote the sets of real, real non-negative, natural numbers, $\mathbb{K} = \{1, 2, \cdots, N\}$ for a natural integer N, and $\Gamma = \{0, 1, 2, \cdots, r\}$, where r is a fixed positive integer, respectively. Finally, we denote $\otimes$ the Kronecker product.

5.2 System Model and Problem Statement

The objective of this section is to present the platoon modelling that is noticeably different from the approach in previous chapters. In particular, the framework is more tailored towards control. Then, we present the feedback linearization proposal, the fuel consumption model, and finally the modified control schemes adopted in this chapter.

5.2.1 Platoon modelling with external forces

In the literature, there is a lack of works that investigate the feasibility of platooning under non-ideal traffic conditions. Therefore, the impact of time-varying traffic conditions on the fuel efficiency of the platoon, and some methods to improve such performance is our main contribution. Different from the previous chapters, we aim at improving the fuel efficiency of the whole platoon. In order to do so, significant changes in the platoon modeling must be made when compared to the previous approach. First, it is necessary to include external forces, and particularly the air-drag resistance, that is one of the main parameters that alter the fuel efficiency of the platoon. Second, we must define the fuel function that will be an essential part of the evaluation process. As earlier mentioned, we adopt the constant spacing policy to exploit the best the platoon gain formation. Therefore, consider the following constant spacing error of the ith vehicle as

$$e_i(t) = p_i(t) - p_{i-1}(t) + L_{i-1} + D_{des} \tag{5.1}$$

and its derivative as

$$\dot{e}_i(t) = v_i(t) - v_{i-1}(t) \tag{5.2}$$

where the index i symbolizes the vehicle index and $i \in \{0, 1, \ldots, N-1\}$, the leader vehicle being 0. L_{i-1} is the length of the vehicle $i-1$ and D_{des} is the constant distance that we seek between vehicles, and $p_i(t)$ and $v_i(t)$ are the position and velocity of the vehicle i, respectively. Different from the previous chapters, here we consider a longitudinal vehicle model with additional external forces as follows

$$\begin{aligned} m_i \cdot \frac{dv_i}{dt} &= F_{eng_i} - F_{air_i} - F_{roll_i} - F_{g_i} \\ &= F_{eng_i} - \frac{1}{2} c_{D_i}(d) \psi_i A_{f_i} \rho_{air} {v_i}^2 - c_{r_i} g m_i \cos\theta - g m_i \sin\theta \end{aligned} \tag{5.3}$$

where the engine force is denoted F_{eng}, the air drag force F_{air}, the roll resistance force F_{roll}, and F_g the gravitational force. Furthermore, m_i designates the vehicle mass for vehicle i, v the vehicle speed, $c_D(d)$ is the air drag coefficient and $\psi \in [0, 1]$ is the possible reduction air-drag, c_r the roll resistance coefficient, A_{f_i} is the front area of vehicle i, ρ_{air} is the air density, θ denotes the road slope, and g the gravitational constant.

Note that (5.3) as it is, presents very complex dynamics, so in order to cope with the non-linearity and simplify its dynamics, we adopt the following control law:

$$F_{eng_i} = u_i m_i + \frac{1}{2} c_{D_i}(d) A_{f_i} \rho_{air} {v_i}^2 + c_{r_i} g m_i \cos\theta + g m_i \sin\theta \tag{5.4}$$

where u_i is the new input signal to be designed. Note that the interest in such feedback linearization controller is to linearize the vehicle dynamics (drop the square dependency on velocity) and to simplify the vehicle dynamics by eliminating other parameters such as road slope, air-drag and roll resistance coefficients. After linearization, we adopt a reasonable model for the vehicle dynamics widely used in the literature [44, 63, 93, 133]:

$$\frac{d}{dt} \begin{bmatrix} p_i(t) \\ v_i(t) \\ a_i(t) \end{bmatrix} = \begin{bmatrix} 0 & 1 & 0 \\ 0 & 0 & 1 \\ 0 & 0 & -\frac{1}{\tau} \end{bmatrix} \begin{bmatrix} p_i(t) \\ v_i(t) \\ a_i(t) \end{bmatrix} + \begin{bmatrix} 0 \\ 0 \\ \frac{1}{\tau_i} \end{bmatrix} u_i(t) \tag{5.5}$$

where $\{p_i, v_i, a_i\}$ are the position, velocity and acceleration of the vehicle i, respectively. The subscript i is the vehicle platoon member index where $i \in \{0, i, \cdots, N-1\}$ and 0 the platoon leader's index. u_i is the control input of vehicle i after linearization, i.e., its desired acceleration. τ_i is the time constant of the first-order low pass filter for each vehicle i. The idea is to approximate the dynamics of the throttle body and vehicle inertia in order to avoid instantaneous response. Furthermore, control input constraints were applied to avoid unpractical acceleration

signals as

$$u_{min} \leq u_i(t) \leq u_{max} \tag{5.6}$$

where u_{min} and u_{max} are the minimum and maximum acceleration signal admitted that compass the control signal. In this chapter, we assume a lag of $\tau = 0.2$ s as in [134]. Note that for implementation reason, the discretization form of (5.5) is required, which can be computed by

$$\begin{bmatrix} p_i(k+1) \\ v_i(k+1) \\ a_i(k+1) \end{bmatrix} = \underbrace{\begin{bmatrix} 1 & T_s & 0 \\ 0 & 1 & T_s \\ 0 & 0 & 1\text{-}\frac{T_s}{\tau_i} \end{bmatrix}}_{\tilde{A}} \begin{bmatrix} p_i(k) \\ v_i(k) \\ a_i(k) \end{bmatrix} + \underbrace{\begin{bmatrix} 0 \\ 0 \\ \frac{T_s}{\tau_i} \end{bmatrix}}_{\tilde{B}} u_i(k) \tag{5.7}$$

Therefore, we adopt a sample time of $T_s = 100$ ms and a zero-order hold for the control input. So, the general notation of the open-loop model of the system in the discrete-time can be written as

$$x(k+1) = Ax(k) + Bu(k) \tag{5.8}$$

$$y(k) = Cx(k) + Dw(k) \tag{5.9}$$

where $x(k) \coloneqq [p_0\ v_0\ a_0\ e_1\ \dot{e}_1\ a_1 \cdots\ e_{N-1}\ \dot{e}_{N-1}\ a_{N-1}]'$, indicates the state-space vector of the system, $u(k) \coloneqq [u_i\ \cdots\ u_{N-1}]'$, is the vector of all control inputs. The vector of measurements available for feedback is defined as $y(k) \coloneqq [e_0\ \dot{e}_0\ v_0\ 0\ e_1\ \dot{e}_1\ v_1\ a_1\ \cdots\ e_{N-1}\ \dot{e}_{N-1}\ v_{N-1}\ a_{N-1}]'$, and $w(k) \coloneqq [p_j\ v_j]'$ is the exogenous input, i.e. the jammer position and velocity. Define $R = (r_{nm}) \in \mathcal{R}^{N \times N}$, where $r_{nm} = \text{-}T_s$ for $n = 3i\text{+}5$ and $m = 3i\text{+}3$, $i = \{0, \cdots, N-1\}$ and 0, otherwise. Thus, $A = I_N \otimes \tilde{A} + R$, $B = I_N \otimes \tilde{B}$, where $\tilde{A}$ and $\tilde{B}$ are defined in (5.7). Finally, note that

$$D = \begin{bmatrix} -I_{2\times 2} \\ 0_{3N-2\times 2} \end{bmatrix}$$

whereas C can be easily identified since the state-space $x(k)$ and the output $y(x)$ are defined. Next, we aim to introduce the fuel consumption model, that will be used to estimate the efficiency of the proposed techniques against classical approaches.

5.2.2 Fuel consumption model

So far, we have introduced the platoon modelling, which includes the external forces, and we derived the system dynamics. In other words, such set of equations describes how the position, velocity and acceleration of the vehicles relates with the control input. However, we are mainly interested in how such dynamics affect the fuel consumption of each vehicle when under different inter-vehicle distances in the

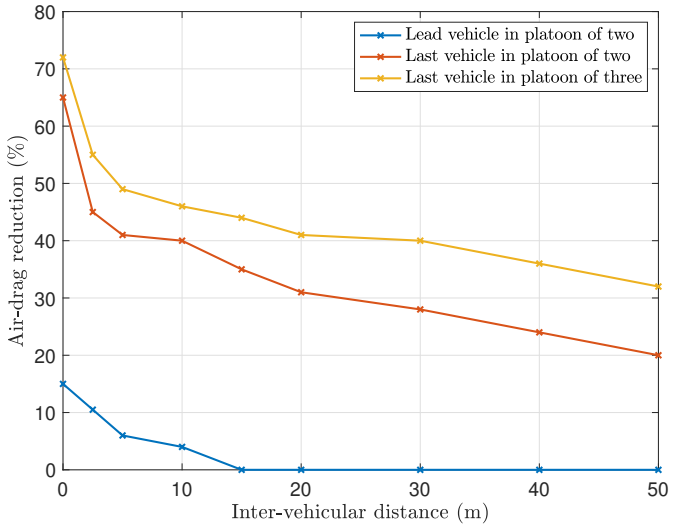

Figure 5.1 – Air-drag reduction for trucks in a platoon at $80km/h$ empirically obtained. The figure is adapted from [2].

platoon. In order to find such influence, we must introduce the fuel consumption modelling. We start by modeling the external forces and the energy loss (W_t) of the system model over time T_f as Oguchi *et al.* [135]:

$$W_t = \begin{cases} \int_0^{T_f} (m_i u_i + c_r g m_i \cos\theta + g m_i \sin\theta \\ \quad + \frac{1}{2} c_{D_i}(d) \psi_i A_{f_i} \rho v_i^2) \cdot v_i \cdot dt & if\ F_{eng_i} > 0 \\ 0 & Otherwise \end{cases} \tag{5.10}$$

where $F_{eng_i} > 0$ indicates that propellant is used to power the vehicle, thus, resulting in losses to be computed. In order to represent such energy losses in terms of fuel consumed, we adopted the following converting method defined by the following cost

$$\begin{aligned} J(u) = & \frac{1}{\rho_{prop} \cdot \eta_{eng}} \int_0^{T_f} (m_i u_i + c_r g m_i \cos\theta + g m_i \sin\theta \\ & + \frac{1}{2} c_{D_i}(d) \psi_i A_{f_i} \rho v_i^2) \cdot v_i \cdot dt \end{aligned} \tag{5.11}$$

where ρ_{prop} and η_{eng} are the energy density of the propellant in $[J/L]$ and the constant efficiency of the engine, respectively. Note that we consider those parameters as $\rho_{pro} = 34.9MJ/L$ and $\eta_{eng} = 30\%$ which correspond to average gasoline density energy and efficiency [136, 137]. So it can be seen that the fuel efficiency

depends mainly on the relative distance between vehicles in the platoon ($c_D(d)$), and relative speed of vehicle relative to air flow. However, there is a consensus about the speed adjustment that even though the air drag can be significantly reduced when the velocity v is decreased, this is generally not economically viable due to tight delivery schedules. Therefore, seeking for fuel consumption efficiency, we must optimize the inter-vehicle distance in the platoon to reduce the air drag coefficient ($c_D(d)$). An illustration of the achievable air-drag reduction in terms of the inter-vehicle distance between platoon members is given in Figure 5.1. We can verify that shorter inter-vehicle distance indeed leads to air-drag reduction for all platoon members. In particular, notice that even the leader vehicle benefits from such small distance between vehicles, as we observe certain air-drag reduction illustrated in blue line in Figure 5.1. The explanation is that the close presence of the follower vehicle contributes to the increase of pressure on the rear of the leader vehicle [15]. Moreover, it is important to understand that the control signal impacts the fuel consumption. Therefore, over the next sections, we aim to evaluate the effect of two different controllers in the fuel efficiency. We start by introducing the models for the relevant controllers.

5.2.3 Classical control schemes for platooning

5.2.3.1 Adaptive Cruise Control

As in the previous chapters, we make use of the Adaptive Cruise Control controller as earlier defined in (2.8)-(2.10). However, so far this controller has been employed in the leader vehicle exclusively, and at this time, we aim to exploit over the platoon members as well. The reason is related to its relevance for deployment application of platooning system in a decentralized design that does not require any type of communication. Additionally, such a controller is string stable with a constant time gap, which translates to very safe outcomes. We aim to evaluate the platooning operation under autonomous operation, where the information of onboard sensors are sufficient for proper control performance. Moreover, we adopt a slightly distinct form in order to handle the control framework. Therefore, consider the following output feedback control law

$$u(t) = -K_0 y(t) \tag{5.12}$$

where K_0 is the controller ACC gain defined by

$$K_0 = \begin{bmatrix} \chi_i & 0 & \cdots & 0 \\ 0 & \chi_{i+1} & & \vdots \\ \vdots & & \ddots & 0 \\ 0 & \cdots & 0 & \chi_{N-1} \end{bmatrix} \tag{5.13}$$

where

$$\chi_i = \begin{bmatrix} \frac{\lambda_i}{h_i} & \frac{1}{h_i} & \lambda_i & 0 \end{bmatrix}, \quad i = \{0, 1, \cdots, N-1\} \tag{5.14}$$

are the ACC controller gains proposed by [45]. Note that this generic notation allows us to consider a homogeneous ($\lambda_i = \lambda \ \wedge \ h_i = h, \ \ \forall i$) or heterogeneous ($\lambda_i \neq \lambda \wedge h_i \neq h, \ \ \forall i$) ACC controller. Furthermore, note that the ACC controller does not make use of the acceleration signal, which explains the zero in the last component of (5.14). Note that we keep this notation to allow K_0 to be written in a diagonal form.

For illustrative purposes, Figure 5.2 exhibits a time simulation of a homogenous platoon of $N = 3$ vehicles with ACC controller under jammer disturbance as Figure 4.5a. The parameters employed are $\tau = 0.2$, $h = 1.4$, $\lambda = 0.5$, and $d_{ss} = 7$ m. We can witness that overall, the controller is able to follow the jammer behavior as in Figure 5.2a, but with some extra lag which is due to actuator lag and the constant time gap policy. In order words, this controller is less sensitive to abrupt changes in the system. Furthermore, very high inter-vehicle distances can be seen, which fluctuate from roughly 20 m up to 40 m as in Figure 5.2c. Next, we aim to introduce the second controller adopted, which will allow us to conclude interesting facts regarding their performance in terms of fuel consumption efficiency that will be exploited along this chapter.

5.2.3.2 Cooperative Adaptive Cruise Control

Besides the ACC controller, we adopt the CACC controller in order to exploit also the communication features of forwarding the acceleration signal. However, in this chapter we adopt the weight of the leader parameter as zero, $C = 0$, which corresponds to the semi-autonomous control. As the previous controller, we do not exploit the leader information as it introduces additional complicated structure from the network design perspective. Therefore, consider the following output feedback control

$$u(t) = -K_1 y(t) \tag{5.15}$$

where K_1 is the controller gain defined by

$$K_1 = \begin{bmatrix} \chi_0 & 0 & \cdots & 0 \\ 0 & \varphi_i & & \vdots \\ \vdots & & \ddots & 0 \\ 0 & \cdots & 0 & \varphi_{n_u} \end{bmatrix} \tag{5.16}$$

where the first term is the ACC controller previously implemented in the leader vehicle to be in conformity with spacing policies imposed by public entities. The

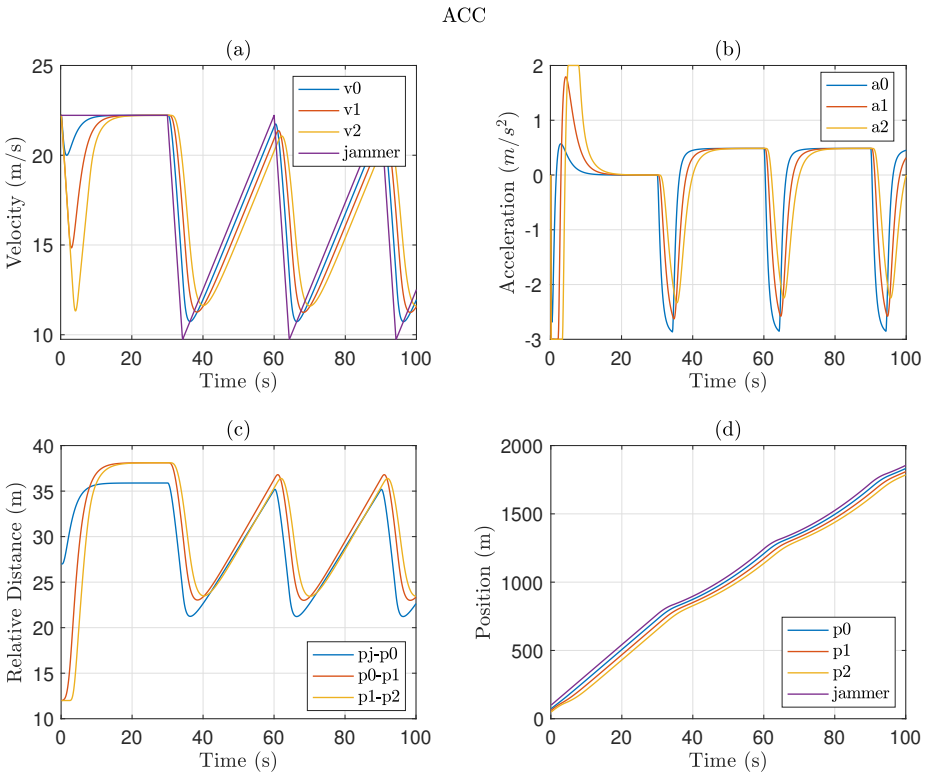

Figure 5.2 – Behavior of ACC controller.

next term is then,

$$\varphi_i = \begin{bmatrix} k_p & k_d & k_c & 1 - C_i \end{bmatrix}, \quad i = \{1, \cdots, n_u - 1\} \tag{5.17}$$

which are the CACC controller gains defined by

$$k_c = (\xi + \sqrt{\xi^2 - 1})\omega_n C_i \tag{5.18}$$

$$k_d = (2\xi - C_i(\xi + \sqrt{\xi^2 - 1}))\omega_n \tag{5.19}$$

$$k_p = \omega_n^2 \tag{5.20}$$

which are the different control gains that depend on the following parameters c_i, ξ and ω_n, as already introduced. As we adopt the semi-autonomous control, the parameter that determines the weight of the leader influence is considered as zero, i.e. $C_i = 0, \quad \forall i$. Similarly to the previous ACC controller, we are able to establish some details of the CACC behavior. Figure 5.3 illustrates characteristics of the semi-autonomous control for a platoon of $N = 3$ vehicles under the same previously indicated jammer. The simulated parameters of the controller are $k_c =$

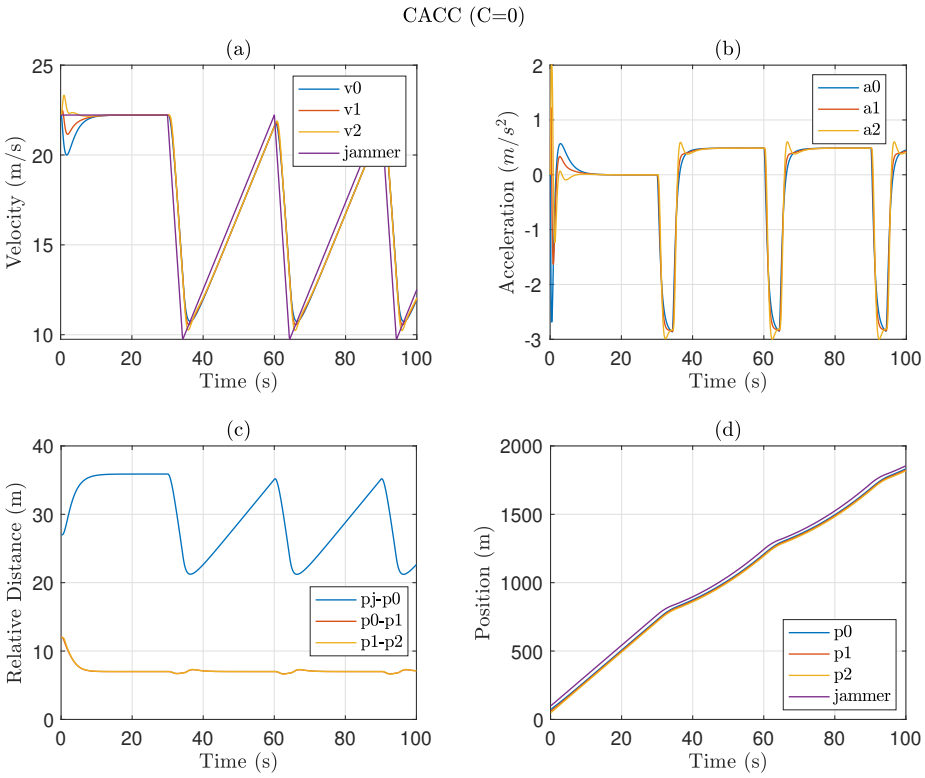

Figure 5.3 – Behavior of CACC controller.

$0, k_d = 1.4, k_p = 0.49$ and desired inter-vehicle distance of $D_{des} = 7$m. Differently from ACC, a more stringent velocity track profile is observed, but now the slight difference is due particularly to the actuator lag, as in Figure 5.3a. Moreover, despite the leader vehicle that is under ACC control, the platoon members under semi-autonomous control present considerably shorter inter-vehicle distances as low as 7 m as shown in Figure 5.3c.

Fuel comparison performance of ACC and CACC

Now that a brief comparison in terms of the controller performance has been presented, we can introduce an additional comparison, but in terms of fuel consumption. In fact, the jammer behavior plays a surprisingly critical role in the system because based on its profile, the platoon system is disturbed with higher or lower intensity. Therefore, consider two opposite and extreme situations where the jammer profile behaves very gentle such as keeping a constant velocity as in Figure 5.4a, and an angressive aspect as shown in Figure 5.4c.

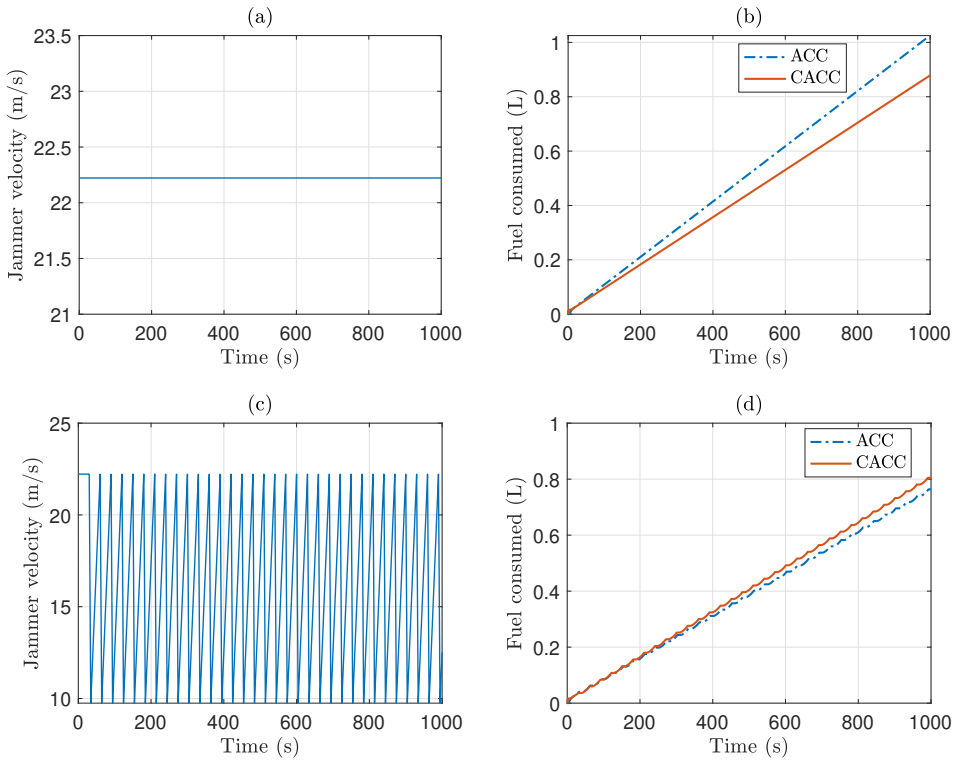

Figure 5.4 – Fuel consumption comparison for ACC and CACC controllers under constant and aggressive condition.

Next to both figures, we present the fuel consumption over time for both controllers under constant and agitated jammer in figures 5.4b and 5.4d, respectively. We can conclude that ACC is better for an aggressive jammer while CACC performs better when the jammer stays at a constant velocity. This is evident when the total fuel consumption of the CACC is lower than the ACC when under a constant jammer profile as in Figure 5.4b. Which is in conformity, since substantial lower inter-vehicle distances are achieved under CACC, and therefore the air-drag reduction ψ_i produces such gains under constant jammer. For this simulation, the CACC achieved +14% of fuel savings comparing to ACC. Surprisingly, the ACC controller performs better in terms of fuel consumption than CACC when the system is under harsh conditions with roughly +6% gains. The rationale behind such result is that the control effort of CACC controller is more stringent than the ACC controller, which translates to higher fuel burden outcomes for CACC under severe disturbances. This can be observed shortly after the start, as exhibited in Figure 5.4d, which the ACC controller performs better in terms of fuel con-

sumption. Additionally, note that the platoon traveled different distances based on the jammer profile, as for instance 22 km for a constant jammer and 16 km for aggressive jammer. We seek to present further analysis, but based on this primary illustrative example we can conclude that each of the controller may be preferable for some jammer profiles. Finally, note that these gains/losses are subject to the parameters we considered and a higher vehicle mass for example might increase the ACC gain. Next, we propose an enhanced controller before bringing formally the objectives of the chapter, and we present further analysis of the switching control burden.

5.2.4 Enhanced proposed controller

From the previous section, we conclude that each controller is more suitable for certain jammer behavior profiles. Therefore, in order to improve the fuel efficiency, we design a new controller that takes into account the jammer profile. However, designing an entirely new optimal controller is extremely difficult due to safety issues, communication issues and uncertainty regarding jammer behavior. Therefore, we propose to design a switching control that alternates between CACC and ACC based on the jammer behavior. Unfortunately, an abrupt switching produces undesired transient responses in the control signal, which translates to misuse of fuel. In order to cope with that, we propose an enhanced controller responsible to mitigate such waste as shown in Figure 5.5. So, having presented the classical control schemes, we introduce the proposed enhanced switching control scheme, and we perform a case comparison over previous control strategies in terms of fuel performance. The particular reason is that in such transient stage, the new controller is taking place which is significantly different from the previous one (ACC to CACC and vice-versa). In other words, the initial conditions are not appropriate, which causes very sharp transient responses leading to non-optimal switching logic in terms of fuel consumption. In order to smooth such unsuitable transient responses, and to improve the fuel efficiency, we propose the following enhanced control

$$u(t) = -(\beta(t)K_1 + (1 - \beta(t))K_0)y(t) \tag{5.21}$$

where $\beta(t) \in \{0, 1\}$ is a control design parameter responsible to weight the influence of each state-feedback gain for the ACC and CACC controller, given by K_0 and K_1, respectively. In other words, it corresponds to the parameter used to smooth the switch transition control. Another important parameter is the set of transitions times defined by $\mathcal{T} = \{t_i, t_{i+1}, \cdots, t_K\}$ where the following holds

$$t_i - t_{i+1} \geq \delta \quad \forall i \in \{1, \cdots, K-1\} \tag{5.22}$$

$$0 < t_1 < t_2 < \cdots < t_K < T \tag{5.23}$$

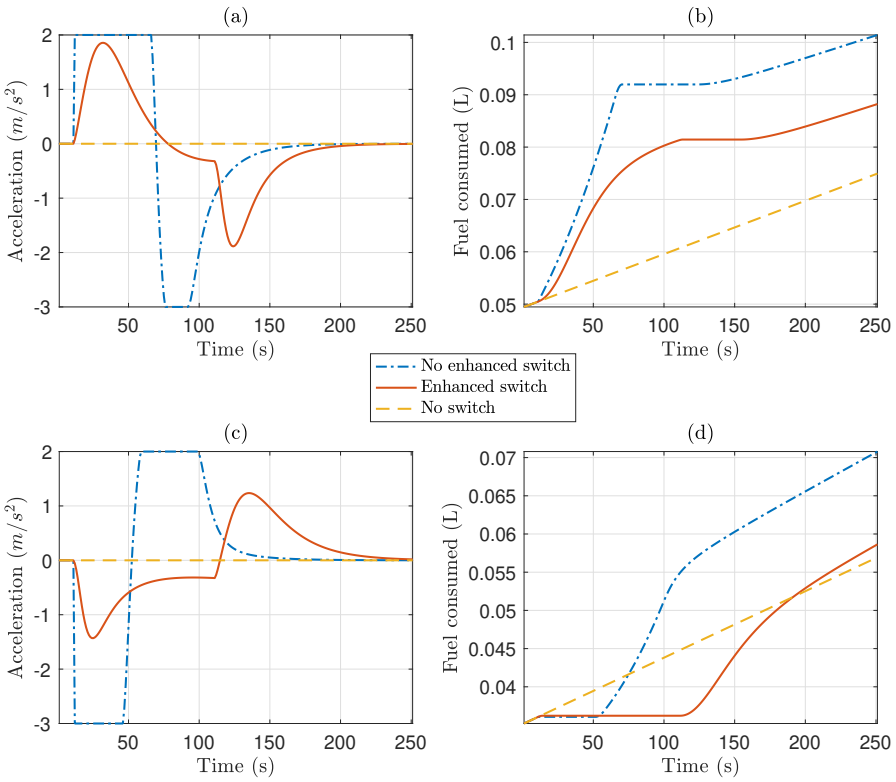

Figure 5.5 – Performance comparison between non-enhanced, enhanced and no switch control in dashed-dotted blue, solid orange, and dashed yellow, respectively, under constant jammer and with transition time $t_1 = 50$ s. The two figures on the top correspond to the switching from ACC to CACC, whereas the bottom two are from CACC to ACC.

where δ is the minimum subinterval considered, in the order of seconds, while T is the maximum simulation time adopted. Furthermore, the dynamics of the smooth switch parameter follows:

$$\dot{\beta}(t) = \begin{cases} -\frac{1}{\delta} & \textit{if } t \in [t_i, t_{i+\delta}] \wedge \beta(t_i) = 1 \\ +\frac{1}{\delta} & \textit{if } t \in [t_i, t_{i+\delta}] \wedge \beta(t_i) = 0 \\ 0 & \textit{if } t \notin [t_i, t_{i+\delta}] \ \forall t_i \in \mathcal{T} \end{cases} \tag{5.24}$$

where we initialize with $\beta(0) = 0$, which corresponds to ACC controller. In order to illustrate the enhancement introduced by the proposed controller, consider the following. First, assume there is no disturbance in the system, which translates to

a platoon moving with a constant speed such as in Figure 5.4a. In order to confirm that such switching produces losses, consider one unique switching transient time at $t_1 = 10$ s, therefore, $\mathcal{T} = \{t_1\}$, and the minimum subinterval $\delta = 50$ s.

Figure 5.5 illustrates the enhanced control performance over non-enhanced approach for the simulated parameters aforementioned. Figures 5.5a and 5.5b correspond to a switching control from ACC to CACC and figures 5.5c and 5.5d from CACC to ACC switch. From figure 5.5a and 5.5c, we can observe that such enhanced approach prevents saturated control outputs as the orange curve is below the threshold $-3 \leq u(t) \leq 2$, which is not the case for non-enhanced switch. Finally, observe for both switching directions, the enhanced switch control is the most efficient in terms of fuel consumption due to a lower total fuel utilization as shown in figures 5.5b and 5.5d. The explanation behind such gains is related to the incorporation of the control parameter β in the final control law, which leads to smoother adjustments over time on the combined control actions. Whereas without such parameter, the non-enhanced control abruptly changes the control law in just one time step, which causes a much larger transient response. Next, we aim to introduce formally the main objective of this chapter, and then the optimal switch policies for deterministic jammers.

5.2.5 Objective

Once the system dynamics, the fuel consumption model and the controllers are defined, we are able to announce the main objectives of this chapter. Therefore, the main objective of this work is as follows.

Minimize the fuel consumption cost (5.11) for a certain set of control $\mathbf{u}$ subject to collisions or platoon disruption.

$$\begin{aligned}
\min_{u} \quad & \frac{1}{\rho_{prop} \cdot \eta_{eng}} \int_0^{T_f} (m_i u_i + c_r g m_i \cos\theta + g m_i \sin\theta \\
& + \frac{1}{2} c_{D_i}(d) \psi_i A_{f_i} \rho v_i^2) \cdot v_i \cdot dt && (5.25) \\
\text{s.t.} \quad & p_{i-1} - p_i - L_{i-1} \geq D_{min} && (5.26) \\
& p_{i-1} - p_i - L_{i-1} \leq D_{max} && (5.27) \\
& v_{min} \leq v_i \leq v_{max} && (5.28) \\
& u_{min} \leq u_i \leq u_{max} && (5.29)
\end{aligned}$$

Additionally, note that $u(t)$ is of the type given in (5.21) with transition times $\mathcal{T} = \{t_i, t_{i+1}, \cdots, t_K\}$ subject to (5.22)-(5.23) as such collection defines the moment that each controller operates. While under no jammer disturbance, CACC is better than ACC in terms of fuel consumption as it accounts with the air drag reduction, $0 \leq \psi < 1$, the same is not true for random/stochastic jammers or

disturbances. Indeed, we have noticed that ACC expends less fuel due to its moderate behavior when compared to CACC stringent constant distance gap policy. Such both features motivates the use of DRL techniques to find locally optimal control policies to cope with the uncertainty of the jammer profile.

5.3 Optimal policy for constant jammers

In this section, we introduce an optimal switching control in terms of fuel consumption when constant jammer is considered in a platoon environment. In order to achieve fuel reduction through platooning, the vehicles must drive at close inter-vehicular distance. We aim to isolate the contribution to fuel consumption by two main factors: air-drag and control effort. The air-drag force F_{air} is modelled as in (4), and its reduction amount $\psi \in [0, 1]$ fluctuates based on the inter-vehicular distances between the vehicles, as presented in Figure 5.1. In order to separate and determine the influence of the control effort on the fuel consumption, all other factors must be kept constant. In this study, we aim to minimize the fuel reduction while keeping safe inter-vehicular distances for a platoon of N vehicles travelling in a highway and facing jammer incidents. First, such jammer profiles are treated as constant, and later the results are extended for stochastic profiles.

The aim is to investigate the specifics of both ACC and CACC control in terms of fuel consumption. It is clear that both controllers are very distinct and require different information in order to adjust their parameters accordingly. First, an ACC generally operates over a constant time-gap policy which, based on relative velocity, distance and absolute velocity, maintains the relative distance. While the latter is usually adopted under constant desired distance policies as the desired inter-vehicular distance can be conveniently controlled. Note that additional information as the acceleration of the preceding vehicle is required, which is possible through V2V communication. Next, in the light of the idea of Liang *et al.* [123] that focus on a method where a platoon member drives faster and catches up with the lead vehicle, we present a theorem that confirms the burden caused by the switching control policies under constant jammer profile.

Theorem 5.1. *Consider the fuel consumption given by (5.11), the controllers ACC and CACC by (5.12) and (5.15), respectively. Define the transition times between controllers as the set* $\mathcal{T} = \{t_i, t_{i+1}, \cdots, t_K\}$ *subject to (5.22)-(5.23). Let* J_{switch} *be the fuel consumed for at least one transition time from one controller to the other, i.e.* $\mathcal{T} \neq \emptyset$*, and* J_{hold} *the fuel consumed when the platoon keeps the same control the whole time, i.e. no possible transition* $\mathcal{T} = \emptyset$*. Then, the following holds true for a constant jammer profile.*

$$J_{switch} \geq J_{hold} \tag{5.30}$$

Proof. In order to evaluate the impact of switching control in terms of fuel burden, we must keep all the other factors constant. Thus, all vehicle parameters are set equal, and no jammer profile is considered, i.e. no disturbance. By contradiction, let's assume that switching control is beneficial, and thus, it produces fuel savings by lowering the total fuel consumption given by (5.11), thus

$$J_{switch} \leq J_{hold} \tag{5.31}$$

Therefore, we can depict the total fuel burden for the switching controls with the following phases:

$$J_{ACC} + J_{transient} + J_{CACC} \leq J_{hold} \tag{5.32}$$

where the first three terms stand for the total fuel spent by the ACC, transient and CACC control, respectively. Moreover, assume that ACC and transient time introduces no air drag reduction ($\psi = 1$) due to larger distances, and negligible component, respectively. Consider that J_{hold} corresponds to maintain the control CACC during the whole time (check *Remark 5.1*), and that *switch* performs a single transition $\mathcal{T} = \{t_1\}$, here namely $t_1 = t_{acc}$, which is the time spent over the first controller that corresponds to ACC controller as previously defined with $\beta(0) = 0$. Thus, inserting (5.11) in (5.32), leads to:

$$\begin{aligned}
&\int_0^{t_{acc}} (mu_{acc} + c_r gm\cos\theta + gm_i \sin\theta + \frac{1}{2}c_D(d)A_f\rho v^2{}_{acc}) \cdot v_{acc}dt \\
&+ \int_{t_{acc}}^{t_{acc}+t_\beta} (mu_\beta + c_r gm\cos\theta + gm_i \sin\theta + \frac{1}{2}c_D(d)A_f\rho v^2{}_{\beta}) \cdot v_{\beta}dt \\
&+ \int_{t_{acc}+t_\beta}^{T_f} (mu_{cacc} + c_r gm\cos\theta + gm_i \sin\theta + \frac{1}{2}c_D(d)\psi A_f\rho v^2{}_{cacc}) \cdot v_{cacc}dt \\
&\leq \int_0^{T_f} (mu_{cacc} + c_r gm\cos\theta + gm_i \sin\theta + \frac{1}{2}c_D(d)\psi A_f\rho v^2{}_{cacc}) \cdot v_{cacc}dt
\end{aligned} \tag{5.33}$$

In addition to no jammer disturbance, assume the vehicle travels to the same destination and maintains its speed constant over the whole trajectory in a flat highway. Furthermore, the following must hold

$$v_\beta > v_{acc}, v_{cacc} \tag{5.34}$$

$$T_f = t_{acc} + t_\beta + t_{cacc} \tag{5.35}$$

$$T_f v_{cacc} = t_{acc}v_{acc} + t_\beta v_\beta + t_{cacc}v_{cacc} \tag{5.36}$$

$$v_{acc} = v_{cacc} = v \tag{5.37}$$

$$\theta = 0 \tag{5.38}$$

where the first inequality means that the transient velocity is greater than ACC and CACC velocity. The second and third equations ensure that the time and

travel distance are the same. The fourth considers that both controllers are able to follow the same cruise speed without error, whereas the latter is the flat road hypothesis. Therefore, considering the set (5.34)-(5.38) in (5.33), we have

$$T_{acc}v^3 + T_\beta v_\beta^3 + T_{cacc}v^3\psi \leq T_f v^3\psi \tag{5.39}$$

which must hold for the feasibility of switching controls in terms of fuel efficiency. Now, from (5.34) and (5.37), we can define $k = v_\beta/v > 1$ which in (5.39) leads to

$$T_\beta(k - \psi) \leq T_{acc}(\psi - 1) \tag{5.40}$$

which does not hold for $k > 1$ and $0 \leq \psi \leq 1$. Therefore, in the absence of jammer, no switching logic is required as it will add a costly transient term that will never be beneficial due to steady conditions after switching. Moreover, the optimal choice is to keep the CACC control which benefits from the air-drag reduction (see *Remark 5.1*).

□

Remark 5.1. *The superiority of CACC over ACC in terms of fuel efficiency is straightforward under constant speed, i.e. no jammer. In order to verify it, the following must hold:*

$$J_{CACC} \leq J_{ACC} \tag{5.41}$$

Then, by inserting (5.11) in (5.41) and considering no air-drag reduction ($\psi = 1$) to ACC due to larger distances, negligible (des)acceleration phases, and a flat road ($\theta = 0$), it yields to

$$\psi v_{cacc}^3 T_f \leq v_{acc}^3 T_f \tag{5.42}$$

which holds when (5.35)-(5.37) and $0 \leq \psi \leq 1$ are true.

5.4 Stochastic disturbances

Previously, we have considered deterministic jammer profiles, which allow us to conveniently address the fuel consumption platooning problem. However, in practical terms such analysis is very limited since the jammer vehicle surely presents stochastic characteristics. Therefore, first of all, we aim to present how we model the uncertainty of the velocity of the jammer. In the sequel, we introduce deep reinforcement learning techniques and a threshold control as solutions for the problem.

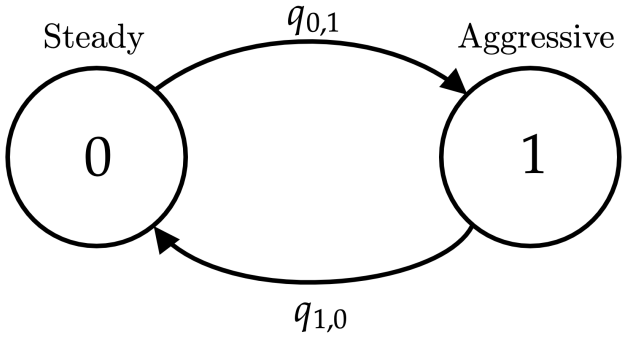

Figure 5.6 – The transition rate for the Markov chain of the Jammer profile.

5.4.1 Jammer profile modeled with Markov chains

In particular, we have adopted a continuous-time Markov process to model the jammer velocity profile as in Figure 5.6. In order to be conservative, we have adopted essentially two different modes. The first one is a constant profile which indicates that the jammer is driving mainly in constant speed described by zero in Figure 5.6. The second is an aggressive velocity profile commonly used in the literature to evaluate the robustness of platoon systems as in [46, 116]. In particular, we have adopted the jammer profile as in Figure 5.4c, but adjusted here to $-2 \leq a_j(t) \leq +2$ in order to produce zero average. More formally, we have the jammer's dynamics given by:

$$w_{\sigma(t)}(k+1) = \begin{bmatrix} p_j(k+1) \\ v_j(k+1) \end{bmatrix} = \begin{bmatrix} 1 & T_s \\ 0 & 1 \end{bmatrix} \begin{bmatrix} p_j(k) \\ v_j(k) \end{bmatrix} + \begin{bmatrix} 0 \\ T_s \end{bmatrix} a_j^{\sigma(t)}(k) \tag{5.43}$$

where v_j its velocity of the jammer for a certain discretization time T_s, and $a_j^{\sigma(t)}$ is the acceleration of the jammer profile dictated by $\sigma(t)$ that is a random variable governed by a continuous-time Markov process. Therefore, we are able to model the jammer dynamics by adjusting its acceleration with the $\sigma(t)$ parameter as introduced next.

Assumption 5.1 (**Markov switching signal for the jammer**). *We adopt a Markov switching signal to model the possible modes of the jammer profile. The switching signal $\sigma(t)$ is said to be Markov, if for $\forall n \in \Gamma$ and $\Delta > 0$,*

$$P\big(\sigma(t+\Delta) = n | \{\sigma(s)\}_{s \leq t}\big) = P\big(\sigma(t+\Delta) = n | \sigma(t)\big)\,. \tag{5.44}$$

A Markov switching signal $\sigma(t) \in \Gamma,\ t \geq 0$ is unequivocally defined by its initial condition $\sigma(0) = \sigma_0 \in \Gamma$, and its generator $Q \in \mathbb{R}^{\Gamma \times \Gamma}$, such that

$$P\big(\sigma(t+\Delta) = m | \sigma(t) = n\big) = \begin{cases} q_{nm}\Delta + o(\Delta), & n \neq m, \\ 1 + q_{nm}\Delta + o(\Delta), & n = m, \end{cases} \tag{5.45}$$

for any $\Delta > 0$*, where* $q_{nn} = -\sum_{m \neq n} q_{nm}$*. If the matrix* Q *is irreducible, then the Markov switching signal has a unique stationary distribution, denoted by* $\pi = [\pi_1, \pi_2, \ldots, \pi_r]$ *[138].*

Therefore, we consider the case where $\sigma(t) \in \Gamma = \{0, 1\}$, which here denotes for steady and aggressive modes, respectively. Both are illustrated in Figure 5.6, and are characterized by the following

$$a_j^{\sigma(t)}(k) = \begin{cases} \vartheta * \mathcal{U}[-\varsigma, \varsigma] & \text{if } \sigma(t) = 0 \\ h(k) & \text{if } \sigma(t) = 1 \end{cases} \tag{5.46}$$

where $\mathcal{U}[-\varsigma, \varsigma]$ is a uniform distributed random number from $-\varsigma$ to $+\varsigma$ included, and $h(k)$ corresponds the following function

$$h(k) = \begin{cases} -\varsigma & \text{if } k \leq \delta/2 \\ +\varsigma & \text{otherwise} \end{cases} \tag{5.47}$$

where δ is the subinterval considered between transitions times defined in (5.22). Note that a triangular shape function is obtained as the jammer's speed. Finally, we can rewrite the output of the system (5.9) as a function of the stochastic disturbance

$$y(k) = Cx(k) + Dw_{\sigma(t)}(k) \tag{5.48}$$

where $\sigma(t) = \{0, 1\}$ is the random variable governed by a continuous-Markov process.

5.4.2 Troublesome conditions

So far, we have successfully treated the jammer behavior as a random process by adopting a continuous-time Markov chains. However, despite that, we are interested in modelling unlikely scenarios such as the case when suddenly the jammer behavior changes to the opposite mode for some fixed interval. In this framework, we have considered for each subinterval time δ a probability of 5% and 10% for such troublesome condition to happen. Therefore, based on the actual state space $\Gamma = \{0, 1\}$ selected, the jammer profile shifts to the opposite state one with the aforementioned probability. The idea behind this additional obstacle is to stress even more the system in order to achieve robust outcomes. More precisely, our goal is to avoid very clear distinction between the profiles, for which simpler threshold control solution would be enough, and to model the real-life behavior of drivers who are not always rational/predictable. Furthermore, we want to evaluate the burden of changing controllers to address such disturbing conditions.

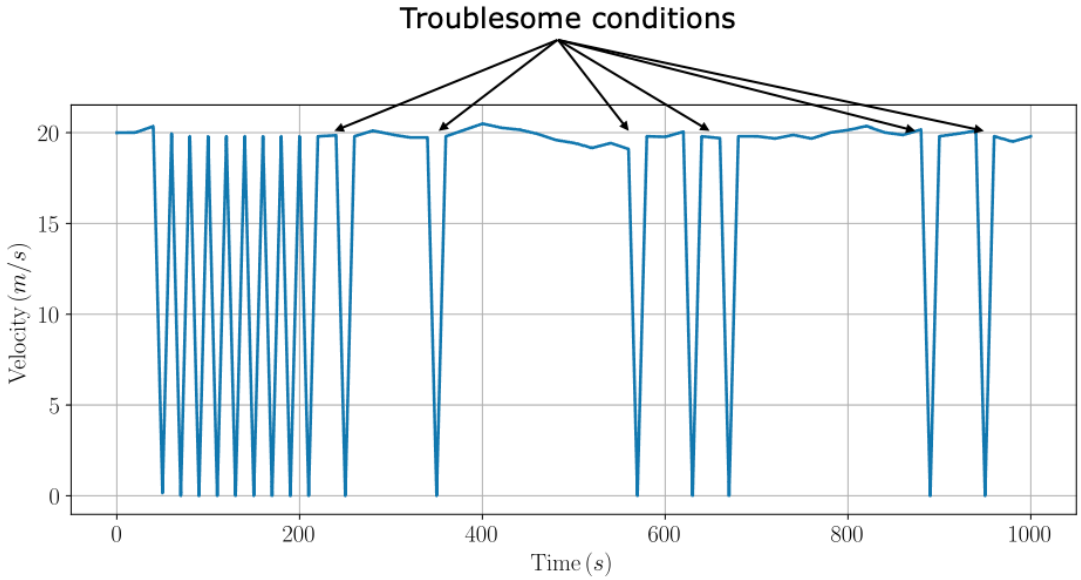

Figure 5.7 – Illustration of troublesome conditions.

5.5 Proposed switch controllers

In this section, we aim to propose two switching controllers approach to handle the stochastic disturbances previously introduced. Note that our first objective is to minimize the fuel consumption cost for a set of control $\mathbf{u}$ constituted by the combination of ACC and CACC, as defined in Section 5.2.5. The burden caused by the switching control policies is confirmed for constant disturbances as proved in Section 5.3. In order to mitigate such losses, we adopt the enhanced proposed controller, as defined in Section 5.2.4, in both following proposed switching controllers approaches.

5.5.1 Threshold control

First, we adopt a simpler approach that requires little computational burden. Our goal is to provide a threshold value that triggers one controller or the other. As already previously confirmed for the deterministic jammers, certain control law is more fuel efficient than the other based on the jammer profile, as seen in Figure 5.4. Therefore, we can extrapolate that similar behavior might occur over stochastic jammer profiles (check *Remark* 5.2).

Therefore, we can design a threshold control based on the parameters of the state-space of the system $x_i(k)$ responsible to specify the controller set ($\mathbf{u}$) that is a combination of ACC and CACC. In order words, such controller generates a

set of transition times $\mathcal{T} = \{t_i, t_{i+1}, \cdots, t_K\}$ based on the jammer behavior. In addition to simply measuring certain state-space parameter of the system $x_i(k)$ each subinterval δ, we assume a moving average where each mean is calculated over a sliding window of length sw across neighboring elements of the state-space parameter $x_i(t)$. More formally, consider the following threshold logic to determine the best set of control

$$u(t) = \begin{cases} K_0 y(t) & \text{if } \sqrt{\frac{1}{sw}\sum_{t-sw}^{t} a_0(t)^2} > \varepsilon_{th} \\ K_1 y(t) & \text{otherwise} \end{cases} \tag{5.49}$$

where $K_0 y(t)$ is defined as (5.12) and $K_1 y(t)$ as (5.15), which are the ACC and CACC controllers, respectively. The variable ε_{th} is the threshold value, that will be determined in the next section. In order words, equation (5.49) indicates that we compare the absolute value of the acceleration signal of the last sw time-steps with certain threshold parameter ϵ_{th} in order to select the control output. Note that such analysis is done each subinterval of time of size δ.

Remark 5.2. *We model the jammer profile with the Markov Chain as in Figure 5.6. As far as the jammer behavior is concerned, the modes of the Markov chain are similarly to the ones evaluated in the fuel comparison as shown in Figure 5.4, which allows us to extrapolate the fuel consumption performance for stochastic disturbances. The remarkable difference is the introduction of a time-varying function that describes the state of the random variable, which is governed by a continuous-time Markov process. Assume negligible interference caused by the troublesome conditions so far.*

5.5.2 Deep reinforcement learning for switching platoon controller

Although simple to implement, the previous controller has its limitation since the threshold parameter ϵ_{th} is adjusted empirically based on observations. Furthermore, it is expected several fluctuations caused by troublesome conditions. Another alternative is to adopt a Neural Network (NN) approach since they are known to be universal non-linear function approximators. Therefore, we have adopted Reinforcement Learning (RL) techniques which seek from trial-and-error algorithms to optimize that agent's actions (maximize the accumulated reward) through the whole interaction moment with the environment. Observe that we exploit Deep Reinforcement Learning (DRL) techniques since we use Deep Neural Networks (DNN) as the function approximation method in the reinforcement learning framework to describe the agent. In this work, we adopt DRL to determine the most appropriate action in terms of fuel efficiency and safety. However,

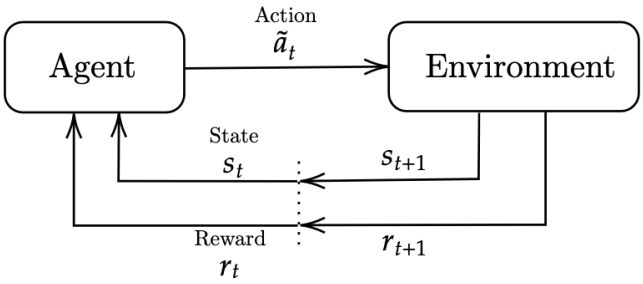

Figure 5.8 – Reinforcement learning overall diagram.

due to safety and convergence issues of DRL, our algorithm establishes transition times and period of operation of both ACC and CACC controllers, instead of directly controlling the vehicles, which translates to the following control

$$u(t) = K_{\mu(t)} y(t) \tag{5.50}$$

where $\mu(t) = \{0, 1\}$ is a function that determines which controller, ACC or CACC, must be adopted, respectively. This function in given by the learning agent at each instant t. In other words, the learning defines the set of transitions times $\mathcal{T}$ where the switching of modes takes place. The appropriate choice is unknown due to the unpredictable behavior of the jammer vehicle. Such challenge motivates the use of DRL algorithms that are able to learn the preceding vehicle dynamics from iterative experiences with the environment.

The problem of longitudinal vehicle platoon control is formulated as an Markovian Decision Process (MDP). In our case, the whole system is modeled as a stochastic environment, where based on the current state observation $s_t \in \mathcal{S} \subseteq \mathbb{R}^{n_s}$ the agent is responsible to chose an action $\tilde{a}_t$[1]$\in \mathcal{A} \subseteq \mathbb{R}^{n_a}$, and then it observes the new state s_{t+1} and receives the correspondent reward value $r_{t+1} \in \mathbb{R}$, which closes the loop as shown in Figure 5.8. Through this interaction with the environment, the agent aims to find a policy $\tilde{\pi} : \mathcal{S} \to \mathcal{A}$ that maximizes the cumulative discounted reward $R_{t_0} = \sum_{t=t_0}^{\infty} \gamma^{t-t_0} r_t$ where $\gamma \in [0, 1)$ is the discounting factor. Therefore, we have adopted the value-based algorithm Double Deep Q-Networks (DDQN) algorithm with a target network proposed by van Hasselt *et al.* [139] which will approximate the Q-function, while addressing the overestimation problem and improving the stabilization of the training, in order to learn the best actions to be chosen. The experience replay buffer is adopted to store past experiences, and randomly use subsets of them to update the Q-network improving the sample-efficient of the training. Finally, in addition to the state space introduced

[1]In the literature, the action is usually denoted by a. However, in order to differentiate from the acceleration of the vehicles, we adopt $\tilde{a}$ to symbolize the action from the agent.

in Section 5.2, we augmented it to include the fuel consumption of the platoon members as defined in (5.11), over one-step simulation.

5.5.2.1 Reward function

A proper design of the reward function is crucial for the convergence of the DRL algorithm. In this study, the interest is to improve fuel efficiency while maintaining safety, we considered the following reward function evaluated at each subinterval δ:

$$r = r_{step} + r_{collision} + r_{idle} \tag{5.51}$$

where r_{step} represents the time-step cost, which can be measured by the number of running cycles, and it is defined as:

$$r_{step} = \begin{cases} 1 & if\ t \leq V\delta \\ \kappa/\delta & otherwise \end{cases} \tag{5.52}$$

where κ is the total number of time-steps in which the limit of fuel supply is attained, δ is the simplified MDP sampling time, and V is the maximum positive integer multiple of δ defined by $V = \frac{T_f - \kappa}{\delta}$, such that $V\delta < T_f$. Note that $0 \leq \kappa/\delta \leq 1$ is a fraction of a unitary reward which is proportional to the remaining time. Finally, $t_p = p\delta$ where $p = 0, \cdots, V-1$. As a result, the agent receives positive reward for each subinterval proportional to the sampling time, and in case of reaching out of fuel condition sooner than the sampling time, only its fraction is considered. Finally, in order to raise safety performance, collisions were treated as penalties with the following reward policy:

$$r_{collision} = \begin{cases} -k_{col} & if\ e(t) < D_{min} \\ 0 & otherwise \end{cases} \tag{5.53}$$

where k_{col} is a positive constant that can be adjusted, and $e(t)$ is the spacing error between vehicles defined in (2.5) which, in this case, is lower bounded by the minimum distance D_{min} in meters. Similarly, we seek to improve fuel efficiency while keeping safe policies, therefore, we introduce an idle reward r_{idle} to penalize ineffective policies in terms of improving fuel efficiency as follows:

$$r_{idle} = \begin{cases} -k_{idle} & if\ e(t) > D_{max} \\ 0 & otherwise \end{cases} \tag{5.54}$$

where k_{idle} is a positive constant, and the spacing policy (2.5) is upper bounded by the maximum distance D_{max} in meters. We aim to prevent policies with very large inter-vehicular distance, which would undo the platoon formation. Note that, if $k_{col} > k_{idle}$ more importance to safety than fuel performance is given, and vice-versa.

5.5.3 Experimental settings

In this subsection, we aim to discuss the main deep neural network elements adopted such as its structure, hyper-parameters, etc. used for the training part. We adopt two hidden layers of rectified non-linearity with 64 units each. The final layer of the DDQN is linear with a scalar output of the Q-value for the possible actions that could be taken. Default hyper-parameters are used for training DNN weights as follows: learning rate $\alpha = 10^{-3}$, discount factor $\gamma = 0.99$ and batch size of 64. The reward constants are set to be $k_{col} = 1$, $k_{idle} = 0.5$, and minimum and maximum distance bounds for reward penalty as $D_{min} = 1$ and $D_{max} = 70$, respectively. The simplified MDP problem is set with a time-step of $T_s = 20$s while the actual/complex MDP problem time-step is $T_s = 0.1$s. State normalization demonstrated to be of utmost importance for the algorithm convergence. Because in DNN training, the scale of the input signal is maintained when it is passed through the DNN.

5.6 Performance evaluation

In this section, we present the performance evaluation of the system according to three different control approaches. First, we assume control strategies that are static despite the changes on the jammer profile. In the sequel, we adopt a threshold approach which aims to trigger the best control action based on certain threshold parameter. Finally, we introduce a deep reinforcement learning approach that attempts to address all the stochastic disturbances of the system through trial-and-error.

5.6.1 Numerical stochastic profiles of the jammer

Before introducing the simulation environment, we highlight the particular class of the stochastic disturbances modeled by the Markov chain as in Figure 5.6. According to Assumption 5.1, we observe that Markov chains have the memoryless property, which translates to past event being irrelevant to decide the dynamic evolution of the process. In other words, the present state is enough for the future development of the process. Furthermore, a Markov process is completely determined by the well known transition rate matrix Q, which for the adopted scenario as in Figure 5.6 is defined by

$$Q = \begin{bmatrix} -q_{n,n} & q_{n,m} \\ q_{m,n} & -q_{m,m} \end{bmatrix} = \begin{bmatrix} -q_{0,0} & q_{0,1} \\ q_{1,0} & -q_{1,1} \end{bmatrix} = \begin{bmatrix} -\frac{1}{40} & \frac{1}{40} \\ \frac{1}{6} & -\frac{1}{6} \end{bmatrix} \tag{5.55}$$

where $q_{n,m}$ is the probability per time unit that the system executes a transition from state n to state m. Note that its diagonal elements $q_{n,n}$ are defined such

that $q_{n,n} = -\sum_{n \neq m} q_{n,m}$ which denotes the total transition rate out of state n, and therefore the rows of the matrix Q sum to zero, $\sum_m q_{n,m} = 0$. Now we can find the stationary distribution π of the Markov chain which is a probability distribution that remains unchanged in the Markov chain in the long run. First of all, note that the probability distribution π is a stationary distribution for the Markov chain if and only if

$$\pi Q = 0 \tag{5.56}$$

is satisfied. Such equation expresses the balance of probability flows, and the proof follows the forward and backward Chapman-Kolmogorov equations, which is out of the scope of this thesis, and the reader is referred to [140] to a deeper discussion. By definition the sum of the probability distribution is equal to one, or more formally

$$\sum_{n \in \Gamma} \pi_n = 1, \tag{5.57}$$

where Γ is the state space $\Gamma = \{0, 1\}$, which here denotes for two modes steady and aggressive, respectively. Therefore, now that such a transition rate matrix Q (5.55) is known, we are able to find the stationary distribution by applying (5.56)

$$\pi Q = \begin{bmatrix} \pi_0 & \pi_1 \end{bmatrix} \begin{bmatrix} -\frac{1}{40} & \frac{1}{40} \\ \frac{1}{6} & -\frac{1}{6} \end{bmatrix} = 0 \tag{5.58}$$

which leads us to $\pi_0 = \frac{40}{6}\pi_1$ and together with (5.57), we have

$$\pi = \begin{bmatrix} \frac{40}{46} & \frac{6}{46} \end{bmatrix} = \begin{bmatrix} 0.8696 & 0.1304 \end{bmatrix} \tag{5.59}$$

Therefore, we can conclude that in the long run roughly 87% of the time the jammer vehicle has a steady profile, and 13% of the time it performs aggressive behaviors. In this study, the transition probabilities of the Markov process are particularized empirically. We assume that most of the time vehicles in a highway progress with relatively constant behavior. Consequently, we adopt a uniform distribution of the acceleration of the jammer as $\varsigma = 2$, so $\mathcal{U}[-2, 2]$ weighted by $\vartheta = 0.01$ constant in order to produce such nearly steady behavior, as seen in (5.46) for $\sigma(t) = 0$. Such value is kept constant over the subinterval δ instant to avoid excessive fluctuation. On the other hand, the aggressive mode follows a deterministic profile to stress the platoon stability, as shown in (5.47). First, until the subinterval $\delta/2$ the acceleration decreases its maximum, thus -2 m/s^2, and during the second half $\delta/2$ it increases its maximum, so $+2$ m/s^2. Our goal is to generate severe traffic conditions under all of which, the designed control must be capable of avoiding collisions.

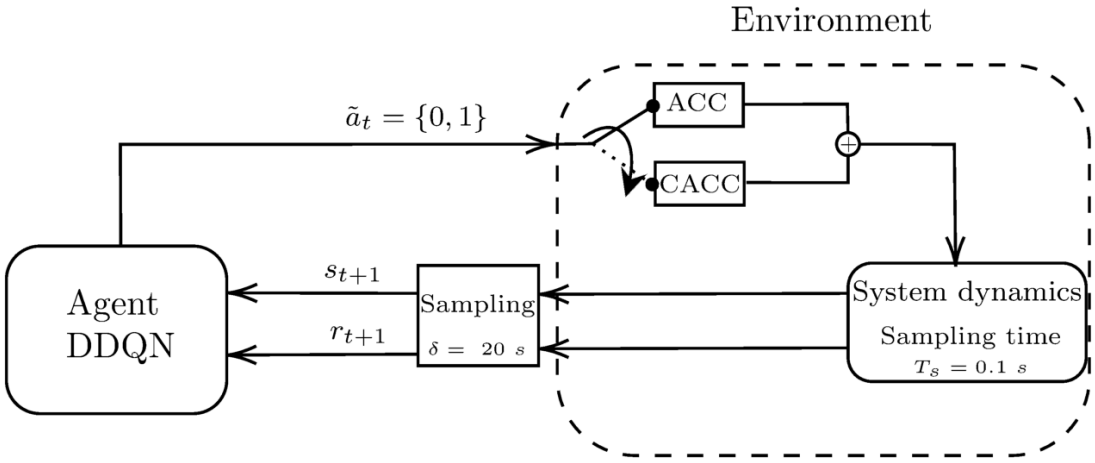

Figure 5.9 – Overview of the DRL framework for our platoon system.

5.6.2 Simulation environment

Different from the previous chapters in which extended platoon size is evaluated, here we aim at smaller homogeneous platoon size such as $N = 3$ and with actuator lag of $\tau_i = 0.2\ s\ \ \forall i$. The main reason for such choice is to mitigate the computation complexity for the deep reinforcement learning approach. Another substantial difference is that we do not use the Simulink environment to model the vehicle dynamics and to implement the control law. Instead a Python simulation is used to verify the feasibility and effectiveness of our proposed controllers in terms of fuel efficiency. Moreover, the communication analysis is simplified since we assume perfect communication for vehicle to neighbor links since we adopt semi-autonomous control i.e. CACC control with $C = 0$. Note that this communication assumption is reasonable due to very low probability of packet error for consecutive links as shown in Figure 4.3.

For convenience, we have used a Python simulator to allow straightforward analysis since the DDQN algorithm is smoothly attainable on it due to the support of external libraries. In particular, we adopt PyTorch [141] which is an open source machine learning library for Python. More precisely, we exploit PyTorch tools to train a Double Deep Q Learning agent in our platooning environment. Notice that, in the learning framework, we adopt a considerable different sampling time when compared to the discretization interval $T_s = 100$ ms of the system dynamics, as shown in Figure 5.9. In fact, we exploit a simpler MDP system with subintervals of $\delta = 20$ s, which translates to updating the learning algorithm less frequently. Such difference is fundamental to reduce the order of the complexity of the problem. Another reason is to avoid large fluctuations caused by the switch of controls once one is chosen. This approach implies that the chosen control does not change, for

Table 5.1 – Neural network, control and traffic simulation parameters

Control and Traffic		**Neural Network**	
Parameter	**Value**	**Parameter**	**Value**
Simulation duration	1000 s	Learning rate (α)	10^{-3}
Jammer profile	Check Fig. 5.6	Discount factor (γ)	0.99
Platoon size (N)	3	Batch size	64
ACC		Reward constants $\{k_{col},\ k_{idle}\}$	$\{1, 0.5\}$
Time-gap (h)	1.4	Reward penalty $\{D_{min,D_{max}}\}$	$\{1, 70\}$
Gain (λ)	0.5	Hidden layers	2
Standstill distance (d_{ss})	7 m	Buffer size	10000
CACC		MDP sampling time (δ)	20 s
Leader factor (C)	0	Steps update target NN	500
Desired distance (D_{des})	7 m	Epsilon greedy method	Check (5.60)
Damping ratio (ξ)	2		
Bandwidth (ω_n)	0.5 Hz		

at least $\delta = 20$ s, which is pertinent to real traffic situations, but the proper value is beyond the scope of this thesis and is left for future evaluation. Finally, all the simulation parameters adopted for both control and deep reinforcement learning framework are depicted in Table 5.1, whereas the values of the parameters of the vehicle and energy consumption model were borrowed from Kulava *et al.* [5], and are illustrated in Table 5.2.

So the environment is initialized with the leader and two platoon members, and a random jammer profile that follows a Markov chain, as previously stated, for each episode. In each step of an episode, the agent examines the most updated state and the reward feedback before deciding which actions to take. In other words, at each subinterval of $\delta = 20$ s, we compute at each $T_s = 0.1$ s the vehicle dynamics, possible collisions and the fuel platoon consumption. The idea is to carefully consider important platooning features, but without excessively increasing the complexity of the DRL framework. Therefore, based on the environment i.e. the disturbances caused by the jammer, the agent gets a reward and calculates the most appropriate action (control ACC or CACC) that leads to the most efficient fuel consumption policy. Note that due to the modification of the sampling time, the agents are only allowed to take decisions at each $\delta = 20$ s. Then, a new state is observed by the agent, and the neural network will update its weights to maximize the total cumulative reward. Finally, the process terminates differently for the training and deployment phase, check Remark 5.3. Note that in the training phase, we adopt the epsilon greedy method as defined by (5.60)

$$g(t) = 0.05 + 0.85e^{-\frac{t}{7}}, \tag{5.60}$$

which means that if a certain random number generated by the model at each step is lower than $g(t)$ (exploration area), the model selects a random action, but if it is higher than $g(t)$ (exploitation area) the model chooses an action based on what it has learned so far [142]. The idea is that in the beginning of training, the

Table 5.2 – Vehicle and energy consumption model parameters used in this chapter (source [5]).

Parameter	**Symbol**	**Value** [Unit]
Vehicle mass	m	1000 kg
Roll resistance	c_r	0.008
Air drag coefficient	c_D	1
Air drag reduction	ψ	Check Fig.5.1
Vehicle front area	A_a	2.1 m^2
Air density	ρ_{air}	1.225 kgm^{-3}
Road slope	θ	0°
Gravitational constant	g	9.8 m/s^2
Max. acceleration	u_{max}	+2 m/s^2
Min. acceleration	u_{min}	−2 m/s^2

agent has very limited information, and therefore, it should explore new actions in different states. Whereas, as it learns from experiences, the agent should exploit its knowledge to maximize the rewards it receives.

Remark 5.3. *During the training phase of the neural network, we adopt the fuel consumption of the platoon members as the terminate condition, i.e. the leader is neglected since it is always under ACC. Whereas in the deployment phase, we consider that the process will be terminated when the simulation duration time of* $T_{final} = 1000$ *s is reached. The reason is that we adopted the fuel consumption of the platoon members as input for the neural network in addition to the state-space* $x(k)$ *previously defined, therefore, we are not able to extrapolate the duration of the simulation by more than the corresponding of the training phase. A more suitable design of the system that does not rely on fuel consumption is left for future work.*

5.6.3 Performance over baseline

In order to evaluate the performance of the proposed controllers, we start by defining the baseline case. Therefore, we considered, as a baseline, the static ACC controller, which produces the safest outcomes due to requiring larger inter-vehicle distance, and does not rely on any type of V2X communication. Moreover, such controller is generally established as a backup system in case of losing the wireless link for an extended period of time [65, 67]. Therefore, to validate the performance of both threshold and DRL approach over static control strategies, we compare them under the same environment settings executed several times to obtain a reliable amount of samples. More precisely, we generate several jammer profiles following the Markov chain described in Figure 5.6, and we employ each

Table 5.3 – Comparison of the average performance **of fuel improvements** against baseline (ACC) for 1k episodes for distribution [40 6].

	Threshold naive	**Threshold optimized**	**DRL**
5% of troublesome cond.	4.68 %	6.13 %	6.83 %
10% of troublesome cond.	3.16 %	5.03 %	5.74 %

control approach while storing some parameters for later analysis such the fuel consumption and control output. Table 5.3 encompasses the average performance for a thousand episodes, i.e. a different jammer profile over a simulation duration of 1000 s for episode, for different control approaches. It includes a naive and an optimized threshold policies, and the DRL approach, as explained next. We can conclude that the Deep Reinforcement Learning approach (DRL) achieves the most suitable behavior among all the evaluated alternatives with in average +6.83% of superiority in terms of fuel consumption efficiency for 5% of troublesome conditions. It should also be noted that the fuel reduction is obtained without reducing the average velocity.

Both threshold policies are defined by the same sliding window of length $sw =$ 50 s as in (5.49), but different threshold parameters values ε_{th} are adopted. For instance, the optimized threshold version, namely $\varepsilon_{th_o} = 1.23$, is obtained after a careful heuristic optimization through the observation of several simulations. Whereas the naive threshold, given by $\varepsilon_{th_n} = 0.1$, approach represents a simpler method acting for small acceleration changes. Therefore, the threshold approach can be interpreted as a moving average of the last 50 s of the acceleration signal that when compared to the threshold parameter triggers the appropriate controller (ACC or CACC). The optimized threshold value is set up experimentally based on the effect of the jammer disturbance and the suitable control signal to react it. Finally, the naive threshold approach granted the last spot in the performance comparison against the baseline. However, based on the transition probabilities of the Markov chain of the jammer profile, different results are expected. In particular, if an additional intermediary mode is considered or the aggressive state stationary distribution π_1 is increased, both threshold performance are expected to decline since a proper adjustment of new threshold values are required. Whereas the DRL approach is able to systematically readjust to it, which motivates its usage.

We next describe the performance in terms of fuel efficiency for a particular jammer profile as shown in Figure 5.10a. We aim to illustrate the ability of different platoon controllers to cope with robust disturbances caused by the jammer. This particular sample clearly displays a robust profile with reasonable troublesome conditions, in addition to aggressive and steady behaviors. Therefore, Figure 5.10b

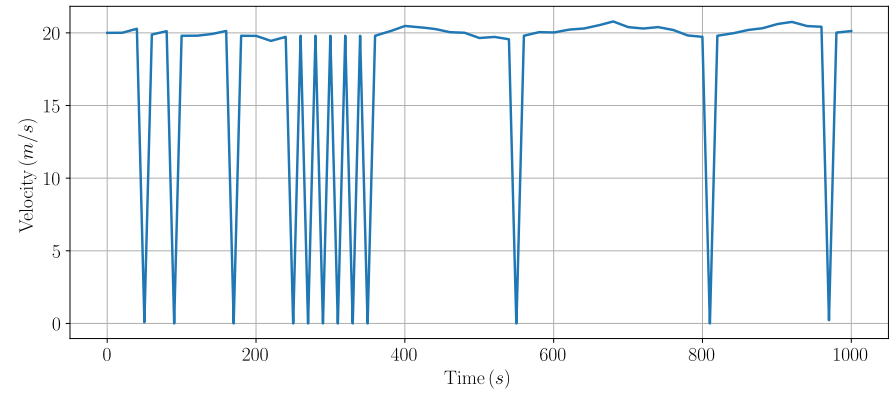

(a)

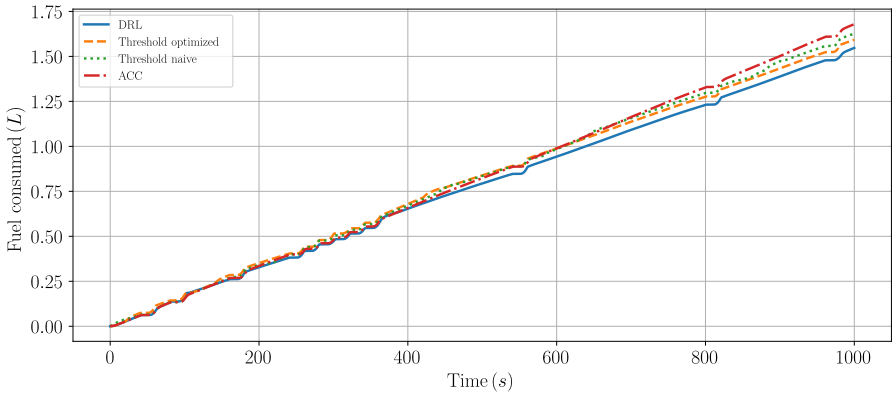

(b)

Figure 5.10 – Illustration of a particular jammer profile investigated in (a), and the corresponding fuel platoon performance for all evaluated cases in (b).

shows the fuel consumption of the platoon members (leader excluded) for different controllers under such same disturbance. As it can be seen, the DRL approach, in solid blue, demonstrates to consume the lowest amount of fuel among all cases.

Moreover, Figure 5.11a exhibits the performance of the evaluated controllers compared against the baseline, i.e. static ACC. We can observe that during the first 100 s, during which the jammer is fairly aggressive, the DRL approach adopts the ACC controller which translates to the zero performance over the baseline. Whereas the threshold approaches act differently operating, in general, worst than the baseline during such interval, as seen in dashed yellow and dotted green, respectively. Note that both threshold controllers, in general, under perform the baseline until roughly 600 s. This fact can be explained by the excessive switching

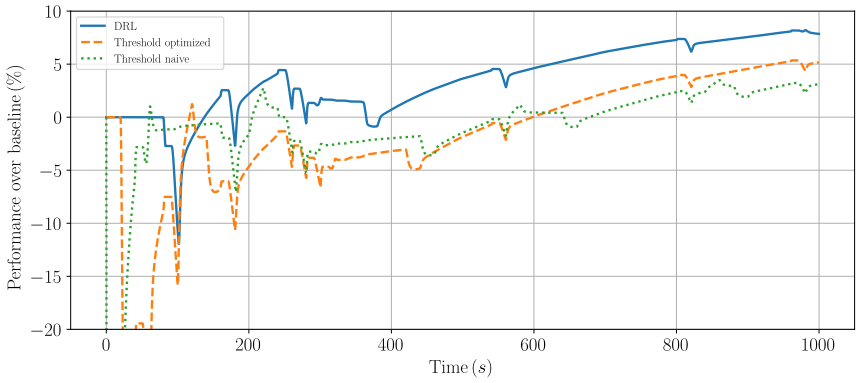

(a)

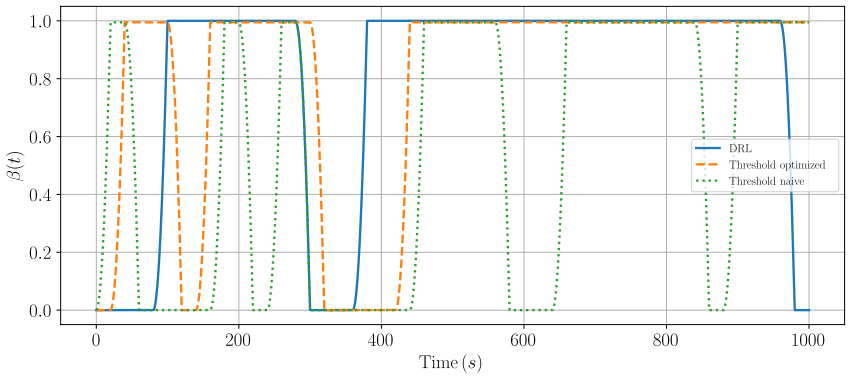

(b)

Figure 5.11 – The fuel performance relative to the baseline approach in (a), and the smooth control design parameter $\beta(t)$ for the DRL and both threshold switch control approaches in (b).

of the threshold approaches for such particular disturbance during the first 250 s, and the requirement of some time of the CACC controller to reduce the inter-vehicular distance and take advantage from the air-drag reduction, as illustrated in Figure 5.4d for a different disturbance.

Finally, Figure 5.11b displays the smooth control design parameter $\beta(t)$ proposed to mitigate the losses caused by the switching control. We can observe the DRL approach properly adopts the ACC control ($\beta(t) = 0$) during the aggressive mode of the jammer (as seen in the time-scale between 200 to 400 s), and refuses to switch during troublesome conditions that do not remain for long. Moreover, the naive threshold control, in dotted green, performs almost three times more switching behavior than the DRL approach, which translates to unnecessary ac-

tions and undesired losses. On the other hand, the optimized threshold control performs better than the naive approach with slightly more switching behavior than the DRL, which highlights the importance of properly tuning the threshold parameter.

5.7 Conclusions

Different from the previous chapters, we have precisely addressed the fuel consumption efficiency in a longitudinal platoon. We started by first identifying the trade-off between control effort and the air-drag reduction when under ACC and CACC controller for deterministic disturbances. We then proposed a enhanced controller based on a linear function of both ACC and CACC controllers, but weighted by a smooth control design parameter, namely $\beta(t)$. Next, we derived equations to prove the inherent losses over switching approaches over constant jammer. We then introduce stochastic disturbances which are modeled by Markov chains. The advantage is the possibility to generate undetermined disturbances profiles, and, therefore, increase the robustness of the system.

To cope with such stochastic framework, we proposed two different switch control strategies: a threshold control and a deep reinforcement learning approach. The former one triggers the proper control action based on the correlation of the acceleration signal with certain threshold value, obtained experimentally. Whereas, the latter seeks from thousands of experiences to learn the most suitable action. Note that it is not easy to optimize the threshold parameter in practice because the jammer profiles, acceleration/braking values etc. are unknown, but the DRL approach can still learn and configure itself. In particular, the neural network is indirectly learning how to behave depending on each jammer disturbance, which is done indirectly through the rewards at each simulation step. Moreover, such approach is expected to overperform the others, since even the probability of the troublesome conditions can be learned, and, therefore, avoid extra switching action. Our simulation results show that, the deep reinforcement learning approach is the most efficient when compared to the ACC controller, namely baseline. Despite the relative small advantage obtained, we expect a substantial improvement when the hyper-parameters of the neural network are properly configured. Also note that we have assumed a simple model for the fuel consumption of the vehicles that is a function of velocity and engine force. In actual vehicles, due to gear shifts the actual fuel consumption may be even higher, which we expect to boost the platoon gains.

Moreover, note that slight improvements in the fuel consumption translate to enormous savings when you consider that fuel corresponds to 35% of the operating costs, which easily reach millions of euros in total per year [1]. Finally, in this

chapter, we demonstrated a careful analysis of the impact of both controllers ACC and CACC, in addition to the burden caused by the switching condition. For future work, we aim at adopting a more complex Markov chain with the introduction of intermediate scenario, and improve the neural network hyper-parameters.

Chapter 6

General conclusion and perspectives

This chapter aims to recapitulate the main conclusions of the research work presented in this thesis. We start by providing a summary of the aspects evaluated in each chapter, and we highlight their correlation to provide transverse considerations. Finally, we present future perspectives, and limitations of our work.

6.1 General conclusion

This thesis has dedicated to the robust control of platooning systems over imperfect wireless channels. We carefully considered the coexistence of communication and control aspects, as both are crucial to the deployments of platooning vehicles.

We covered several important features in this work, the first one is a proposition of an adaptive control scheme based on the communication link quality, as reported in Chapter 3. In this context, we introduce the proposed dynamic algorithm, for which we conduct an offline heuristic optimization to establish the best control parameters for any given value of PER. Such proposition is verified via our platoon simulation environment built on Simulink and Matlab that are responsible to allow the interplay between control and communication systems. We successfully accomplish our objective since our dynamic approach outperforms static control strategies. Furthermore, we identified a substantial reliance on the channel quality link of the leader with the last vehicle in the platoon, which considerably restricted even our compelling dynamic approach.

Looking for channel quality enhancements, we proposed in Chapter 4 an analytical modelling of platoon under two different relaying schemes. In particular, we considerably improved the channel access model by introducing a Markov chain model that quantifies the reliability of the different communication links such as

vehicle-to-vehicle and vehicle-to-RSU. We then propose a cross-layer approach that adjusts the application layer, i.e the inter-vehicle distance of the platoon, to the observed medium access control layer performance. In addition, we provide optimization of the communication protocol for the platoon taking into consideration the platoon performance. More precisely, we determine the best trade-off between the contention window size, which directly affects the packet delay, and the control platoon performance, which translates to shorter inter-vehicle distances. In addition to the above performances analysis, we provided a comparison with classical approaches that do not consider the bi-directional interplay between control and communication parameters in Chapter 4. As shown, it becomes evident the necessity to carry analysis of such interaction since outcomes with collisions were observed when only partial analysis was conducted. This observation reinforces the main goal of this thesis.

Nevertheless, note that until now, all attention is focused on optimizing the inter-vehicle distance of the platoon taking into account the essential features of the joint communication/control design. Despite the relevance of such approach, we lack analysis to quantify such developments in terms of fuel consumption, which it is the most important aspect in the economical perspective and feasibility of platooning for commercial purposes. In order to fill this gap, we propose in Chapter 5 a comprehensive analysis to improve fuel efficiency improvements to platooning system.

We started Chapter 5 addressing the external forces and the fuel consumption model in a more control framework point of view. The reason is that we aim to observe the effect of the inter-vehicle distance, which is a control parameter, on the platoon fuel efficiency. We then presented a fuel comparison performance of both evaluated controllers, ACC and CACC, which allowed us to observe the following interesting fact. There is a non-trivial trade-off between a higher fuel consumption due to control effort and lowered fuel consumption due to platooning. Therefore, our goal in this chapter is to attempt to address such dilemma. In this context, we proposed an enhanced control, which is a linear combination of both ACC and CACC control, but parameterized by a smoothing factor β to allow mild transitions, and to reduce fuel losses. However, now we face one question: when each controller should be used during platooning operation? In fact, such question is associated with the non-trivial trade-off aforementioned, and it is a very complex task since the platoon is subject to unknown disturbances. We model such unknown dynamics as a stochastic process, for which we propose a Markov chain model that quantifies the jammer vehicle speed profile. In order to attempt to answer the above question, we propose two different approaches.

The first approach is a threshold control that, based on certain function of the acceleration of the vehicle, determines the best controller to be adopted by

the platoon. The second one adopts a Deep Reinforcement Learning approach which, based on trial-and-error experiences, learns the behavior of the disturbances and adapts the action that maximizes certain reward function. To overcome the safety and convergence issues of DRL algorithms, our approach defines the period of operation of the well-known ACC and CACC controllers, instead of directly controlling the vehicles. Note that in both approaches, we adopt a homogeneous controller, which translates to all platoon members acting under the same control policy. We showed that both proposed approaches are promising solutions to determine the set of transition times, and, therefore, to answer the question. In particular, the DRL outperforms all the evaluated cases in our platooning scenario, but, on the other hand, imposes some deployment challenges to process all the information and take decision in real time.

Note that a lot of effort has been done to apply machine learning techniques in connected autonomous vehicles. Undoubtedly, advances in faster convergent algorithms and more powerful computational resources are technical key points for a massive deployment of them. Additionally, the understanding of drivers' trust and reliance in such system is equally important [143], since it may not be possible to demonstrate the safety of autonomous vehicles in terms of fatalities and injuries [144]. Regardless, the environmental awareness progress and technology evolution make the implementation of such systems very likely in the near future.

6.2 Future perspectives

In this thesis, we demonstrated the importance of the joint design of network and control systems for platooning systems. We provided appealing insights from both communication and control point of view along this work. The fuel efficiency consumption problem is the final question we tackled. Nevertheless, some possible direct extensions and applications to other domains are presented next.

6.2.1 Direct extensions

In Chapter 2, we limited our work to evaluate the platooning operation under the mature IEEE 802.11p technology, however, 3GPP Cellular-V2X (C-V2X) technology can further improve the performance due to its dual operation modes: base-station-scheduling and autonomous-scheduling. Therefore, works that address both technologies [46, 87–89] could be extended to address the platooning performance under our proposed dynamic control approach. Furthermore, very limited attention has been given to platooning systems under the next generation of radio access technologies for V2X communications, known as IEEE 802.11bd

and NR V2X, which are expected to substantially improve the latency, reliability and the throughput of the platoon.

Following the line of the work done in Chapter 3, the adaptation of the weight of the leader parameter (C) based on the communication link condition can further improve the system performance together with the proposed V2X relaying schemes as exposed in Chapter 4. Therefore, the analytical model used to compute the probability of packet loss in a platoon with and without a relay support could be evaluated under an offline optimization of the control parameter, leader factor (C), in addition to the inter-vehicle distance (D_{des}). Moreover, the packet loss probability for V2V links, disclosed in Chapter 4, can be further improved by taking into consideration virtual collisions, channel switch, hidden terminals and AIFS differentiation [76, 113].

The deep reinforcement learning approach, introduced in Chapter 5, paves the way for interesting extensions. In particular, improvements on the stochastic disturbances model with an intermediary mode [129] or even real-word driving data, can allow the velocity profile of the jammer to be more realistic. Another extension is to consider a heterogeneous platoon, in which individual platoon members carry an agent that must be trained. Another straightforward extension is to theoretically prove that switching between the ACC and CACC controllers with a certain minimum dwell time maintains string stability of the platoon.

The DRL framework of Chapter 5 can be used for considerably different approaches. For instance, in a more communication point of view, the DRL can be extended to identify the best network parameters, so that the channel access delay is reduced without excessively increasing the packet loss in the system. In this framework, a multi-agent deep reinforcement learning approach [145] might be used to coordinate the platoon vehicles for learning the communication protocols between V2X entities. A distinct approach is to address the packet delay problem in platooning [146], as introduced in Chapter 4, using deep reinforcement learning, which can be used to design an adaptive controller to outperform our proposition.

6.2.2 Application to other domains

Even though less intuitive, the tools and models developed in this thesis may be adapted for application in other domains. In particular, the rationale behind Chapter 3 in which we evaluate the control performance under loose wireless communication can be extended for general Networked Control Systems (NCS) applications. It consists of control systems with control loops closed through a communication network such as remote control of drones and robotic systems. Alternatively, we can extend for applications that requires human interaction, namely human-in-the-loop. There are many applications such as having an surgeon operating surgery in another location, a technician performing repair or maintenance operations in

areas inaccessible to humans or virtual reality applications [147–150]. So in the presence of imperfections on the wireless feedback channel, control algorithms can make corrective actions either by emulating a feedback to the human, or applying a local offline control. Note that local control in the case of platooning systems corresponds to switching to semi-autonomous CACC or ACC or even splitting the platoon into smaller ones that run autonomously.

Bibliography

[1] Scania AB. Annual report. `https://www.scania.com/content/dam/group/investor-relations/financial-reports/annual-reports/2014-en-scania-annual-report.pdf`, 2014. [Online].

[2] Wolf-Heinrich Hucho. Aerodynamics of road vehicles, 1998. *Warrendale, PA: Society of Automotive Engineers*, 1998.

[3] Yunpeng Zang, Lothar Stibor, Georgios Orfanos, Shumin Guo, and Hans-Juergen Reumerman. An error model for inter-vehicle communications in highway scenarios at 5.9 GHz. In *Proceedings of the 2nd ACM international workshop on Performance evaluation of wireless ad hoc, sensor, and ubiquitous networks*, pages 49–56, 2005.

[4] Hannes Hartenstein and Kenneth Laberteaux. *VANET: vehicular applications and inter-networking technologies*, volume 1. John Wiley & Sons, 2009.

[5] Sai Teja Kaluva, Aditya Pathak, and Aybike Ongel. Aerodynamic drag analysis of autonomous electric vehicle platoons. *Energies*, 13(15):4028, 2020.

[6] Jean-Paul Rodrigue, Claude Comtois, and Brian Slack. *The geography of transport systems*. Routledge, 2016.

[7] Dongyao Jia, Kejie Lu, Jianping Wang, Xiang Zhang, and Xuemin Shen. A survey on platoon-based vehicular cyber-physical systems. *IEEE communications surveys & tutorials*, 18(1):263–284, 2015.

[8] 3GPP TR 22.886 (V16.2.0). Study on enhancement of 3GPP support for 5G V2X services, [Dec. 2018.].

[9] Kuo-Yun Liang, Jonas Mårtensson, and Karl H Johansson. Heavy-duty vehicle platoon formation for fuel efficiency. *IEEE Transactions on Intelligent Transportation Systems*, 17(4):1051–1061, 2015.

[10] Sebastian Van De Hoef, Karl Henrik Johansson, and Dimos V Dimarogonas. Fuel-efficient en route formation of truck platoons. *IEEE Transactions on Intelligent Transportation Systems*, 19(1):102–112, 2017.

[11] Valerio Turri, Bart Besselink, and Karl H Johansson. Cooperative look-ahead control for fuel-efficient and safe heavy-duty vehicle platooning. *IEEE Transactions on Control Systems Technology*, 25(1):12–28, 2016.

[12] Pedro Fernandes and Urbano Nunes. Multiplatooning leaders positioning and cooperative behavior algorithms of communicant automated vehicles for high traffic capacity. *IEEE Transactions on Intelligent Transportation Systems*, 16(3):1172–1187, 2014.

[13] Farhad Farokhi and Karl H Johansson. A study of truck platooning incentives using a congestion game. *IEEE Transactions on intelligent transportation systems*, 16(2):581–595, 2014.

[14] Can Zhao, Li Li, Jingwei Li, Keqiang Li, and Zhiheng Li. The impact of truck platoons on the traffic dynamics around off-ramp regions. *IEEE Access*, 9:57010–57019, 2021.

[15] Assad Alam, Bart Besselink, Valerio Turri, Jonas Mårtensson, and Karl H Johansson. Heavy-duty vehicle platooning for sustainable freight transportation: A cooperative method to enhance safety and efficiency. *IEEE Control Systems Magazine*, 35(6):34–56, 2015.

[16] Randolph Hall and Chinan Chin. Vehicle sorting for platoon formation: Impacts on highway entry and throughput. *Transportation Research Part C: Emerging Technologies*, 13(5-6):405–420, 2005.

[17] Michael P Lammert, Adam Duran, Jeremy Diez, Kevin Burton, and Alex Nicholson. Effect of platooning on fuel consumption of class 8 vehicles over a range of speeds, following distances, and mass. *SAE International Journal of Commercial Vehicles*, 7(2014-01-2438):626–639, 2014.

[18] Assad Al Alam, Ather Gattami, and Karl Henrik Johansson. An experimental study on the fuel reduction potential of heavy duty vehicle platooning. In *13th International IEEE Conference on Intelligent Transportation Systems*, pages 306–311. IEEE, 2010.

[19] World health organization. `https://www.who.int/news-room/fact-sheets/detail/road-traffic-injuries`, [Online].

[20] Observatoire National Interministériel de la Sécurité Routière. Accidentalité routière 2020. https://www.onisr.securite-routiere.gouv.fr/sites/default/files/2021-05/20210531_Bilan_D%C3%A9finitif_ONISR_2020%20vMS.pdf, [Online].

[21] Volvo Trucks. European accident research and safety report 2013. https://www.truckaccidentattorneysroundtable.com/wp-content/uploads/2013/07/Volvo-European-Accident-Safety-and-Research-Report-00467651.pdf, [Online].

[22] A James McKnight and George T Bahouth. Analysis of large truck rollover crashes. *Traffic injury prevention*, 10(5):421–426, 2009.

[23] Robert E Chandler, Robert Herman, and Elliott W Montroll. Traffic dynamics: studies in car following. *Operations research*, 6(2):165–184, 1958.

[24] Bob Pishue. Inrix 2020 global traffic scorecard. https://inrix.com/scorecard/, [Online].

[25] Pedro Fernandes and Urbano Nunes. Platooning with IVC-enabled autonomous vehicles: Strategies to mitigate communication delays, improve safety and traffic flow. *IEEE Transactions on Intelligent Transportation Systems*, 13(1):91–106, 2012.

[26] Scania AB. Annual report. https://www.scania.com/content/dam/group/investor-relations/annual-review/download-full-report/scania-annual-and-sustainability-report-2020.pdf, 2020. [Online].

[27] Our World in Data. Cars, planes, trains: where do co2 emissions from transport come from? https://ourworldindata.org/co2-emissions-from-transport, 2020. [Online].

[28] International Energy Agency. Trucks and buses. https://www.iea.org/reports/trucks-and-buses, 2020. [Online].

[29] Simon Kemp. Digital 2021: Global overview report. https://datareportal.com/reports/digital-2021-global-overview-report, [Online].

[30] Andreas Festag. Cooperative intelligent transport systems standards in europe. *IEEE communications magazine*, 52(12):166–172, 2014.

[31] John B Kenney. Dedicated short-range communications (DSRC) standards in the united states. *Proceedings of the IEEE*, 99(7):1162–1182, 2011.

[32] David Eckhoff, Nikoletta Sofra, and Reinhard German. A performance study of cooperative awareness in ETSI ITS G5 and IEEE WAVE. In *2013 10th Annual Conference on Wireless On-demand Network Systems and Services (WONS)*, pages 196–200. IEEE, 2013.

[33] Yasser L Morgan. Notes on DSRC & WAVE standards suite: Its architecture, design, and characteristics. *IEEE Communications Surveys & Tutorials*, 12(4):504–518, 2010.

[34] Khadige Abboud, Hassan Aboubakr Omar, and Weihua Zhuang. Interworking of DSRC and cellular network technologies for V2X communications: A survey. *IEEE transactions on vehicular technology*, 65(12):9457–9470, 2016.

[35] Stephan Eichler. Performance evaluation of the IEEE 802.11 p WAVE communication standard. In *2007 IEEE 66th Vehicular Technology Conference*, pages 2199–2203. IEEE, 2007.

[36] J Karl Hedrick, Masayoshi Tomizuka, and Pravin Varaiya. Control issues in automated highway systems. *IEEE Control Systems Magazine*, 14(6):21–32, 1994.

[37] Sinan Öncü, Jeroen Ploeg, Nathan Van de Wouw, and Henk Nijmeijer. Cooperative adaptive cruise control: Network-aware analysis of string stability. *IEEE Transactions on Intelligent Transportation Systems*, 15(4):1527–1537, 2014.

[38] Jie Mei, Kan Zheng, Long Zhao, Lei Lei, and Xianbin Wang. Joint radio resource allocation and control for vehicle platooning in LTE-V2V network. *IEEE Transactions on Vehicular Technology*, 67(12):12218–12230, 2018.

[39] Bingyi Liu, Dongyao Jia, Kejie Lu, Dong Ngoduy, Jianping Wang, and Libing Wu. A joint control–communication design for reliable vehicle platooning in hybrid traffic. *IEEE Transactions on Vehicular Technology*, 66(10):9394–9409, 2017.

[40] Rajesh Rajamani, Seibum B Choi, BK Law, JK Hedrick, Robert Prohaska, and Paul Kretz. Design and experimental implementation of longitudinal control for a platoon of automated vehicles. *J. Dyn. Sys., Meas., Control*, 122(3):470–476, 2000.

[41] Rajesh Rajamani. *Vehicle dynamics and control*. Springer Science & Business Media, 2011.

[42] Diana Yanakiev and Ioannis Kanellakopoulos. Variable time headway for string stability of automated heavy-duty vehicles. In *Proceedings of 1995 34th IEEE Conference on Decision and Control*, volume 4, pages 4077–4081. IEEE, 1995.

[43] Xavier Huppé, Jean de Lafontaine, Mathieu Beauregard, and François Michaud. Guidance and control of a platoon of vehicles adapted to changing environment conditions. In *SMC'03 Conference Proceedings. 2003 IEEE International Conference on Systems, Man and Cybernetics. Conference Theme-System Security and Assurance (Cat. No. 03CH37483)*, volume 4, pages 3091–3096. IEEE, 2003.

[44] Jeroen Ploeg, Nathan Van De Wouw, and Henk Nijmeijer. Lp string stability of cascaded systems: Application to vehicle platooning. *IEEE Transactions on Control Systems Technology*, 22(2):786–793, 2013.

[45] Petros A Ioannou and Cheng-Chih Chien. Autonomous intelligent cruise control. *IEEE Transactions on Vehicular technology*, 42(4):657–672, 1993.

[46] Vladimir Vukadinovic, Krzysztof Bakowski, Patrick Marsch, Ian Dexter Garcia, Hua Xu, Michal Sybis, Pawel Sroka, Krzysztof Wesolowski, David Lister, and Ilaria Thibault. 3GPP C-V2X and IEEE 802.11p for vehicle-to-vehicle communications in highway platooning scenarios. *Ad Hoc Networks*, 74:17–29, 2018.

[47] Michał Sybis, Vladimir Vukadinovic, Marcin Rodziewicz, Paweł Sroka, Adrian Langowski, Karolina Lenarska, and Krzysztof Wesołowski. Communication aspects of a modified cooperative adaptive cruise control algorithm. *IEEE Transactions on Intelligent Transportation Systems*, 20(12):4513–4523, 2019.

[48] DVAHG Swaroop and J Karl Hedrick. Constant spacing strategies for platooning in automated highway systems. *J. Dyn. Sys., Meas., Control.*, 1999.

[49] DVAHG Swaroop. *String stability of interconnected systems: An application to platooning in automated highway systems*. PhD thesis, University of California, Berkeley, 1994.

[50] Shengbo Eben Li, Yang Zheng, Keqiang Li, and Jianqiang Wang. An overview of vehicular platoon control under the four-component framework. In *2015 IEEE Intelligent Vehicles Symposium (IV)*, pages 286–291. IEEE, 2015.

[51] Prabir Barooah and Joao P Hespanha. Error amplification and disturbance propagation in vehicle strings with decentralized linear control. In *Proceedings of the 44th IEEE conference on Decision and Control*, pages 4964–4969. IEEE, 2005.

[52] Sadayuki Tsugawa, Sabina Jeschke, and Steven E Shladover. A review of truck platooning projects for energy savings. *IEEE Transactions on Intelligent Vehicles*, 1(1):68–77, 2016.

[53] Carl Bergenhem, Steven Shladover, Erik Coelingh, Christoffer Englund, and Sadayuki Tsugawa. Overview of platooning systems. In *Proceedings of the 19th ITS World Congress, Oct 22-26, Vienna, Austria (2012)*, 2012.

[54] Steven E Shladover. Path at 20history and major milestones. *IEEE Transactions on intelligent transportation systems*, 8(4):584–592, 2007.

[55] Ottmar Gehring and Hans Fritz. Practical results of a longitudinal control concept for truck platooning with vehicle to vehicle communication. In *Proceedings of Conference on Intelligent Transportation Systems*, pages 117–122. IEEE, 1997.

[56] Christophe Bonnet and Hans Fritz. Fuel consumption reduction in a platoon: Experimental results with two electronically coupled trucks at close spacing. Technical report, SAE technical paper, 2000.

[57] Carl Bergenhem, Qihui Huang, Ahmed Benmimoun, and Tom Robinson. Challenges of platooning on public motorways. In *17th world congress on intelligent transport systems*, pages 1–12, 2010.

[58] Jeroen Ploeg, Steven Shladover, Henk Nijmeijer, and Nathan van de Wouw. Introduction to the special issue on the 2011 grand cooperative driving challenge. *IEEE Transactions on Intelligent Transportation Systems*, 13(3):989–993, 2012.

[59] Cristofer Englund, Lei Chen, Jeroen Ploeg, Elham Semsar-Kazerooni, Alexey Voronov, Hoai Hoang Bengtsson, and Jonas Didoff. The grand cooperative driving challenge 2016: boosting the introduction of cooperative automated vehicles. *IEEE Wireless Communications*, 23(4):146–152, 2016.

[60] The h2020 project ensemble. `https://ec.europa.eu/inea/en/horizon-2020/projects/h2020-transport/automated-road-transport/ensemble`, [Online].

[61] JK Hedrick, Y Chen, and S Mahal. Optimized vehicle control/communication interaction in an automated highway system, institute of transportation studies. Technical report, Research Reports, Working Papers, Institute of Transportation Studies, UC, 2001.

[62] Pete Seiler and Raja Sengupta. Analysis of communication losses in vehicle control problems. In *Proceedings of the 2001 American Control Conference.(Cat. No. 01CH37148)*, volume 2, pages 1491–1496. IEEE, 2001.

[63] Pete Seiler and Raja Sengupta. An $\mathcal{H}_\infty$ approach to networked control. *IEEE Transactions on Automatic Control*, 50(3):356–364, 2005.

[64] Rajesh Rajamani, Han-Shue Tan, Boon Kait Law, and Wei-Bin Zhang. Demonstration of integrated longitudinal and lateral control for the operation of automated vehicles in platoons. *IEEE Transactions on Control Systems Technology*, 8(4):695–708, 2000.

[65] Jeroen Ploeg, Elham Semsar-Kazerooni, Guido Lijster, Nathan van de Wouw, and Henk Nijmeijer. Graceful degradation of cooperative adaptive cruise control. *IEEE Transactions on Intelligent Transportation Systems*, 16(1):488–497, 2014.

[66] Haitao Xing, Jeroen Ploeg, and Henk Nijmeijer. Smith predictor compensating for vehicle actuator delays in cooperative acc systems. *IEEE Transactions on Vehicular Technology*, 68(2):1106–1115, 2018.

[67] Jeroen Ploeg, Bart TM Scheepers, Ellen Van Nunen, Nathan Van de Wouw, and Henk Nijmeijer. Design and experimental evaluation of cooperative adaptive cruise control. In *2011 14th International IEEE Conference on Intelligent Transportation Systems (ITSC)*, pages 260–265. IEEE, 2011.

[68] Liren Zhang, Abderrahmane Lakas, Hesham El-Sayed, and Ezedin Barka. Mobility analysis in vehicular ad hoc network (vanet). *Journal of Network and Computer Applications*, 36(3):1050–1056, 2013.

[69] Alessandro Amoroso, Gustavo Marfia, and Marco Roccetti. Going realistic and optimal: A distributed multi-hop broadcast algorithm for vehicular safety. *Computer networks*, 55(10):2504–2519, 2011.

[70] Osama Rehman and Mohamed Ould-Khaoua. A hybrid relay node selection scheme for message dissemination in vanets. *Future Generation Computer Systems*, 93:1–17, 2019.

[71] Mani Amoozadeh, Hui Deng, Chen-Nee Chuah, H Michael Zhang, and Dipak Ghosal. Platoon management with cooperative adaptive cruise control enabled by vanet. *Vehicular communications*, 2(2):110–123, 2015.

[72] Yunpeng Wang, Xuting Duan, Daxin Tian, Guangquan Lu, and Haiyang Yu. Throughput and delay limits of 802.11 p and its influence on highway capacity. *Procedia-Social and Behavioral Sciences*, 96:2096–2104, 2013.

[73] Dongyao Jia, Rui Zhang, Kejie Lu, Jianping Wang, Zhongqin Bi, and Jingsheng Lei. Improving the uplink performance of drive-thru internet via platoon-based cooperative retransmission. *IEEE Transactions on Vehicular Technology*, 63(9):4536–4545, 2014.

[74] Chong Han, Mehrdad Dianati, Rahim Tafazolli, Ralf Kernchen, and Xuemin Shen. Analytical study of the IEEE 802.11 p MAC sublayer in vehicular networks. *IEEE Transactions on Intelligent Transportation Systems*, 13(2):873–886, 2012.

[75] Yuan Yao, Yujiao Hu, Gang Yang, and Xingshe Zhou. On MAC access delay distribution for IEEE 802.11 p broadcast in vehicular networks. *IEEE Access*, 7:149052–149067, 2019.

[76] Caixia Song. Performance analysis of the IEEE 802.11 p multichannel MAC protocol in vehicular ad hoc networks. *Sensors*, 17(12):2890, 2017.

[77] Periklis Chatzimisios, Anthony C Boucouvalas, and Vasileios Vitsas. IEEE 802.11 packet delay-a finite retry limit analysis. In *GLOBECOM'03. IEEE Global Telecommunications Conference (IEEE Cat. No. 03CH37489)*, volume 2, pages 950–954. IEEE, 2003.

[78] Michele Segata, Bastian Bloessl, Stefan Joerer, Christoph Sommer, Mario Gerla, Renato Lo Cigno, and Falko Dressler. Toward communication strategies for platooning: Simulative and experimental evaluation. *IEEE Transactions on Vehicular Technology*, 64(12):5411–5423, 2015.

[79] Gaurang Naik, Biplav Choudhury, and Jung-Min Park. IEEE 802.11 bd & 5G NR V2X: Evolution of radio access technologies for V2X communications. *IEEE access*, 7:70169–70184, 2019.

[80] Nikita Lyamin, Alexey Vinel, Magnus Jonsson, and Boris Bellalta. Cooperative awareness in vanets: On etsi en 302 637-2 performance. *IEEE Transactions on Vehicular Technology*, 67(1):17–28, 2017.

[81] Michele Segata, Falko Dressler, and Renato Lo Cigno. Jerk beaconing: A dynamic approach to platooning. In *2015 IEEE vehicular networking conference (VNC)*, pages 135–142. IEEE, 2015.

[82] Amrita Ghosal, Sang Uk Sagong, Subir Halder, Kalana Sahabandu, Mauro Conti, Radha Poovendran, and Linda Bushnell. Truck platoon security: State-of-the-art and road ahead. *Computer Networks*, 185:107658, 2021.

[83] Jonathan Petit and Steven E Shladover. Potential cyberattacks on automated vehicles. *IEEE Transactions on Intelligent transportation systems*, 16(2):546–556, 2014.

[84] Eman Mousavinejad, Fuwen Yang, Qing-Long Han, Quanwei Qiu, and Ljubo Vlacic. Cyber attack detection in platoon-based vehicular networked control systems. In *2018 IEEE 27th International Symposium on Industrial Electronics (ISIE)*, pages 603–608. IEEE, 2018.

[85] Sofian Ali Ben Mussa, Mazani Manaf, Kayhan Zrar Ghafoor, and Zouina Doukha. Simulation tools for vehicular ad hoc networks: A comparison study and future perspectives. In *2015 International Conference on Wireless Networks and Mobile Communications (WINCOM)*, pages 1–8. IEEE, 2015.

[86] Chenxi Lei, Emiel Martijn van Eenennaam, Wouter Klein Wolterink, Jeroen Ploeg, Georgios Karagiannis, and Geert Heijenk. Evaluation of cacc string stability using sumo, simulink, and OMNeT++. *EURASIP Journal on Wireless Communications and Networking*, 2012(1):1–12, 2012.

[87] Rafael Molina-Masegosa and Javier Gozalvez. LTE-V for sidelink 5G V2X vehicular communications: A new 5G technology for short-range vehicle-to-everything communications. *IEEE Vehicular Technology Magazine*, 12(4):30–39, 2017.

[88] Min Wang, Martin Winbjork, Zhang Zhang, Ricardo Blasco, Hieu Do, Stefano Sorrentino, Marco Belleschi, and Yunpeng Zang. Comparison of LTE and DSRC-based connectivity for intelligent transportation systems. In *2017 IEEE 85th vehicular technology conference (VTC Spring)*, pages 1–5. IEEE, 2017.

[89] Manuel Gonzalez-Martín, Miguel Sepulcre, Rafael Molina-Masegosa, and Javier Gozalvez. Analytical models of the performance of C-V2X mode 4 vehicular communications. *IEEE Transactions on Vehicular Technology*, 68(2):1155–1166, 2018.

[90] Alexey Vinel, Lin Lan, and Nikita Lyamin. Vehicle-to-vehicle communication in C-ACC/platooning scenarios. *IEEE Communications Magazine*, 53(8):192–197, 2015.

[91] Fabio Arena, Giovanni Pau, and Alessandro Severino. A review on IEEE 802.11 p for intelligent transportation systems. *Journal of Sensor and Actuator Networks*, 9(2):22, 2020.

[92] Lijian Xu, George Yin, Hongwei Zhang, et al. Communication information structures and contents for enhanced safety of highway vehicle platoons. *IEEE Transactions on vehicular Technology*, 63(9):4206–4220, 2014.

[93] Victor S Dolk, Jeroen Ploeg, and WP Maurice H Heemels. Event-triggered control for string-stable vehicle platooning. *IEEE Transactions on Intelligent Transportation Systems*, 18(12):3486–3500, 2017.

[94] Giulia Giordano, Michele Segata, Franco Blanchini, and Renato Lo Cigno. The joint network/control design of platooning algorithms can enforce guaranteed safety constraints. *Ad Hoc Networks*, 94:101962, 2019.

[95] Meng Wang, Serge Paul Hoogendoorn, Winnie Daamen, Bart van Arem, Barys Shyrokau, and Riender Happee. Delay-compensating strategy to enhance string stability of adaptive cruise controlled vehicles. *Transportmetrica B: Transport Dynamics*, 6(3):211–229, 2018.

[96] Mani Amoozadeh, Hui Deng, Chen-Nee Chuah, H Michael Zhang, and Dipak Ghosal. Platoon management with cooperative adaptive cruise control enabled by VANET. *Vehicular communications*, 2(2):110–123, 2015.

[97] ETSI. Specification of cooperative awareness basic service", ETSI EN 302 637-2 v1.3.2, November 2014.

[98] MATLAB WLAN toolbox 802.11p. `https://fr.mathworks.com/help/wlan/ug/802-11p-packet-error-rate-simulation-for-a-vehicular-channel.html`, [Online].

[99] Paul Alexander, David Haley, and Alex Grant. Cooperative intelligent transport systems: 5.9-GHz field trials. *Proceedings of the IEEE*, 99(7):1213–1235, 2011.

[100] Pekka Kyosti and et al. WINNER II channel models. *IST, Tech. Rep. IST-4-027756 WINNER II D1. 1.2 V1. 2*, 2007.

[101] Giammarco Cecchini, Alessandro Bazzi, Barbara M Masini, and Alberto Zanella. Performance comparison between IEEE 802.11 p and LTE-V2V in-coverage and out-of-coverage for cooperative awareness. In *2017 IEEE Vehicular Networking Conference (VNC)*, pages 109–114. IEEE, 2017.

[102] Jingwei Fu, Gang Wu, and Ran Li. Performance analysis of sidelink relay in SCMA-based multicasting for platooning in V2X. In *2020 IEEE International Conference on Communications Workshops (ICC Workshops)*, pages 1–6. IEEE, 2020.

[103] Dongyao Jia, Kejie Lu, and Jianping Wang. A disturbance-adaptive design for VANET-enabled vehicle platoon. *IEEE Transactions on Vehicular Technology*, 63(2):527–539, 2014.

[104] Giuseppe Bianchi et al. Performance analysis of the IEEE 802.11 distributed coordination function. *IEEE Journal on selected areas in communications*, 18(3):535–547, 2000.

[105] Md Noor-A-Rahim, GG Md Nawaz Ali, Hieu Nguyen, and Yong Liang Guan. Performance analysis of IEEE 802.11 p safety message broadcast with and without relaying at road intersection. *IEEE Access*, 6:23786–23799, 2018.

[106] Qingji Wen and Bin-Jie Hu. Joint optimal relay selection and power control for reliable broadcast communication in platoon. In *2020 IEEE 92nd Vehicular Technology Conference (VTC2020-Fall)*, pages 1–6. IEEE, 2020.

[107] Le-Nam Hoang, Elisabeth Uhlemann, and Magnus Jonsson. An efficient message dissemination technique in platooning applications. *IEEE Communications Letters*, 19(6):1017–1020, 2015.

[108] Tiago R Gonçalves, Vineeth S Varma, and Salah E Elayoubi. Performance of vehicle platooning under different v2x relaying methods. In *2021 IEEE 32nd Annual International Symposium on Personal, Indoor and Mobile Radio Communications (PIMRC)*, pages 1018–1023. IEEE, 2021.

[109] Ge Guo and Wei Yue. Hierarchical platoon control with heterogeneous information feedback. *IET control theory & applications*, 5(15):1766–1781, 2011.

[110] Liwei Xu, Weichao Zhuang, Guodong Yin, and Chentong Bian. Stable longitudinal control of heterogeneous vehicular platoon with disturbances and information delays. *IEEE Access*, 6:69794–69806, 2018.

[111] Yuan Yao, Yujiao Hu, Gang Yang, and Xingshe Zhou. On MAC access delay distribution for IEEE 802.11p broadcast in vehicular networks. *IEEE Access*, 7:149052–149067, 2019.

[112] Mario di Bernardo, Paolo Falcone, Alessandro Salvi, and Stefania Santini. Design, analysis, and experimental validation of a distributed protocol for platooning in the presence of time-varying heterogeneous delays. *IEEE Transactions on Control Systems Technology*, 24(2):413–427, 2016.

[113] Haixia Peng, Dazhou Li, Khadige Abboud, Haibo Zhou, Hai Zhao, Weihua Zhuang, and Xuemin Shen. Performance analysis of IEEE 802.11p DCF for multiplatooning communications with autonomous vehicles. *IEEE Transactions on Vehicular Technology*, 66(3):2485–2498, 2017.

[114] Tiago R Gonçalves, Vineeth S Varma, and Salah E Elayoubi. Performance and design of robust platoons under different communication technologies. In *2021 IEEE 93rd Vehicular Technology Conference (VTC2021-Spring)*, pages 1–6. IEEE, 2021.

[115] Dongyao Jia and Dong Ngoduy. Enhanced cooperative car-following traffic model with the combination of V2V and V2I communication. *Transportation Research Part B: Methodological*, 90:172–191, 2016.

[116] Tiago R Gonçalves, Vineeth S Varma, and Salah E Elayoubi. Vehicle platooning schemes considering V2V communications: A joint communication/control approach. In *2020 IEEE Wireless Communications and Networking Conference (WCNC)*, pages 1–6. IEEE, 2020.

[117] Jelena Mišić, Ghada Badawy, and Vojislav B Mišić. Performance characterization for IEEE 802.11 p network with single channel devices. *IEEE Transactions on Vehicular Technology*, 60(4):1775–1787, 2011.

[118] Claudia Campolo, Antonella Molinaro, Alexey Vinel, and Yan Zhang. Modeling prioritized broadcasting in multichannel vehicular networks. *IEEE Transactions on Vehicular Technology*, 61(2):687–701, 2011.

[119] Francesco Romeo, Claudia Campolo, Antonella Molinaro, and Antoine O Berthet. Asynchronous traffic on the sidelink of 5G V2X. In *2020 IEEE International Conference on Communications Workshops (ICC Workshops)*, pages 1–6. IEEE, 2020.

[120] Apratim Choudhury, Tomasz Maszczyk, Muhammad Tayyab Asif, Nikola Mitrovic, Chetan B Math, Hong Li, and Justin Dauwels. An integrated V2X simulator with applications in vehicle platooning. In *2016 IEEE 19th International Conference on Intelligent Transportation Systems (ITSC)*, pages 1017–1022. IEEE, 2016.

[121] Valerio Turri, Bart Besselink, and Karl H Johansson. Cooperative look-ahead control for fuel-efficient and safe heavy-duty vehicle platooning. *IEEE Transactions on Control Systems Technology*, 25(1):12–28, 2016.

[122] Valerio Turri, Bart Besselink, and Karl H Johansson. Gear management for fuel-efficient heavy-duty vehicle platooning. In *2016 IEEE 55th Conference on Decision and Control (CDC)*, pages 1687–1694. IEEE, 2016.

[123] Kuo-Yun Liang, Jonas Mårtensson, and Karl Henrik Johansson. When is it fuel efficient for a heavy duty vehicle to catch up with a platoon? *IFAC Proceedings Volumes*, 46(21):738–743, 2013.

[124] Gening Yu and Ishwar K Sethi. Road-following with continuous learning. In *Proceedings of the Intelligent Vehicles' 95. Symposium*, pages 412–417. IEEE, 1995.

[125] Luke Ng, Christopher M Clark, and Jan P Huissoon. Reinforcement learning of adaptive longitudinal vehicle control for dynamic collaborative driving. In *2008 IEEE Intelligent Vehicles Symposium*, pages 907–912. IEEE, 2008.

[126] Charles Desjardins and Brahim Chaib-Draa. Cooperative adaptive cruise control: A reinforcement learning approach. *IEEE Transactions on intelligent transportation systems*, 12(4):1248–1260, 2011.

[127] Gustav Ling, Klas Lindsten, Oskar Ljungqvist, Johan Löfberg, Christoffer Norén, and Christian A Larsson. Fuel-efficient model predictive control for heavy duty vehicle platooning using neural networks. In *2018 Annual American Control Conference (ACC)*, pages 3994–4001. IEEE, 2018.

[128] Farwa Jaffar, Taha Farid, Muhammad Sajid, Yasar Ayaz, and Muhammad Jawad Khan. Prediction of drag force on vehicles in a platoon configuration using machine learning. *IEEE Access*, 8:201823–201834, 2020.

[129] Zhaojian Li, Tianshu Chu, Ilya V Kolmanovsky, and Xiang Yin. Training drift counteraction optimal control policies using reinforcement learning: An adaptive cruise control example. *IEEE Transactions on Intelligent Transportation Systems*, 19(9):2903–2912, 2017.

[130] Tianshu Chu and Uroš Kalabić. Model-based deep reinforcement learning for cacc in mixed-autonomy vehicle platoon. In *2019 IEEE 58th Conference on Decision and Control (CDC)*, pages 4079–4084. IEEE, 2019.

[131] Xiaoxiang Li, Xinyou Qiu, Jian Wang, and Yuan Shen. A deep reinforcement learning based approach for autonomous overtaking. In *2020 IEEE*

International Conference on Communications Workshops (ICC Workshops), pages 1–5. IEEE, 2020.

[132] Chen Chen, Jiange Jiang, Ning Lv, and Siyu Li. An intelligent path planning scheme of autonomous vehicles platoon using deep reinforcement learning on network edge. *IEEE Access*, 8:99059–99069, 2020.

[133] J Karl Hedrick, Masayoshi Tomizuka, and Pravin Varaiya. Control issues in automated highway systems. *IEEE Control Systems Magazine*, 14(6):21–32, 1994.

[134] Meng Wang, Serge Paul Hoogendoorn, Winnie Daamen, Bart van Arem, Barys Shyrokau, and Riender Happee. Delay-compensating strategy to enhance string stability of adaptive cruise controlled vehicles. *Transportmetrica B: Transport Dynamics*, 6(3):211–229, 2018.

[135] Takashi Oguchi, Masahiko Katakura, and Masaaki Taniguchi. Available concepts of energy reduction measures against road vehicular traffic. In *Intelligent Transportation: Realizing the Future. Abstracts of the Third World Congress on Intelligent Transport SystemsITS America*, 1996.

[136] M Rashid Khan. *Advances in clean hydrocarbon fuel processing: Science and technology*. Elsevier, 2011.

[137] Global Marketing. Diesel fuels technical review, 2007.

[138] Sheldon M Ross, John J Kelly, Roger J Sullivan, William James Perry, Donald Mercer, Ruth M Davis, Thomas Dell Washburn, Earl V Sager, Joseph B Boyce, and Vincent L Bristow. *Stochastic processes*, volume 2. Wiley New York, 1996.

[139] Hado Van Hasselt, Arthur Guez, and David Silver. Deep reinforcement learning with double q-learning. In *Proceedings of the AAAI conference on artificial intelligence*, volume 30, 2016.

[140] Oswaldo Luiz do Valle Costa, Marcelo D Fragoso, and Marcos G Todorov. *Continuous-time Markov jump linear systems*. Springer Science & Business Media, 2012.

[141] Adam Paszke, Sam Gross, Francisco Massa, Adam Lerer, James Bradbury, Gregory Chanan, Trevor Killeen, Zeming Lin, Natalia Gimelshein, Luca Antiga, Alban Desmaison, Andreas Kopf, Edward Yang, Zachary DeVito, Martin Raison, Alykhan Tejani, Sasank Chilamkurthy, Benoit Steiner, Lu Fang, Junjie Bai, and Soumith Chintala. Pytorch: An imperative

style, high-performance deep learning library. In H. Wallach, H. Larochelle, A. Beygelzimer, F. d'Alché-Buc, E. Fox, and R. Garnett, editors, *Advances in Neural Information Processing Systems 32*, pages 8024–8035. Curran Associates, Inc., 2019.

[142] Iman Sajedian, Heon Lee, and Junsuk Rho. Double-deep q-learning to increase the efficiency of metasurface holograms. *Scientific reports*, 9(1):1–8, 2019.

[143] Murat Dikmen and Catherine Burns. Trust in autonomous vehicles: The case of tesla autopilot and summon. In *2017 IEEE International conference on systems, man, and cybernetics (SMC)*, pages 1093–1098. IEEE, 2017.

[144] Nidhi Kalra and Susan M Paddock. Driving to safety: How many miles of driving would it take to demonstrate autonomous vehicle reliability? *Transportation Research Part A: Policy and Practice*, 94:182–193, 2016.

[145] Ashley Peake, Joe McCalmon, Benjamin Raiford, Tongtong Liu, and Sarra Alqahtani. Multi-agent reinforcement learning for cooperative adaptive cruise control. In *2020 IEEE 32nd International Conference on Tools with Artificial Intelligence (ICTAI)*, pages 15–22. IEEE, 2020.

[146] Ikumi Ichikawa and Toshimitsu Ushio. Application of reinforcement learning to adaptive control of connected vehicles. *Nonlinear Theory and Its Applications, IEICE*, 10(4):443–454, 2019.

[147] F Gosselin, C Megard, S Bouchigny, F Ferlay, F Taha, P Delcampe, and C DHauthuille. A vr training platform for maxillo facial surgery. In *Applied human factors and ergonomics (AHFE) international conference, Miami, Florida, USA, Advances in Cognitive Ergonomics*, 2010.

[148] C Andriot and J Perret. Immersive virtual prototyping with haptic feedback and virtual manikins. *Proceedings of IDMME-Virtual Concept, Beijing, China*, 2008.

[149] James Calvin, Alan Dickens, Bob Gaines, Paul Metzger, Dale Miller, and Dan Owen. The simnet virtual world architecture. In *Proceedings of IEEE Virtual Reality Annual International Symposium*, pages 450–455. IEEE, 1993.

[150] Michael R Macedonia, Michael J Zyda, David R Pratt, Paul T Barham, and Steven Zeswitz. Npsnet: a network software architecture for largescale virtual environments. *Presence: Teleoperators & Virtual Environments*, 3(4):265–287, 1994.

université PARIS-SACLAY
ÉCOLE DOCTORALE
Sciences et technologies de l'information et de la communication (STIC)

Titre: Contrôle robuste de pelotons de véhicules sur un canal radio avec imperfections

Mots clés: Pelotons de véhicules, régulateur de vitesse adaptatif coopératif (CACC), relais, communication sans fil

Résumé: Les systèmes de transport sont essentiels pour la société, car le rythme soutenu de la croissance économique est étroitement lié à l'accroissement des activités de transport. Dans ce contexte, le domaine des systèmes de transport intelligents (ITS) est apparu comme un sujet de recherche d'actualité pour améliorer et relever les nouveaux défis des systèmes de circulation. Les systèmes de pelotons représentent une approche relativement simple en termes de déploiement vers des solutions économes en carburant, la réduction de la congestion du trafic et l'amélioration de la sécurité routière. En particulier, le peloton de véhicules est une formation spécifique par un groupe de véhicules coordonnés, dans laquelle une courte distance intervéhicules est maintenue grâce à l'automatisation et aux technologies de communication entre véhicules. Le déploiement de tels systèmes est étroitement lié à une évaluation minutieuse de la synergie entre les deux technologies de base.

Dans cette thèse, nous formulons et analysons une classe de problèmes de platooning en abordant les aspects de communication et de contrôle avec les défis connexes introduits par le chevauchement de ces deux domaines. Nous évaluons d'abord la robustesse de la performance du platoon dans des conditions sévères pour les communications Véhicule-à-Véhicule (V2V), exprimées par de longues rafales de pertes et dans des conditions difficiles de brouillage sur la route. Nous proposons un mécanisme de contrôle dynamique dans lequel les paramètres du schéma de contrôle le plus avancé, le Predicted Cooperative Adaptive Cruise Control (PCACC), sont adaptés en fonction de la qualité observée de l'interface radio.

La fiabilité du réseau est de la plus haute importance car elle limite le fonctionnement du système de contrôle. Afin de surmonter l'impact des messages abandonnés et retardés, nous proposons une modélisation analytique d'un nouveau schéma de relais V2V et une étude de l'impact du relais des unités de bord de route (RSU) comme alternatives pour étendre la couverture du message du véhicule en tête du peloton. Nous commençons par développer un modèle de Markov pour les différents liens de communication, et nous évaluons soigneusement l'impact des paramètres du réseau (erreurs et retards) sur la performance du contrôleur (distance intervéhicules). Pour ce faire, nous intégrons le taux d'erreurs de paquets résultant à la distribution des retards et évaluons son impact sur les performances du peloton.

L'analyse formulée jusqu'à présent est limitée à l'amélioration des performances du système de peloton tout en considérant soigneusement la présence d'un grand nombre de liaisons V2V point à point. Malgré cette importance, nous manquons d'une évaluation explicite pour quantifier ces développements en termes de consommation de carburant, qui est l'aspect le plus important du point de vue économique et de la faisabilité du platooning à des fins commerciales. Dans ce contexte, le dernier objectif de cette thèse est d'aborder explicitement le problème de la consommation de carburant dans les systèmes de platooning. Nous réduisons la consommation de carburant atteignable par la commutation de deux politiques de contrôle, le contrôle de vitesse adaptatif (ACC) et le contrôle de vitesse adaptatif coopératif (CACC), dans les systèmes de platooning. Parmi d'autres propositions, nous adoptons des techniques d'apprentissage par renforcement profond (DRL) comme solution alternative pour contrôler indirectement le système. Les simulations effectuées démontrent la faisabilité de notre système, même en cas de forte congestion du trafic.

Université Paris-Saclay
Espace Technologique / Immeuble Discovery
Route de lOrme aux Merisiers RD 128 / 91190 Saint-Aubin, France

université PARIS-SACLAY
ÉCOLE DOCTORALE
Sciences et technologies de l'information et de la communication (STIC)

Title: Robust control of platooning systems over imperfect wireless channels

Keywords: Vehicle platoons, Cooperative Adaptive Cruise Control (CACC), relaying, wireless communication

Abstract: Transportation systems are critical for society, as the persistent pace of economic growth and increase of demands are closely related to more transportation activity. In this framework, the field of Intelligent Transportation Systems (ITS) has emerged as a research trending topic to enhance and address new traffic-system challenges. Platooning systems represent a relatively simple approach in terms of deployment towards fuel efficient solutions, traffic congestion reduction, and road safety improvements. In particular, vehicle platoon is a specific formation by a group of coordinated vehicles, in which a short inter-vehicle distance is maintained by virtue of automation and vehicular communication technologies. The deployment of such systems are closely related to a careful evaluation of the synergy between both core technologies.

In this thesis, we formulate and analyze a class of platooning problems by addressing communication and control aspects with the related challenges introduced by the overlap of both areas. We first evaluate the robustness of the platoon performance under severe conditions for Vehicle-to-Vehicle (V2V) communications, expressed in long bursts of losses and in difficult traffic jamming conditions on the road. We propose a dynamic control mechanism where the parameters of the well-known Predicted Cooperative Adaptive Cruise Control (PCACC) are adapted based on the observed network link quality.

The network reliability is of utmost importance as it limits the control system operation. In order to overcome the impact of dropped and delayed messages, we propose an analytical modeling of a novel V2V relaying scheme and a study of the impact of Roadside Unit (RSU) relaying as alternatives to extend the coverage range of the leader message. We start by developing a Markov model for the different communication links, and we carefully evaluate the impact of network parameters (errors and delays) on the controller performance (inter-vehicle distance). This is done by integrating the resulting packet error rate with the delay distribution and evaluating its impact on the platoon performance.

The analysis formulated so far is narrowed to improve the performance of the platoon system while carefully considering the presence of a large number of point-to-point V2V links. Despite significant, we lack an explicit evaluation to quantify such developments in terms of fuel consumption, which is the most important aspect from the economical perspective and feasibility of platooning for commercial purposes. In this context, the last objective in this thesis is to address explicitly the fuel consumption problem in platooning systems. We reduce the fuel consumption attainable by the switching of two control policies, Adaptive Cruise Control (ACC) and Cooperative Adaptive Cruise Control (CACC), in platooning systems. Among the propositions, we adopt Deep Reinforcement Learning (DRL) techniques as an alternative solution to indirectly control the system. The carried out simulations demonstrate the feasibility of our scheme even under strong traffic congestion.

Université Paris-Saclay
Espace Technologique / Immeuble Discovery
Route de lOrme aux Merisiers RD 128 / 91190 Saint-Aubin, France